



Experimental testing of fillet welded T-joints to evaluate the NZS3404 specified safety factors for seismic fillet welds

In partial fulfilment of the requirements for the degree of Master of Engineering

By: Mark Zhang (ID: 1316399)

Supervised by: Dr. Shahab Ramhormozian

Auckland University of Technology

October 2023

Abstract

Welding is widely used in the construction and manufacturing industry. The quality of the weld on-site and weld design become the most important factors for structural safety and cost-effectiveness. Mainly there are five basic weld categories which are butt weld, fillet weld, corner joint weld, lap joint weld, and edge joint weld. This research is focused on fillet weld which is one of the most widely used welding methods.

In this project, five groups of fillet welding specimens with different weld sizes are experimentally tested in the lab. The data from the tests are collected and analyzed to obtain the safety factors for the simplified method formula currently used in New Zealand standard, NZS3404. These experimental safety factors from the test are compared to the existing factors recommended in NZS3404.

The project is undertaken in three main steps:

The first step is the test setup, specimens, and procedure design phase, which includes designing the test setup and different specimens as well as defining the testing procedure including the loading regime and measurement plan. This requires predicting the modes of failures of the specimens according to the provisions of the current standard.

The second step is the experiments which include lab work and data collection. The specimens are under an axial cyclic loading regime. The welds are equal leg fillet weld. Using the equation $\phi V_w = \phi \times 0.6 \times f_{uw} \times t_t \times k_r$, which is a simplified method from NZS3404, the shear capacity of weld is identified. The recorded data such as load values from the actuator and the displacements are analyzed and compared with the current design methods.

The third step consists of the analysis of the obtained data along with the recommendations.

Table of Contents

Attestation of Authorship	1
Acknowledgements.....	1
Dedication	1
1.0 Introduction:	1
1.1 Steel and weld	1
1.2 Literature review:	2
1.2.1 Fillet weld design	2
1.2.2 Simplified method	4
1.2.3 Direction method:	6
1.2.4. Traction stress method.....	7
1.3 The need to improve the weld design provisions:.....	8
1.4 The details of the test samples:	9
2.0 Test setup design and detail	13
2.1 the philosophy of the test setup design.....	13
2.2 The testing load path.	13
2.3 Test set up design.....	17
2.3.1 Introduction	17
2.3.2 Test Setup and Specimen’s structural design:.....	20
2.4 The setup and specimen (i.e. testing sample) drawings.....	52
3. 0 Experiments procedure:.....	55
3.1 Introduction of the Loading regime:	55
3.2 Converting the drift deformation to axial displacement	56
3.3 The facilities used in AUT labs:.....	59
3.3.1 the equipment used in the cyclic/dynamic tests and general procedure:	59
3.2.2 The instrumentation used in the test:.....	65
3.2.3 Data recording tools and software - Data Acquisition (DAQ) Systems and the controllers/commanders:.....	69
3.2.4 The common tools used in the test preparation.....	70
3.3 Installation of strain gauges:	73
3.4 Test sample assembling:	78
3.5 Bolts installation for the sample’s assembling:.....	82

4.0 Dimensions and observations on samples:	91
5.0 Etching test:	98
6.0 Results and analysis:	104
6.1 General goal:	104
6.2 Determination of the throat thickness of the samples:.....	104
6.2.1 Determination of the throat thickness from the etching test	106
6.2.2 The physical measurements of the critical throat thickness.....	108
6.3 Failure mode results and static analysis:	110
6.3.1 Tested samples fractured in weld.	110
6.3.2 Tested samples fractured in stem	114
6.3.3 The test failed (terminated) due to slipping.....	116
6.4 comparison between the actual capacity and/or demand and theoretical capacity 118	
6.5 Summary of the experimental results.....	119
7.0 Conclusion and recommendations	123
7.1 Further potential improvements and/or considerations regarding the test setup.....	123
7.2 Further research.....	123
7.3 Conclusion	124
8.0 Bibliography	125

Table of Figures

FIGURE 1: EXAMPLES OF A MOMENT END PLATE CONNECTION (LEFT) FROM (COWIE & FUSSELL, 2015) AND WELDED MOMENT CONNECTION (RIGHT) FROM SCNZ STEELWORK CONNECTIONS GUIDE (HYLAND, COWIE, & BIRD, 2010)	1
FIGURE 2: EQUAL LEG FILLET WELD (LEFT) AND UNEQUAL LEG FILLET WELD (RIGHT FROM) IN NZS: 3404:1997	2
FIGURE 3: AWS STANDARD SHEAR TEST SPECIMENS (AWS B4.0, 2016): (A) LONGITUDINAL SHEAR WELD; (B) TRANSVERSE SHEAR WELD	3
FIGURE 4: TYPICAL FAILURE ANGLE: (A) FAILURE ANGLE OF LONGITUDINAL SHEAR WELD; (B) FAILURE ANGLE OF TRANSVERSE SHEAR WELD	6
FIGURE 5: STRESSES ON THE THROAT SECTION OF A FILLET WELD (COMMITTEE, 2005)	6
FIGURE 6: LINEAR REPRESENTATION AND DECOMPOSITION OF TRACTION STRESSES (NIE & DONG, 2012)	8
FIGURE 7: DRAWING OF TEST SAMPLES WITHOUT GAPS (DIMENSIONS IN MM)	9
FIGURE 8: THE DRAWING OF TEST SAMPLES WITH GAP	10
FIGURE 9: THE DETAIL DRAWING OF TEST SAMPLES WITH GAP	11
FIGURE 10: SETUP MEMBERS RELATED TO LOAD PATH FROM FRONT VIEW	14
FIGURE 11: SETUP MEMBERS RELATED TO LOAD PATH FROM SIDE VIEW	15
FIGURE 12: SETUP MEMBERS RELATED TO LOAD PATH FROM CLOSE VIEW	16
FIGURE 13: GENERAL TEST SETUP LAYOUT-MID CROSS SECTION	18
FIGURE 14: GENERAL TEST SETUP DESIGN-3D VIEW	19
FIGURE 15: WEB PLATE	21
FIGURE 16: WEB PLATE A_G AREA	22
FIGURE 17: CLAMPING ANGLE	23
FIGURE 18: CLAMPING ANGLE A_g area	24
FIGURE 19: CLAMPING ANGLE A_n area	25
FIGURE 20: 250 GRADE STEEL DATA SHEET	25
FIGURE 21: CLAMPING ANGLE STRESS DISTRIBUTION AROUND BOLT HOLE	26
FIGURE 22: DIMENSIONS FOR THE STEEL CANTILEVER PART IN CALCULATION-FRONT VIEW	28
FIGURE 23: DIMENSIONS FOR THE STEEL CANTILEVER PART IN CALCULATION-INSIDE VIEW	29
FIGURE 24: CLAMPING ANGLE A_E , T_P DIMENSION	33
FIGURE 25: CLAMPING ANGLE UNDER TENSION-FRICTION MODE	34
FIGURE 26: CRITICAL SECTION OF CLAMPING ANGLE UNDER TENSION-FRICTION MODE	35
FIGURE 27: DIMENSION $L1$	37
FIGURE 28: COVER PLATE	39
FIGURE 29: YIELDLINE THEORY CASE 1: COMPLETE TEE STUB YIELDING	40
FIGURE 30: COVER PLATE YIELDLINE THEORY DIMENSION	40
FIGURE 31: YIELDLINE THEORY CASE 2: BOLT STRETCHING WITH FLANGE YIELDING	41
FIGURE 32: FLANGE BASE PLATE	42

FIGURE 33: T-STUB IDENTIFICATION AND ORIENTATION (GIRAO COELHO, 2006)	42
FIGURE 34: FLANGE BASE PLATE YIELDLINE THEORY DIMENSION	43
FIGURE 35: CLAMPING ANGLE.....	43
FIGURE 36: DIMENSIONS OF THE CLAMPING ANGLE BASE PLATE IN YIELDLINE THEORY	44
FIGURE 37: CLAMPING ANGLE RESTRAINT AGAINST SPECIMEN BUCKLING	46
FIGURE 38: DIMENSIONS USED IN THE CALCULATION.	47
FIGURE 39: WEB PLATE SUBJECT TO COMPRESSION (G300)	48
FIGURE 40: FRONT VIEW OF THE TEST SETUP AND TEST SAMPLE	52
FIGURE 41: SIDE VIEW FOR TEST SAMPLE.....	53
FIGURE 42: SEPARATED PARTS FOR TEST SAMPLE	54
FIGURE 43: 3D VIEW OF THE SAMPLE	54
FIGURE 44: THE FIGURE E-1 IN SAC STEEL PROJECT: REPORT NO. SAC/BD-97/02	55
FIGURE 45: DETAIL DIMENSIONS OF THE 460UB82.1	56
FIGURE 46: HPU IN AUT LABS	60
FIGURE 47: HPU'S PUMPS (PHOTO TAKEN FROM INSIDE OF THE HOOD).....	60
FIGURE 48: THE PIPES AND VALVES FOR DELIVERING THE HYDRAULIC FLUID	61
FIGURE 49: AN HSM IN AUT LABS.....	62
FIGURE 50: THE PRESSURE GAUGES OF AN HSM IN AUT LABS	63
FIGURE 51: THE ACTUATOR AND ITS REACTION FRAME IN AUT LABS.....	65
FIGURE 52: THE DETAILS ON THE PACKAGE OF STRAIN GAUGE FROM BESTECH AUSTRALIA PTY LTD	66
FIGURE 53: THE STRAIN GAUGES ON TRAIL TEST SAMPLE	67
FIGURE 54: TYPICAL LVDT LAYOUT AND WORKING PRINCIPLE (MASI, DANISI, LOSITO, MARTINO, & SPIEZIA, 2011)	68
FIGURE 55: THE TYPE OF LVDT USED IN THESE TESTS FROM AUT LABS	68
FIGURE 56: AG125-15DB CORDED ANGLE GRINDER.....	70
FIGURE 57: AG 125-A22 CORDLESS ANGLE GRINDER	71
FIGURE 58: SHOWN PLAN FOR THE SIZE OF PODGER SPANNER(PODGER RATCHET WRENCH-KING TONY-1500).....	71
FIGURE 59: THE DIMENSION OF THE STANDARD PODGER SPANNER (HTTP://WWW.WRENCHMM.COM/ENGLISH/PRODUCT/7026814542.HTML)	72
FIGURE 60: THE TORQUE WRENCH USED IN AUT LABS.....	72
FIGURE 61: THE DRAWING FOR THE STRAIN GAUGES POSITIONS ON SAMPLES	73
FIGURE 62: THE DISC 100 X 16MM RAPID STRIP DISC NORTON BLAZE.....	74
FIGURE 63: THE FINISHED STEEL SURFACE PREPARATION WORK FOR STRAIN GAUGE INSTALLATION.....	75
FIGURE 64: THE CIRCUIT BOARD FOR QUARTER BRIDGE CONNECTION	76
FIGURE 65: THE SUPER GLUE FOR THE WIRE FIXING	76
FIGURE 66: THE SAMPLE WITH STRAIN GAUGES INSTALLED.....	77
FIGURE 67: THE OUTLINE OF THE TEST STRUCTURE	78
FIGURE 68: MARKED UP CENTRAL LINES ON THE CLAMPING ANGLE AND GROUND PROTECTION PLATE FOR ALIGNMENT PURPOSE	79
FIGURE 69: MARKED UP CENTRAL LINES ON THE T-JOINT FOR ALIGNMENT PURPOSE	80

FIGURE 70: PLACING THE TEST SAMPLE IN A POSITION CLOSE TO ONE OF THE CLAMPING ANGLES.	81
FIGURE 71: PLACING THE COVER PLATES ON THE TEST SAMPLE (FLANGE BASE PLATE)	82
FIGURE 72: THE ELECTRIC TORQUE WRENCH (TORQUE GUN) TYPE: V-RAD 16	83
FIGURE 73: THE TORQUE CALIBRATION CHART FOR ELECTRIC TORQUE WRENCH TYPE: V-RAD 16.....	84
FIGURE 74: THE CALIBRATION VALUES TABLE FOR ELECTRIC TORQUE WRENCH TYPE: V-RAD 16.....	85
FIGURE 75: CONFIRM THE PITCH SIZE OF M20 10.9 BOLT.....	89
FIGURE 76: THE EZIJAC SOCKET TYPE MODEL: B3S-L5	90
FIGURE 77: THE DOCUMENTED SIZE OF THE SAMPLE FW10G0R1N3S2.....	92
FIGURE 78: THE 6 POINTS ON THE WEB PLATE TO MEASURE LEG LENGTH(3D VIEW)	92
FIGURE 79: THE 6POINTS ON THE FLANGE BASE PLATE TO MEASURE ROOT LENGTH (PLAN VIEW).....	93
FIGURE 80: THE ILLUSTRATION OF LEG LENGTH, THROAT, AND ROOT LENGTH	93
FIGURE 81:CAM TYPE GAGE.....	94
FIGURE 82: UNFINISHED STEEL SURFACE WITH SPUR ON THE FLANGE BASE PLATE	96
FIGURE 83: UNFINISHED STEEL SURFACE WITH SPUR ON THE STEM WEB PLATE.....	96
FIGURE 84: HARD DISC TYPE: A RHODIUS RS28 125x7,0.....	97
FIGURE 85: FINISHED STEEL SURFACE AFTER 80-GRIT GRIND	99
FIGURE 86: FINISHED STEEL SURFACE AFTER 120 AND 240 GRIT GRIND.....	100
FIGURE 87: FINISHED STEEL SURFACE READY FOR ETCHING TEST	100
FIGURE 88: THE PROCESSING OF THE ETCHING TEST	101
FIGURE 89: RECORD A SAMPLE AFTER THE ETCHING TEST	103
FIGURE 90: THE FILLET WELD SIZE IN NZS: 3404:1997	105
FIGURE 91: DESIGN THROAT THICKNESS OF COMPOUND WELDS WITH INCOMPLETE PENETRATION WELDS.....	106
FIGURE 92: TWO WELD TOES LOCATED	107
FIGURE 93: THE LINE EXCLUDING CONCAVITY	107
FIGURE 94: FIND THE THROAT THICKNESS FROM THE ACTUAL ROOT	107
FIGURE 95: FINDING THE THROAT THICKNESS FROM THE WELD LEGS (WITHOUT GAP).....	108
FIGURE 96: FINDING THE THROAT THICKNESS FROM THE L1AND L2 (WITH GAP)	109
FIGURE 97: THE MEASURED ANGLES FROM FRACTURED SAMPLE	111
FIGURE 98:THE COMPARISON OF THE FORCE CAPACITY BETWEEN DIFFERENT MEASUREMENT METHODS FOR GROUPFW8.....	113
FIGURE 99: THE FRACTURE ON WELD OFTHE SAMPLEFW8G0R1N4S2	114
FIGURE 100: THE FRACTURE IN STEM OF THE SAMPLEFW12G3R1N2S5	115
FIGURE 101: FAILED (TERMINATED) IN SLIPPING OF THE TEST SAMPLEFW10G0RON3S4.....	117
FIGURE 102: SUMMARY OF THE DATA FOR FW8 GROUP	119
FIGURE 103: SUMMARY OF THE DATA FORFW10 GROUP.....	120
FIGURE 104: SUMMARY OF THE DATA FOR FW12 GROUP.....	120
FIGURE 105: SUMMARY OF THE DATA FOR FW10+1.5 GAP GROUP.....	121
FIGURE 106: SUMMARY OF THE DATA FOR FW12+3 GAP GROUP.....	121
FIGURE 107: SUMMARY OF THE DATA FOR FW16 GROUP.....	122

List of Tables

TABLE 1: DIMENSIONS OF DIFFERENT PARTS.....	19
TABLE 2: LOADING REGIME VALUES:.....	58
TABLE 3: TABLE OF THE DIMENSION OF SAMPLEFW10G0R1N3S2 – DIMENSIONS ARE ALL IN MM.	94
TABLE 4: TABLE OF ETCHING TEST SOLUTION	98
TABLE 5: THE SUMMARY OF THE TEST FAILURE MODE	110
TABLE 6: THE SUMMARY FOR TESTED SAMPLES FRACTURED ON WELD (NOTE: THE ANALYSIS INCLUDES BOTH SIDE OF THE FILLET WELD.)	112
TABLE 7: THE SUMMARY FOR TESTED SAMPLES FRACTURED IN STEM. (NOTE: THE ANALYSIS INCLUDES BOTH SIDE OF THE FILLET WELD.)	114
TABLE 8: THE SUMMARY FOR TESTED SAMPLES FAILED (TERMINATED) DUE TO SLIPPING (NOTE: THE ANALYSIS INCLUDES BOTH SIDE OF THE FILLET WELD.)	116
TABLE 9: THE RATIO OF THE WELD ACTUAL CAPACITY AND/OR DEMAND TO THE THEORETICAL CAPACITY (RED: FRACTURE IN WELD, ORANGE: FRACTURE IN STEM (I.E. WEB), GREEN: TEST TERMINATED DUE TO SLIDING, AND BLACK: THE SAMPLE USED IN FIRST TRAIL TEST)	118

Table of equations

EQUATION 1: STRESS ON CRITICAL PLANE FROM (NIE & DONG, 2012) – P IS THE SHEAR FORCE	3
EQUATION 2: CALCULATION OF WELD DESIGN CAPACITY FOR FILLET WELD FROM (SHAHAB RAMHORMOZIAN, 2020c)	5
EQUATION 3: THE DESIGN RESISTANCE OF THE FILLET WELD FROM EN 1993-1-8:2005 (2005)	7
EQUATION 4: STEEL NOMINAL (I.E. UNFACTORED) SECTION CAPACITY IN NZS3404	21
EQUATION 5: DESIGN SECTION CAPACITY IN NZS3404	21
EQUATION 6: NOMINAL SECTION CAPACITY OF A TENSION MEMBER IN NZS3404	26
EQUATION 7: THE EFFECTIVE SECTION MODULUS CALCULATION	30
EQUATION 8: NORMAL SECTION MOMENT CAPACITY IN NZS3404	30
EQUATION 9: CALCULATION OF NOMINAL WEB SHEAR CAPACITY IN THE PRESENCE OF BENDING MOMENT IN NZS3404	32
EQUATION 10: CALCULATION OF NOMINAL SHEAR CAPACITY OF A FLAT PLATE WITH NON-UNIFORM SHEAR STRESS DISTRIBUTION IN NZS3404	32
EQUATION 11: STEEL PLY IN A BOLTED CONNECTION IN BEARING IN NZS3404	32
EQUATION 12: STEEL PLY IN A BOLTED CONNECTION IN TEAROUT IN NZS3404	33
EQUATION 13: HOLDING MOMENT FOR LATERAL MOMENT IN NZS:3404	46
EQUATION 14: EFFECTIVE LENGTH IN NZS3404	48
EQUATION 15: RADIUS OF GYRATION FOR Y-AXIS IN NZS3404	48
EQUATION 16: SLENDERNESS RATIO IN NZS3404	49
EQUATION 17: NOMINAL SECTION CAPACITY IN NZS3404	49
EQUATION 18: MODIFIED COMPRESSION MEMBER SLENDERNESS IN NZS3404	49
EQUATION 19: CALCULATION FOR MEMBER AXIAL FORCE CAPACITY IN NZS3404	50
EQUATION 20: CALCULATION FOR REQUIRED TORQUE (FROM:	85
EQUATION 21: CALCULATION FOR <i>longitudinal elastic stiffness of the bolt</i>	86
EQUATION 22: CALCULATION FOR ELONGATION OF THE BOLT DUE TO THE PRELOAD	86
EQUATION 23: CALCULATION FOR ROTATION OF THE NUT FOR M24 BOLTS IN RADIANS	86
EQUATION 24: CALCULATION FOR <i>longitudinal elastic stiffness of the bolt</i>	87
EQUATION 25: CALCULATION FOR ROTATION OF THE NUT FOR M24 BOLTS IN RADIANS	87
EQUATION 26: CALCULATION FOR ROTATION OF THE NUT FOR M20 BOLTS IN RADIANS	88
EQUATION 27: CALCULATING THE THROAT LENGTH USING THE LEG DIMENSIONS AND ANGLE	109
EQUATION 28: CALCULATING THE THROAT THICKNESS BASED ON THE WELD DIMENSIONS L1 AND L2, AS WELL AS THE ANGLE, FOR WELD SAMPLES WITH A GAP	110

Attestation of Authorship

I hereby declare that this submission is my own work and that, to the best of my knowledge and belief, it contains no material previously published or written by another person, nor material which to a substantial extent has been submitted for the award of any other degree or diploma of a university or other institution of higher learning, except where explicitly defined in the acknowledgements.

Signature:

Date: 29/11/2023

Acknowledgements

I am writing to convey my heartfelt gratitude and deep appreciation to my supervisor, Dr. Shahab Ramhormozian, for the unwavering support, invaluable guidance, and tremendous assistance provided during the course of this research project. Through his mentorship, which has been both profoundly knowledgeable and truly inspirational, I have garnered the strength, expertise, abilities, and opportunities necessary to undertake and effectively conclude this study. I would also like to express my gratitude to the weld research group, comprising primarily Dr. Charles Clifton, Dr. Michail Karpenko, Dr. Pingsha Dong, Dr. Hafez Taheri, Mr Kevin Yip and Mr. Nandor Mago. I am profoundly impressed by the vast of knowledge possessed by Dr. Charles Clifton. Equally noteworthy is his willingness and enthusiasm to impart this knowledge and share his wealth of experience with others. All the group members' extensive knowledge and wealth of expertise played a crucial role in ensuring that the research project stayed on the correct course and yielded the desired results.

I extend the same gratitude to the AUT lab managers and technicians, including Dave Crofts, Stephen Hartley, Allan Dixon, and Louise Burnett. Their invaluable assistance and dedicated efforts were instrumental in overcoming numerous challenging tasks and practical issues encountered during the testing stage.

Last but certainly not least, I am immensely grateful to HERA for their significant technical and financial supports for this research project, which has provided me with the opportunity to contribute in. Additionally, I extend my heartfelt appreciation to John Jones Steel and Konnect Fastening Systems for their generous and selfless contributions to this research endeavour. The support from New Zealand Ministry of Business, Innovation and Employment (MBIE) through an Endeavour Fund for the Research Programme (Sustainable Earthquake Resilient Buildings for a Better Future - PROP-83779-ENDRP-AUT) is greatly appreciated.

Dedication

This thesis is proudly dedicated to:

My dear mother, Mrs. Yuying Qin

(For all her selflessness, for her strength and support even in toughest times when she was seriously ill during this project, for a kind lady)

My dear father, Mr. Shouhe Zhang

(For his endless support and kindness)

My lovely home country, China

(for its diversity and gracefulness)

My beautiful country of living, New Zealand

(for its peacefulness and beauty)

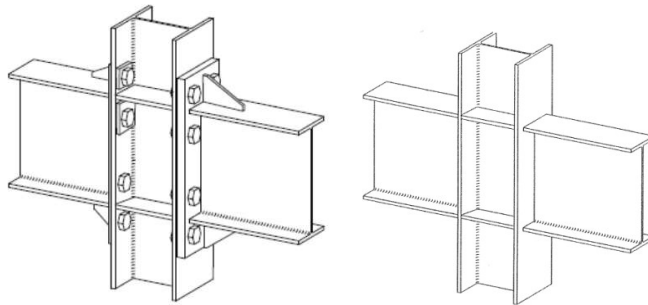
1.0 Introduction:

1.1 Steel and weld

Welding is widely used in the construction and manufacturing industry.

Steel is among the primary construction materials, alongside wood and concrete, and it holds a significant role in the construction sector. According to a 2014 report, the steel utilized in the construction industry accounted for over half of the total steel production, with 60% specifically dedicated to building construction (Moynihan & Allwood, 2014). As one of the main steel connection methods, welding is widely used in the mechanical and construction industry. Mainly there are five basic weld categories which are butt weld, fillet weld, corner joint weld, lap joint weld, and edge joint weld. This research will focus on the fillet weld which is one of the most widely used welding methods.

The weld is capable to be used as a connection for carrying normal force, shear force, and bending moment. As two examples of beam-column moment connections, Figure 1 below shows a bolted beam-column joint and a welded beam-column joint, in which the moment end plate (Figure 1: (a)) connection needs to bolt the end plate to both sides of the column and the welded moment (Figure 1: (b)) do not need bolting, hence expected to be more cost effective.



(a) (b)

Figure 1: Examples of a Moment End Plate connection (left) from (Cowie & Fussell, 2015) and Welded Moment connection (right) from SCNZ Steelwork Connections Guide (Hyland, Cowie, & Bird, 2010)

The weld design in New Zealand must be compliant with NZS3404(New Zealand Standard, 1997). According to the feedback from industry, the fillet welds are likely to be oversized based on current standards design provisions, likely requiring excessive costs.

1.2 Literature review:

1.2.1 Fillet weld design

The design for fillet weld is based on the weld geometrical dimensions. The weld leg length and weld throat thickness (also known as throat length) are the two essential factors for weld design.

The leg length is defined as “The lengths (t_{w1}, t_{w2}) of the sides lying along legs of a triangle inscribed within the cross section of the weld (see Figure 2 (left) and (right)). When the legs are of equal length, the size shall be specified by a single dimension (t_w). ” The leg length is the distance from the root of the weld (the point where the two pieces of metal meet) to the toe of the weld (the end of the weld bead). There are two legs in a fillet weld, one along each piece of metal being joined. The leg size is a critical factor because it determines the throat size, which is the shortest distance from the root to the face of the weld, and ultimately affects the strength of the weld. The root of weld is the point where the two pieces of metal meet at the bottom of the weld and the toe of the weld is the end of the weld bead where it meets the base metal surface.

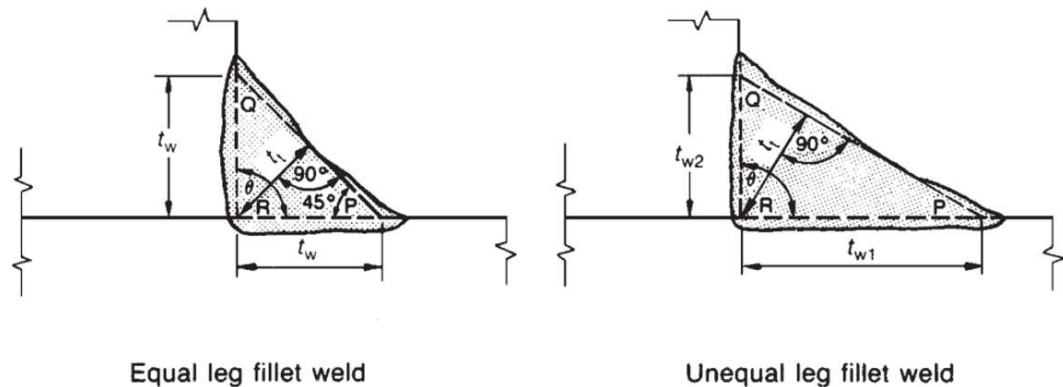


Figure 2: Equal leg fillet weld (left) and Unequal leg fillet weld (right from) in NZS3404:1997

The other important weld dimension is throat thickness (t_t), see Figure2, the design throat thickness on the critical surface is calculated assuming it has an angle of 45° Degrees from the baseplate and assume the failure always happens on this plane. Also,

it can be understood that it is the minimum distance minus any reinforcement between the weld root and the face of a fillet weld.

It needs to be noted that in New Zealand, America and Australia, the leg length (t_{w1}, t_{w2}) is used to describe the fillet weld size, but in Europe, the fillet weld size is described as the throat thickness (t_t).

Another important parameter in weld design is the Critical failure plane. The critical failure plane area equals throat thickness (a) multiplied the total length of the weld (L), as shown in Figure 3. The critical failure plane is used for the calculation of shear stress (τ).

$$\tau = \frac{P}{L \times a}$$

Equation 1: Stress on critical plane from (Nie & Dong, 2012) – P is the shear force

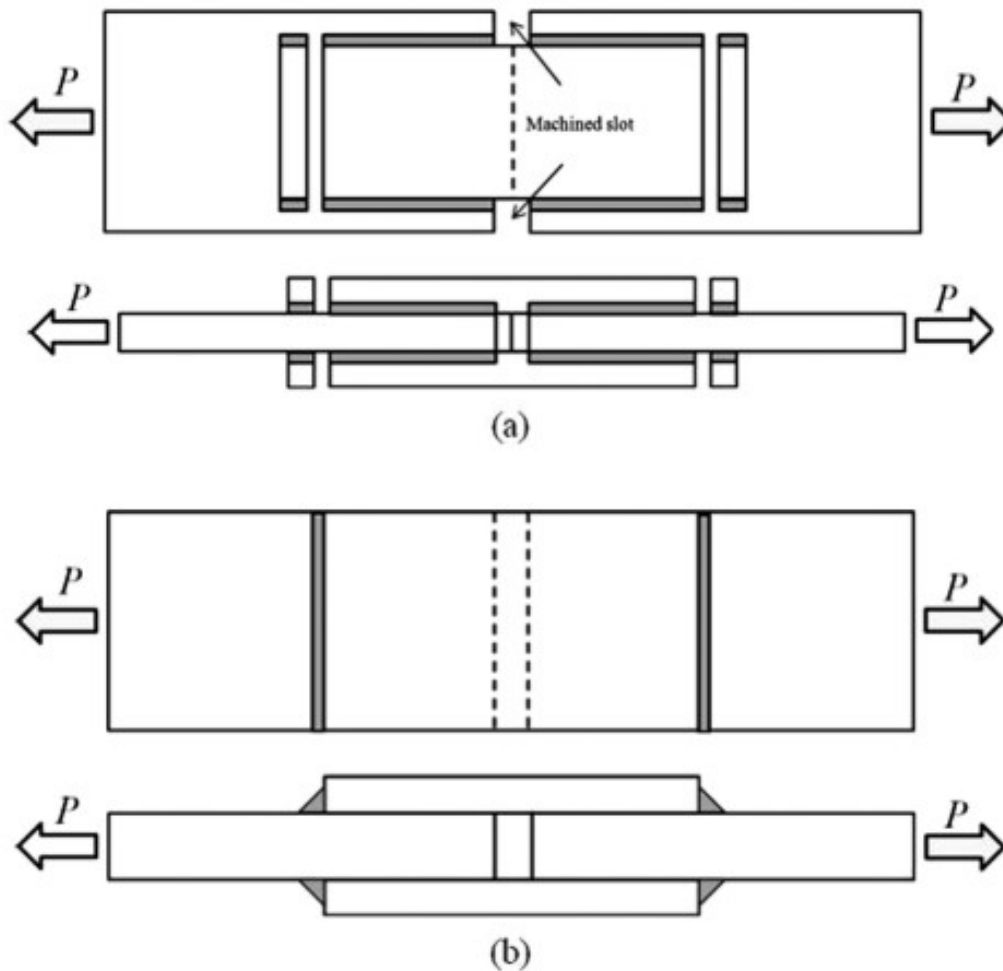


Figure 3: AWS standard shear test specimens (Society, 2007): (a) longitudinal shear weld; (b) transverse shear weld

The main currently used weld design methods in different standards around the world are mostly based on the simplified method, the directional method, and traction stress method. The simplified method and the directional method are mature in philosophy and used with competence in research and practice over a long period of time. The concept of the traction stress method is proposed by Prof. Pingsha Dong (Dong, 2001), and this method is quickly developing and has received increasing attention because of its more advanced and expected more accurate predictions.

For the same load case, there would be different design results of the weld size under different methods and design standards. As mentioned above, weld size is essential for safety and cost effectiveness of design. The size of the weld influences the structural safety and cost-efficiency of the connection, thus avoiding over or under designing is desirable. This requires the identification of reliable and realistic safety factors for welds. This is the main objective of this study.

Three primary methods for weld design used by most standards are described below.

1.2.2 Simplified method

As the current weld design method used in New Zealand standard NZS3404 (New Zealand Standard, 1997), compared to the other two methods, the simplified method is easy to understand and used in practice because it is a relatively simple design philosophy. That is assuming the critical throat plane area which is the effective length of the weld multiplied by the effective throat thickness, as the effective internal force resistant area (described as critical failure plane, $L \times a$ as per Equation 1) or even more simply described as the minimum area within the weldment. Under this assumption, the internal stress can be calculated from the external force divided by the effective throat area, and the design will be satisfied if the internal stress is less than factored weld metal capacity. Due to its simplicity, the simplified method was chosen instead of the direction method which is difficult to understand and hard to be used in practical design work compared to the simplified method.

NZS3404 (New Zealand Standard, 1997) has the following design formula:

$$V_w^* < \phi V_w$$

where

ϕ : strength reduction factor

V_w : nominal capacity of a fillet weld per unit length.

V_w^* : a design force per unit length of weld

The design formula for the nominal capacity of a fillet weld per unit length (v_w) are as follow:

$$\phi V_w = \phi 0.6 f_{uw} t_t k_r$$

Equation 2: Calculation of weld design capacity for fillet weld from (Shahab Ramhormozian, 2020c)

Where

f_{uw} : nominal tensile strength of weld metal

t_t : design throat thickness

k_r : reduction factor given in table 9.7.3.10(2) of NZS3404 to account for the length of a welded lap connection (L_w). For all other connection types, $k_r = 1.0$ (New Zealand Standard, 1997).

As it is clearly understood from the formula, the thickness of the design throat t_t is an important parameter to determine capacity of the weld, and this parameter depends on the angle of fracture. In other words, the formula of this simplified method design philosophy, considers the effective area of a fillet weld as a key parameter to identify nominal capacity of the weld to resist the external force.

The design theory for the simplified method is easy to understand and use in practice, however there are still shortcomings associated with this method.

The simplified method considers only the throat plane to identify the design strength and ignores all the geometry-depended parameters. The weld stress distribution is more complex than what is considered in the simplified method which, for example, considers only one shear failure angle and shear strength regardless the geometrical influences on such angle. The shear strength obtained from transverse shear specimens can be 40% to 60% higher than those obtained from longitudinal shear specimens (Nie & Dong, 2012), see Figure 3 for the definition of longitudinal and transverse shear specimens.

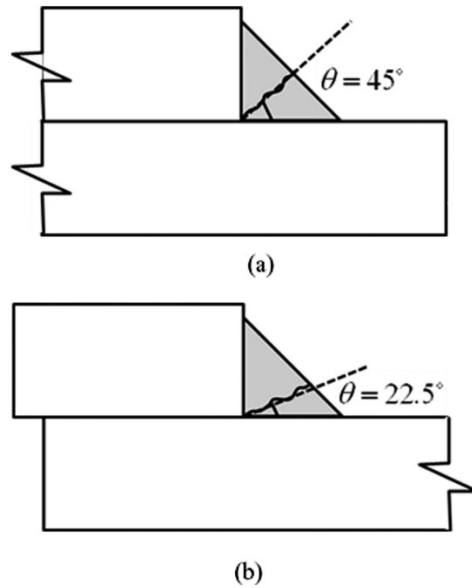


Figure 4: Typical failure angle: (a) failure angle of longitudinal shear weld; (b) failure angle of transverse shear weld

Another shortcoming of the theory of the simplified method is that it only considers the elastic condition and ignores the elastic-plastic strength and capacity of the material.

1.2.3 Direction method:

The direction method is currently used in EN 1993-1-8:2005 (European Committee for Standardization [CEN], 2005). The direction method formula is illustrated below, and the stress analysis is shown in Figure 5.

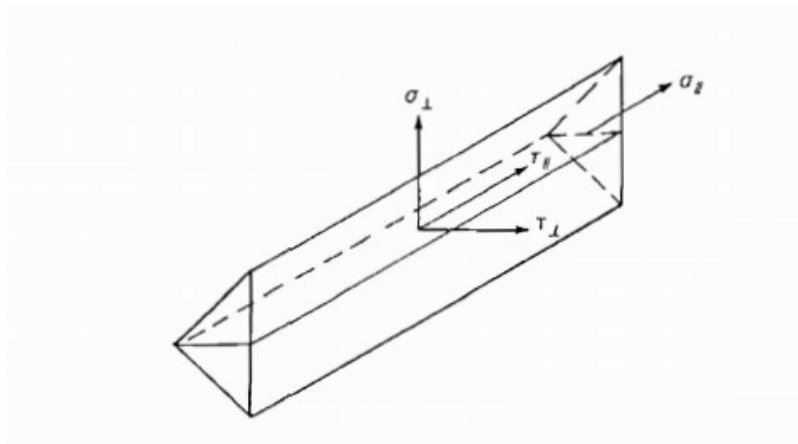


Figure 5: Stresses on the throat section of a fillet weld (Committee, 2005)

- σ_{\perp} is the normal stress perpendicular to the throat.

- σ_{\parallel} is the normal stress parallel to the axis of the weld.
- τ_{\perp} is the shear stress (in the plane of the throat) perpendicular to the axis of the weld.
- τ_{\parallel} is the shear stress (in the plane of the throat) parallel to the axis of the weld.

σ_{\parallel} is normally a very minor load in practice that can be ignored in the design calculation.

The weld design will be considered qualified if the following two formulas are satisfied:

$$[\sigma_{\perp}^2 + 3(\tau_{\perp}^2 + \tau_{\parallel}^2)]^{0.5} \leq f_u / \beta_w \gamma M_2$$

$$\sigma_{\perp} \leq 0.9 f_u / \beta_w \gamma M_2$$

Equation 3: The design resistance of the fillet weld from EN 1993-1-8:2005 (2005)

where:

f_u is the nominal ultimate tensile strength of the weaker part joined.

β_w is the appropriate correlation factor taken from table 2.1.

γM_2 is a partial safety factor for the resistance of weld equal to 1.25 (Heravi, 2019)

The direction method is developed based on the von Mises stress failure criterion. Unlike the simplified method, the direct method analyzes the internal stress distribution of the weld by considering the normal and shear stresses according to the direction of the external force.

The shortcoming of the direction method, same as that of the simplified method, is that it only considers the elastic condition and ignores elastic-plastic material strength. Moreover, the weld stress distribution under the external force is assumed to be uniform.

1.2.4. Traction stress method

The traction stress method is proposed by Professor Pingsha Dong (Dong, 2001). And after that, the traction stress method was improved and systemized. The fundamental design philosophy of this method is based on considering a hypothetical cutting plane (or series of planes) within a material where the stress distribution is analyzed. Assuming this cutting plane with an angle (θ) to the base plate along the welding line, and linearly analysing three traction stress components which are longitudinal shear (τ_L), transverse shear (τ_T), and normal stress (σ) (Nie & Dong, 2012).

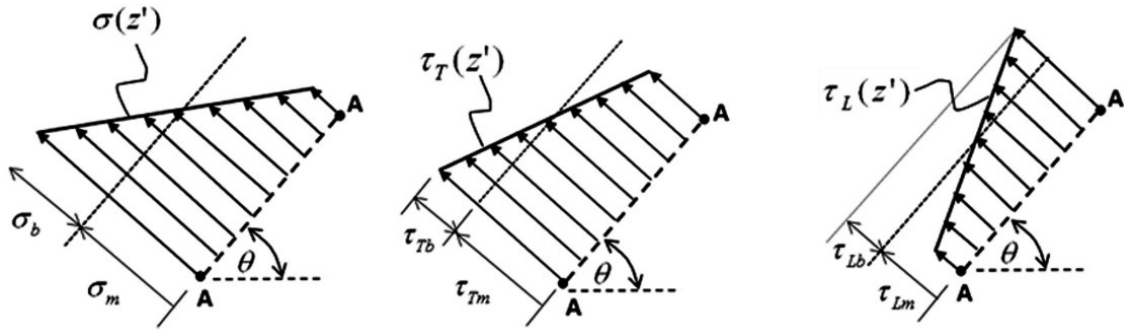


Figure 6: Linear representation and decomposition of traction stresses(Nie & Dong, 2012)

Compared to the simplified method and direction method, the traction stress method is the only design method considering the weld internal stress from an assumed angle of the cutting plane through the weld. Thus, in theory, the traction stress method is able to make stress analysis of resistance at any internal point of the weld.

However, the calculation formula for the traction stress method is too complicated to be widely used in practice.

1.3 The need to improve the weld design provisions:

The weld design approach plays a crucial role in structural safety and cost-effectiveness. This research focuses on the fillet welds, as one of the most common types of welded connections between structural elements, such as the beam and column. The primary focus is the seismic application of such welds in which the structural components that are connected by the weld, are expected to experience inelastic (plastic) actions.

The past earthquakes, for example in India (2001), Iran (2003), China (2008), New Zealand (2011) and Japan (2011), have highlighted the importance of structural safety. An important factor of weld design is having reliable performance under seismic actions. Moreover, the cost of construction is a factor that needs to be carefully considered. Hence an optimum balance between strength/safety and cost is desirable. This main purpose of the experiments undertaken in this research is exploring weld sample's performance under a simulated seismic load. The loading regime for these tests is designed after adopting from the loading protocols from (AISC, 2016) modified to fit the requirements of this research, as explained in the following sections.

The safety factors for the simplified method formula currently used in the New Zealand standard NZS3404 will be re-evaluated and assessed according to the experimental test results obtained in this research to propose potential improvements for the current provisions.

1.4 The details of the test samples:

The test is conducted with the assumption that the test specimens represent the connection between the flange of a steel beam and the column flange in a moment resisting frame welded beam-column connection. The beam's flange is represented by a web plate with dimensions of 60mm x 16mm, while the column's flange is represented by a thick flange baseplate with dimensions of 60mm x 60mm. The test includes four groups of samples, each featuring different fillet weld leg sizes: 8mm, 10mm, 12mm, and 16mm. Additionally, two more groups of samples are included, with weld size of 10mm and 12mm, in which 1.5mm and 3mm gaps were introduced. Hence in total, there are six groups of samples, and their design is illustrated in the Figure 7 below. Each sample group were tested with few repeats, as explained in the following sections.

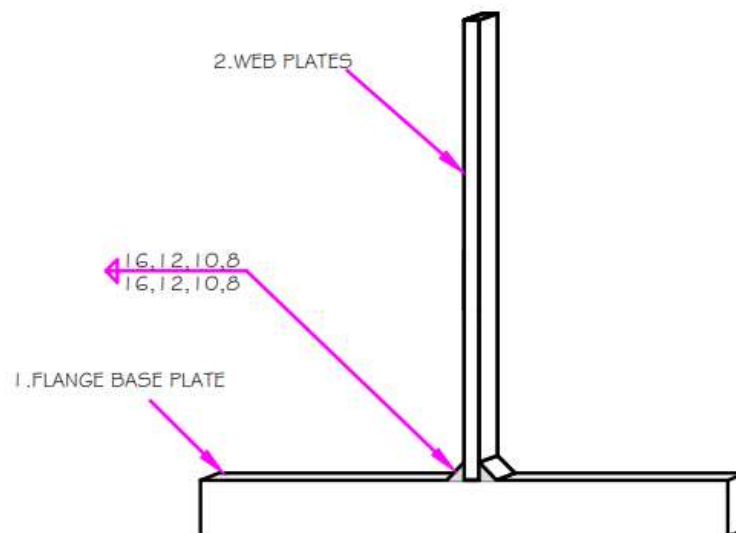


Figure 7: Drawing of test samples without gaps (dimensions in mm)

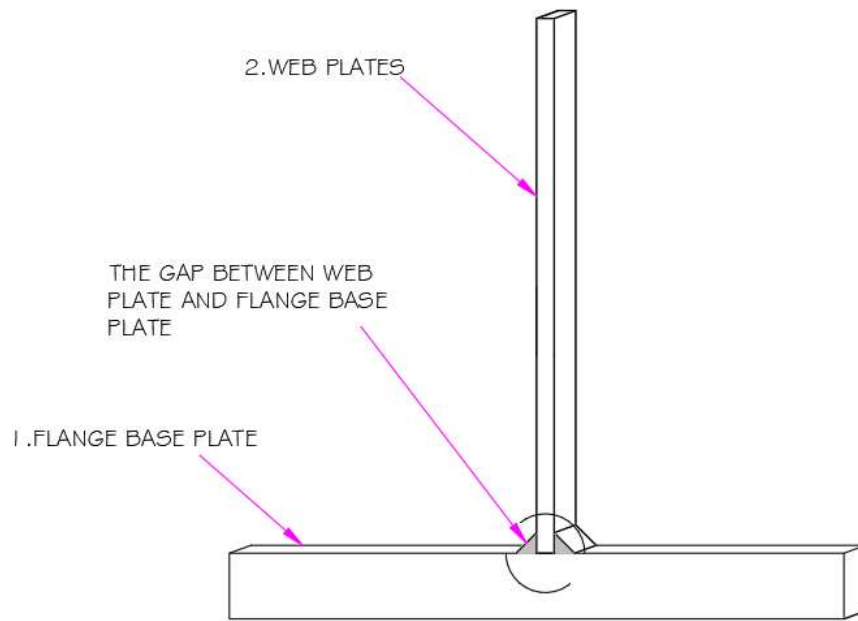
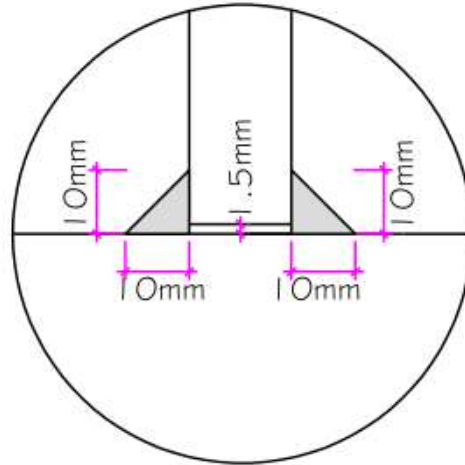
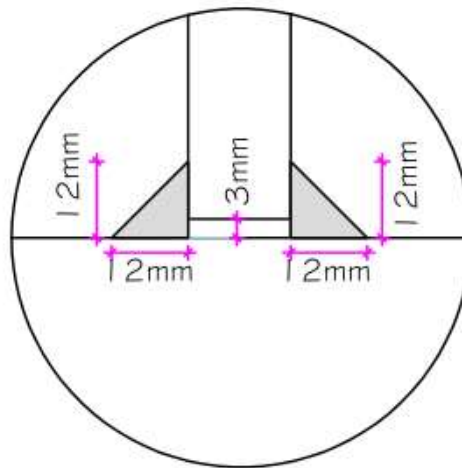


Figure 8: The drawing of test samples with gap

T-FILLET WELDED WITH GAP SPECIMEN DETAIL



T-FILLET WELDED WITH GAP SPECIMEN TYPE 1: 1.5mm GAP WITH 10mm WELD SIZE



T-FILLET WELDED WITH GAP SPECIMEN TYPE 2: 3mm GAP WITH 12mm WELD SIZE

Figure 9: The detail drawing of test samples with gap

To designate these samples, specific codes are utilized: FWxx represents the weld size, Gxx denotes the size of the gap between the flange base plate and the web plate, and R1 indicates one side of the sample with a round weld. During the manufacturing process, each sample is assigned a unique serial number, which is then included as a suffix. The factory's series number is denoted as NxSy, where x corresponds to the group number to which the sample belongs, and y represents the sample number within that group. For example, if a sample has a 12mm weld length, a 3.0mm gap size, and a round weld, with the serial number N4S2, it would be named FW12G3.0R1N4S2.

2.0 Test setup design and detail

2.1 The philosophy of the test setup design

The test setup design is undertaken by several crucial considerations that require careful attention:

1. Ensuring Flange Base Plate Stiffness: To ensure superior rigidity in the flange base plate (column flange) compared to the web plate (beam flange), the flange base plate's size must be relatively larger.
2. Focus on Elastic and Post-Elastic Behaviour: The test primarily examines the elastic and post-elastic performance of the weld and web. The test continues until the web plate undergoes plastic deformation until fracture, if possible. The load applied is always within the equipment's capacity.
3. Application of Friction Load to the Web Plate: Instead of using shear force from bolts to pull and push the stem plate (i.e., web plate), the test applies a friction load to the web plate. Two clamping angles are designed to securely hold the web plate, allowing pulling, and pushing through the frictional force between the clamping angles and the web plate, using a conservative friction factor (i.e., coefficient) of 0.3.
4. Repeating Samples Testing: To ensure the reliability of the test results, at least five samples are tested in each group for different weld sizes.
5. Secure Flange Base Plate Fixation: The flange base plate is firmly fixed to the strong floor using a thick cover plate to minimize deformation and/or detachment caused by the tension force.
6. Test setup reusability: the test setup was designed to remain in the elastic range allowing its reusability for many tests.

2.2 The testing load path.

The test setup's general load path can be summarized as follows and the following figures illustrate these primary members:

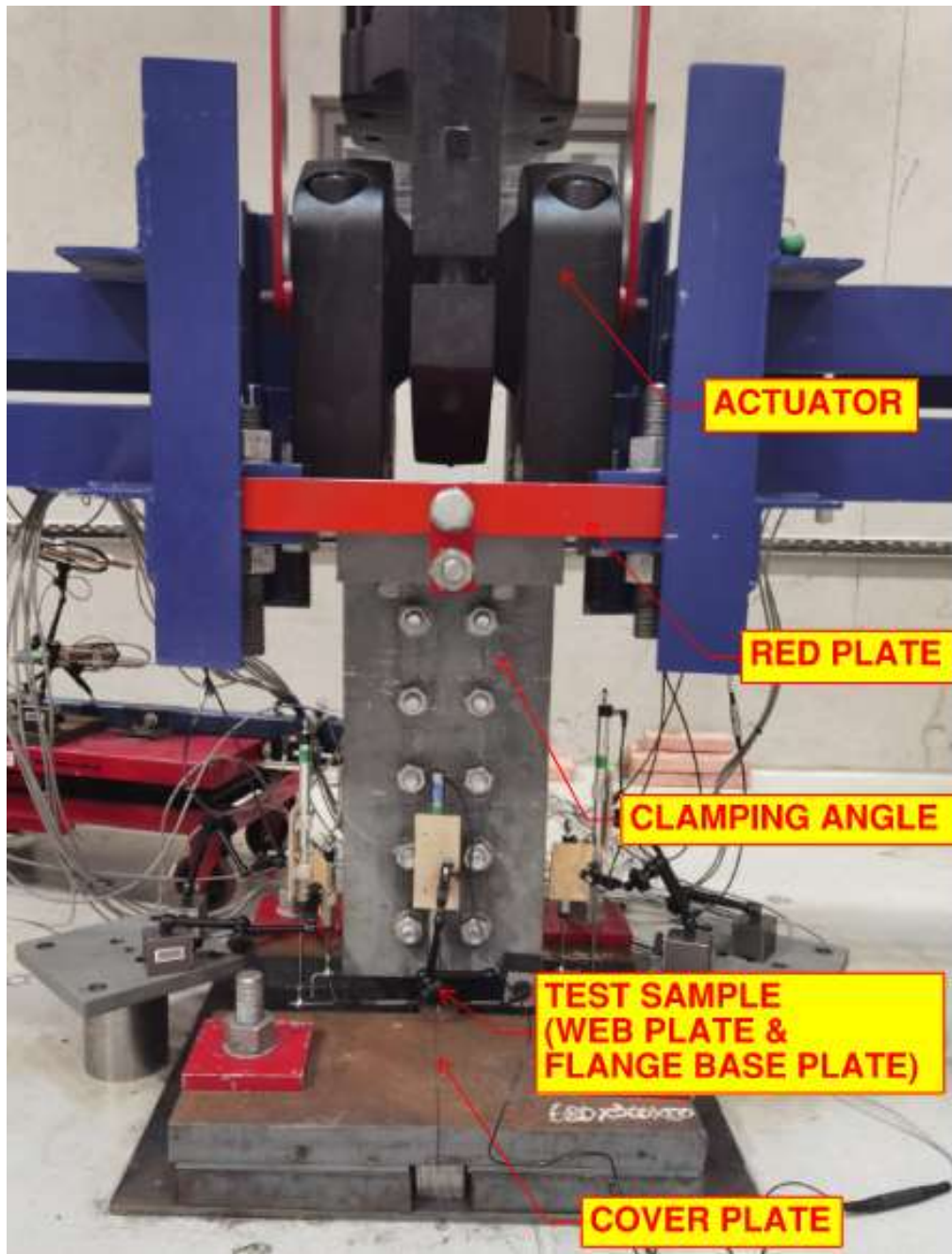


Figure 10: Setup members related to load path from front view

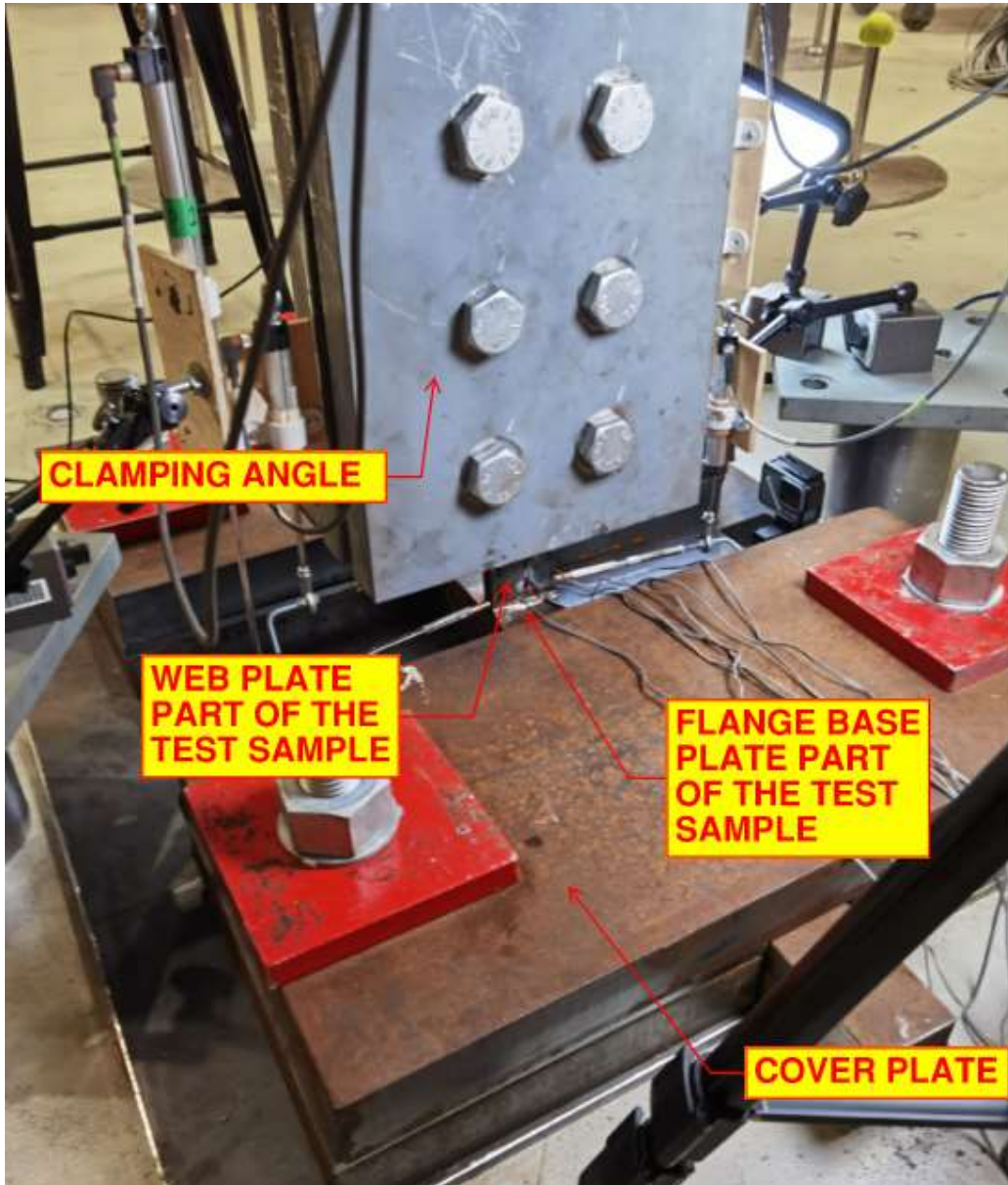


Figure 11: Setup members related to load path from side view

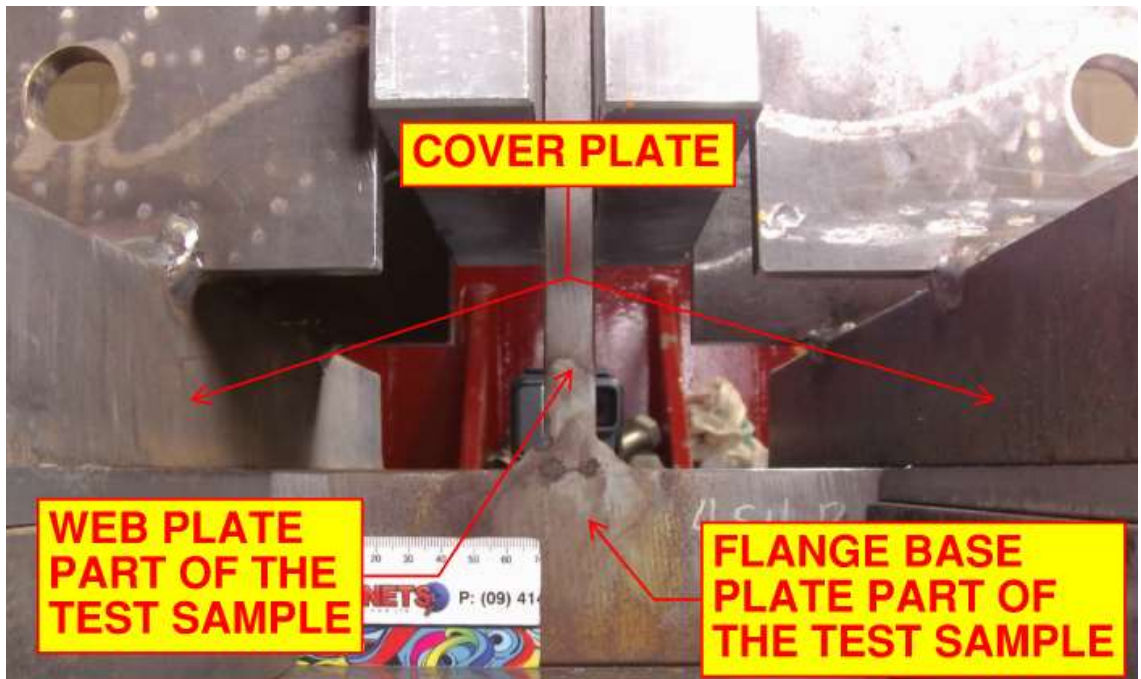


Figure 12: Setup members related to load path from close view

1. The actuator applies force to the clamping angles through a red plate, connecting them together.
2. The clamping angles securely hold the web plate in place using strong friction force. When the actuator pulls or pushes the clamping angles, the frictional force between the clamping surface of the web plate and the clamping angles allows the load to be transferred to the web plate.
3. The load then travels from the web plate through the weld to the flange base plate.
4. The flange base plate is firmly attached to the strong floor using cover plates, ensuring its stability, and minimizing deformation from the tension force.

In this way, the load path effectively transmits the forces applied to the clamping angles to the web plate through friction, and then through the welds to the flange base plate.

2.3 Test set up design

2.3.1 Introduction

The general test setup including a specimen (See Figure 13&Figure 14) consists of six main parts, i.e., two clamping angles, one Web-plate, one Flange base plate, and two cover plates. The web-plate is welded to the flange base plate which together make a sample (a T-stub sample also known as Stem in this thesis). As the general drawing Figure 13 and Figure 14 show, the clamping angles are connected to the actuator's endplate (also known as red plate in this thesis) through their short legs each one by 2×M30 High Strength Friction Grip (HSFG) Property Class (PC) 8.8 bolts and connected to the Web-plate through their long legs by 10×M24 HSFG PC8.8 bolts (and for some experiments by M20 PC10.9 bolts, as explained in the following sections). The Web-plate is welded to the middle of the Flange base plate, and the fillet weld leg sizes to be tested are 8mm, 10mm, 12mm, and 16mm. The flange base plate is covered by the cover plate at both sides. The cover plates also cover the backup plates as shown in the drawings Figure 13 and Figure 14. The cover plate is connected to the strong floor by 2×M36 HSFG PC8.8 threaded rods and nuts. The actuator endplate is designed to remain elastic at 1000kN force which is the maximum force that may be imposed by the dynamic actuator. All the dimensions of bolts, nuts, and washers in the design are compliant with the AS/ANZ 1252:1996 (AS/NZS, 1996a).

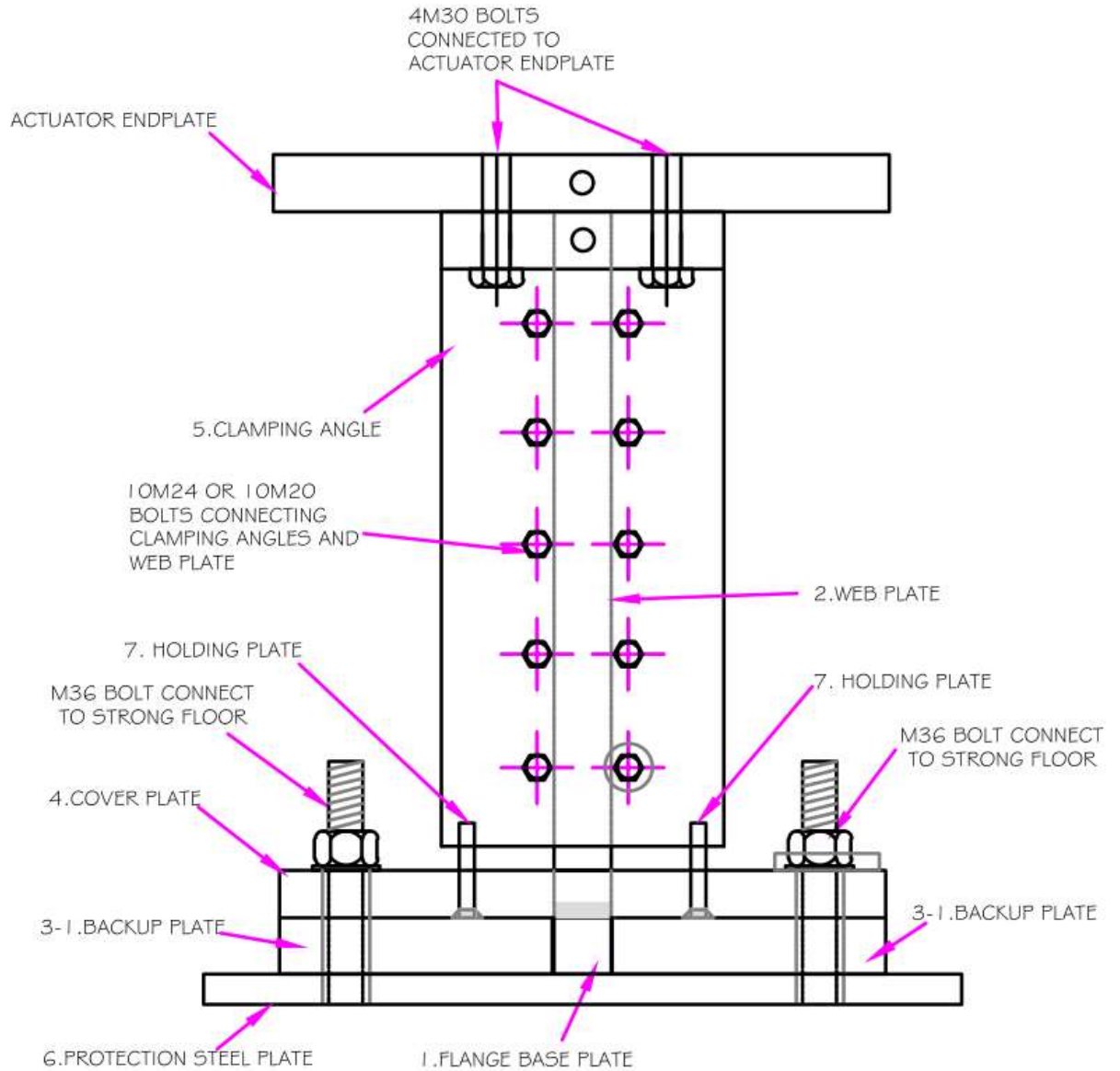


Figure 13: General test setup layout-mid cross section

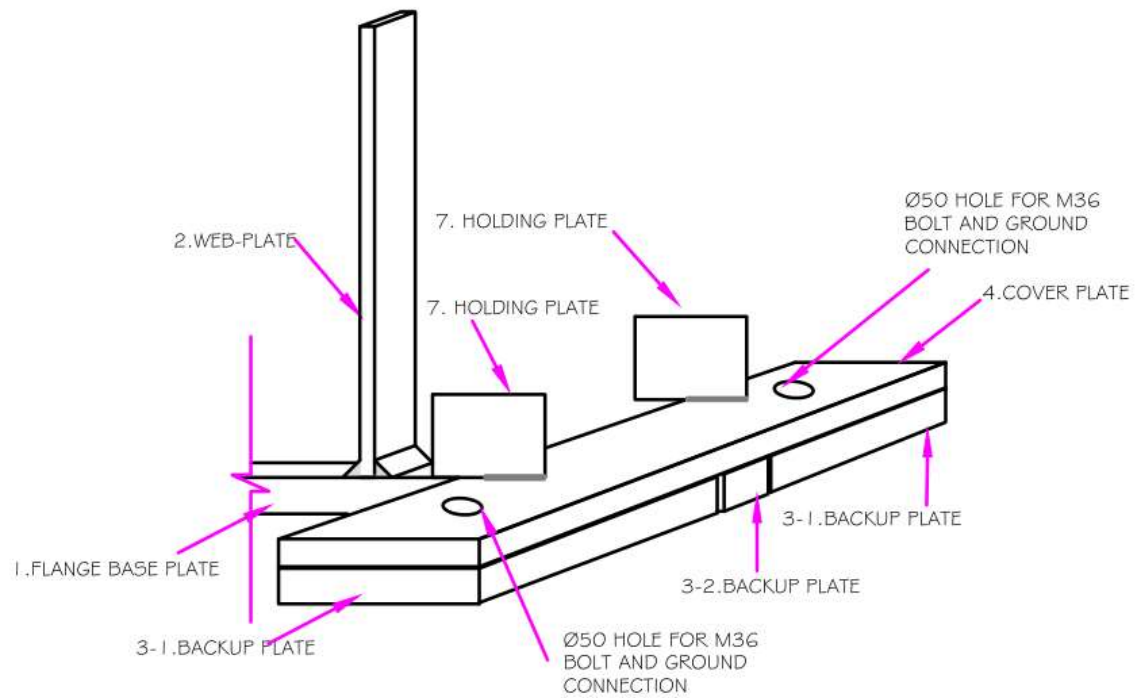


Figure 14: General test setup design-3D view

The dimension of the test setup and specimens' parts are shown in Table 1.

Table 1: Dimensions of different parts

Name	Dimension	Length (mm)	Width(mm)	Thickness(mm)
Web-Plate		745	60	16
Flange base plate		560	60	60
Cover plate		640	300	50
Backup plate		300 and 120	280 and 60	60
Clamping angle		670 and 140	298	40 and 70

2.3.2 Test Setup and Specimen's structural design:

Nominal Capacity of the fillet Weld compared with the Web-plate yield strength.

Weld capacity of leg sizes of 16mm, 12mm, 10mm and 8mm according to NZS3404 are as follows:

Leg size 16mm:

$$V_w = 0.6 \times f_{uw} \times t_t \times K_\gamma = 0.6 \times 490000 \text{ kN/m} \times 0.016 \text{ m} \times \cos 45^\circ \times 1 \\ = 3326 \text{ kN/m}$$

Weld capacity of $F_{w16} = 2 \times V_w \times L_w = 2 \times 3326 \times 0.06 = 399.32 \text{ kN/m} < 1000 \text{ kN}$ hence, the actuator capacity is higher than that of weld, according to NZS3404

V_w : nominal capacity per unit length of weld

L_w : longitudinal length of the weld

t_t : design throat thickness

Leg size 12mm:

Weld capacity of $F_{w12} = 299.27 \text{ kN/m}$

Leg size 10mm:

Weld capacity of $F_{w10} = 249.39 \text{ kN/m}$

Leg size 8mm:

Weld capacity of $F_{w8} = 199.52 \text{ kN/m}$

2.3.2.1 Web-plate tensile yield strength (G300):

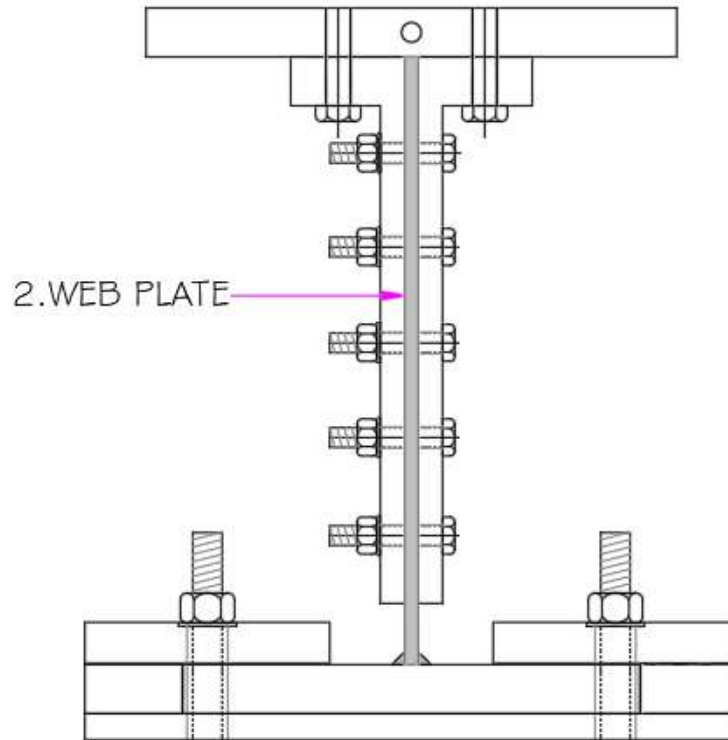


Figure 15: Web plate

Web plate normal section capacity (excluding strength reduction factor of $\phi=0.9$):

$$N = f_y \times A = 300 \div 1000 \times (0.06 \times 1000) \times (0.016 \times 1000) = 288\text{kN}$$

Equation 4: Steel nominal (i.e. unfactored) section capacity in NZS3404

$f_y=f_{yp}$: metal yield strength

A: normal cross section area of the web plate

Web-plate tensile capacity (gross and net):

Design tension capacity:

$$\begin{aligned} N_t &= 0.9 \times A_g \times f_y = 0.9 \times (0.06 \times 1000) \times (0.016 \times 1000) \times 300 \div 1000 \\ &= 259.2\text{kN} \end{aligned}$$

Equation 5: Design section capacity in NZS3404

$$F_{w16} = 399.32\text{kN} > F_{w12} = 299.27\text{kN} > F_{w10} = 249.39\text{kN} > F_{w8} = 199.52\text{kN}$$

259.2kN is Web plate design capacity in tension which is between 12mm and 10mm fillet welds capacity

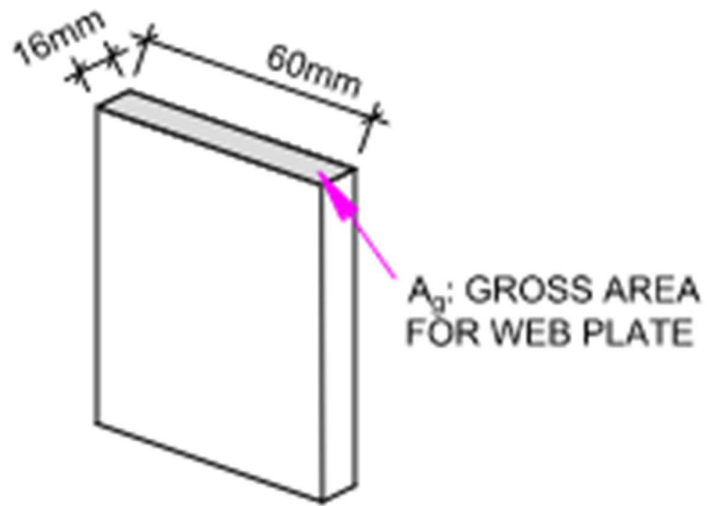


Figure 16: Web plate A_g area

A_g : the gross area of the cross section

2.3.2.2 Clamping angle Capacity(G250) :

2.3.2.2.1 Friction between the clamping angles and the Web-plate:

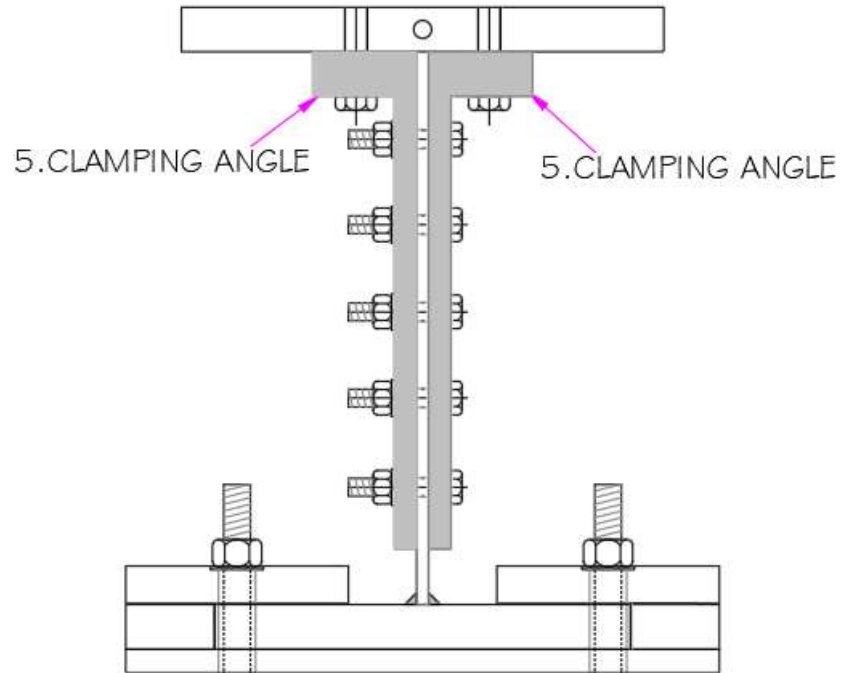


Figure 17: Clamping angle

Friction between clamping angle and web-plate under TF mode:

5M24 Bolts

$$F = 0.3 \times n \times 2 \times T = 0.3 \times 10 \times 2 \times 210 = 1260\text{kN} > F_{w16} = 399.32\text{kN}$$

$$F = 0.3 \times 8 \times 2 \times T = 1218\text{kN} > F_{w16} = 399.32\text{kN}$$

T = 203kN (Assumed if M20, 10.9 Class are used, as in some tests.)

Where:

0.3: assumed coefficient of friction

n: number of bolts bolting the clamping angles and the web plate

T: minimum bolt tension according to NZS3404: Part1: 1997, Table 15.2.5.1, fully tensioned M24: 210 kN,

2.3.2.2.2 Tensile capacity (gross and net):

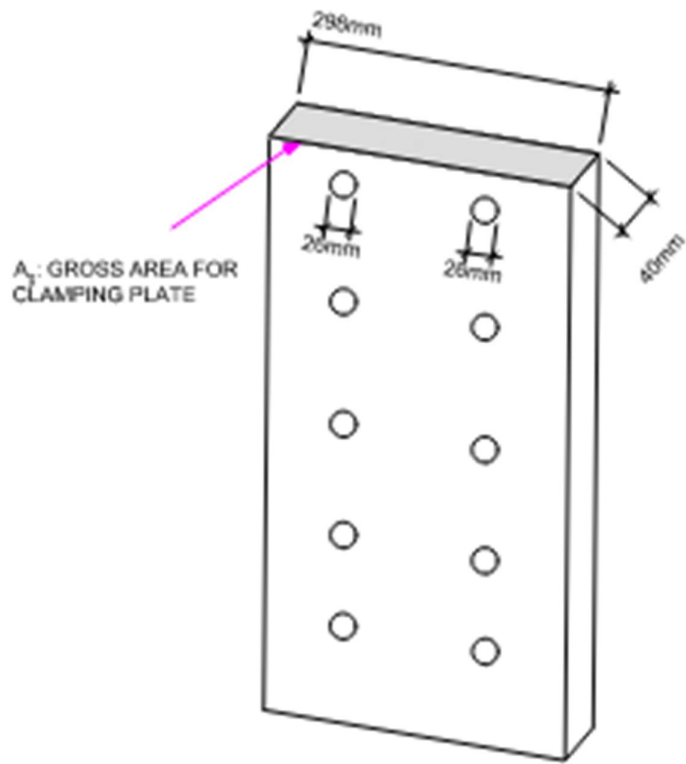


Figure 18: Clamping angle A_g area

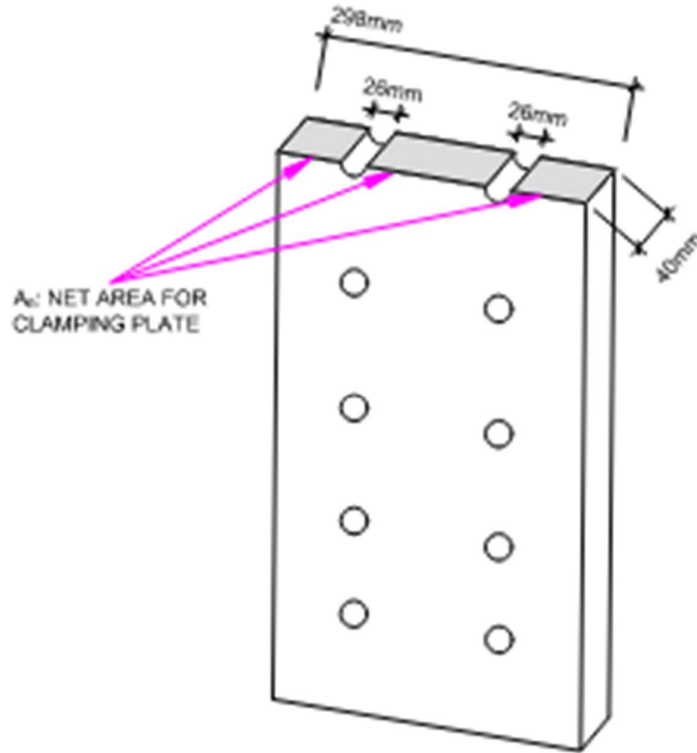


Figure 19: Clamping angle A_n area

250 GRADE STRUCTURAL STEEL PLATE

AS/NZS 3678 - 250

GENERAL DESCRIPTION

A high strength structural steel product with 250MPa nominal yield strength.

TYPICAL USES

- General fabrication
- Structural members
- High-rise buildings
- Bridges
- Storage tanks

KEY FEATURES

- Guaranteed minimum strength levels
- Excellent weldability
- Excellent formability

CUSTOM RANGE

The Calibre Steel custom range offers flexible order quantities and a wide variety of grade and size combinations ordered to specification on a standard mill lead-time.

Optional mechanical testing options are available upon enquiry.

Tensile Properties (Transverse)		Thickness [mm]					
		$t \leq 8$	$8 < t \leq 12$	$12 < t \leq 20$	$20 < t \leq 25$	$25 < t \leq 80$	$80 < t \leq 100$
Yield Strength [MPa]	Guaranteed Min	280	260	250	240	230	230
	Typical	290-480	260-360	260-380	250-370	240-370	240-340
Tensile Strength [MPa]	Guaranteed Min	410	410	410	410	410	410
	Typical	420-540	420-500	420-510	440-520	440-510	450-510

Stocked Range		
Thickness [mm]	Width [mm]	Length [mm]
6	2400	6000
	2400	9000
	3000	9000
8	2400	6000
	3000	9000
	3200	12000
10	2400	6000
	3000	9000
	3200	12000
12	2400	6000
	3000	9000
	3200	12000

Stocked Range		
Thickness [mm]	Width [mm]	Length [mm]
16	2400	6000
	3000	9000
20	2400	6000
	3000	9000
25	2400	6000
	3000	9000
32	2400	6000
	40	6000
50	2400	6000

Custom Size Guidelines		
Width [mm]	Thickness [mm]	Length [m]
1300mm to 3200mm in multiples of 100mm (e.g. 1300mm, 1400mm...3200mm)	6, 8, 10, 12, 16, 20, 25, 28, 32, 36, 40, 45, 50, 55, 60, 70, 80, 90, 100, 110, 120, 140, 150, 160, 170, 180, 190, 200	<p>8mm to 12mm thick: 4.0m to 12.0m in increments of 0.1m (e.g. 4.0m, 5.1m, 6.3m...25.0m)</p> <p>>12mm to 32mm thick: 4.0m to 13.5m in increments of 0.1m (e.g. 4.0m, 5.1m...25.0m)</p> <p>>32mm thick: 2.4m to 13.5m in increments of 0.1m (e.g. 2.4m, 4.1m, 5.1m...25.0m)</p>

Figure 20: 250 Grade steel data sheet

The clamping angle normal section tensile capacity across the plate (Two clamping angles – gross section capacity and net section capacity):

$$N_t = 0.9 \times A_g \times f_y = 0.9 \times (0.04 \times 1000) \times (0.298 \times 1000) \times 230 \div 1000 \times 2 = 4934.88 \text{ kN OK}$$

or

$$0.9 \times 0.85 \times k_{et} \times A_n \times f_{up} = 0.9 \times 0.85 \times 0.75 \times [(0.298 - 2 \times 0.026) \times 1000] \times (0.04 \times 1000) \times 410 \div 1000 \times 2 = 4629.47 \text{ kN OK}$$

Equation 6: Nominal section capacity of a tension member in NZS3404

Load factor: 1.5 for a safe design

1500kN dynamic actuator < 4968.21kN

Clamping angle would not fail, and this was obviously expected compared with web plate capacity.

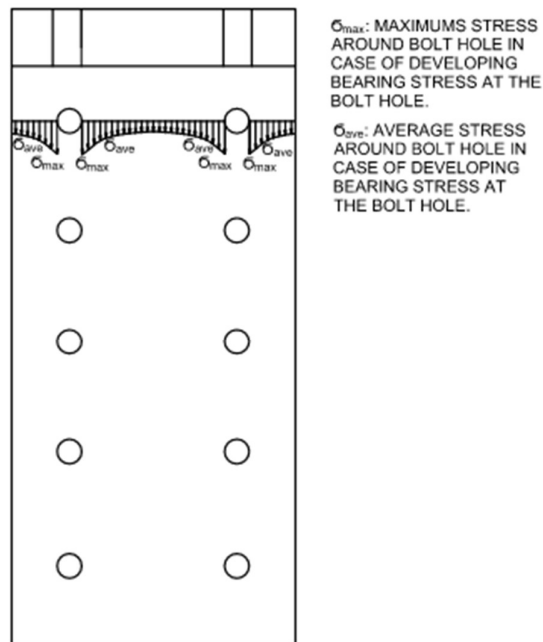


Figure 21: Clamping angle stress distribution around bolt hole

In case of developing bearing stress at the bolt hole:

$$\sigma_{ave} = (1500 \div 2) / [(0.298 - 2 \times 0.026) \times 0.04 \times 2 \times 1000] = 37.71 \text{ MPa} < 230 \text{ MPa}$$

The maximum stress around the bolt hole in case of developing bearing:

$$\sigma_{max} = 3 \times 37.71 = 113.13 \text{ MPa} < 230 \text{ MPa}$$

hence yielding in clamping angles will not occur.

3: assumed maximum stress magnification factor around the holes

A_g : the gross area of the cross section

K_{te} : the correction factor for distribution of forces

A_n : the net area of the cross section.

f_{up} : the tensile strength

2.3.2.2.3 Check the applied moment generated by tensioned bolts on clamping angle:

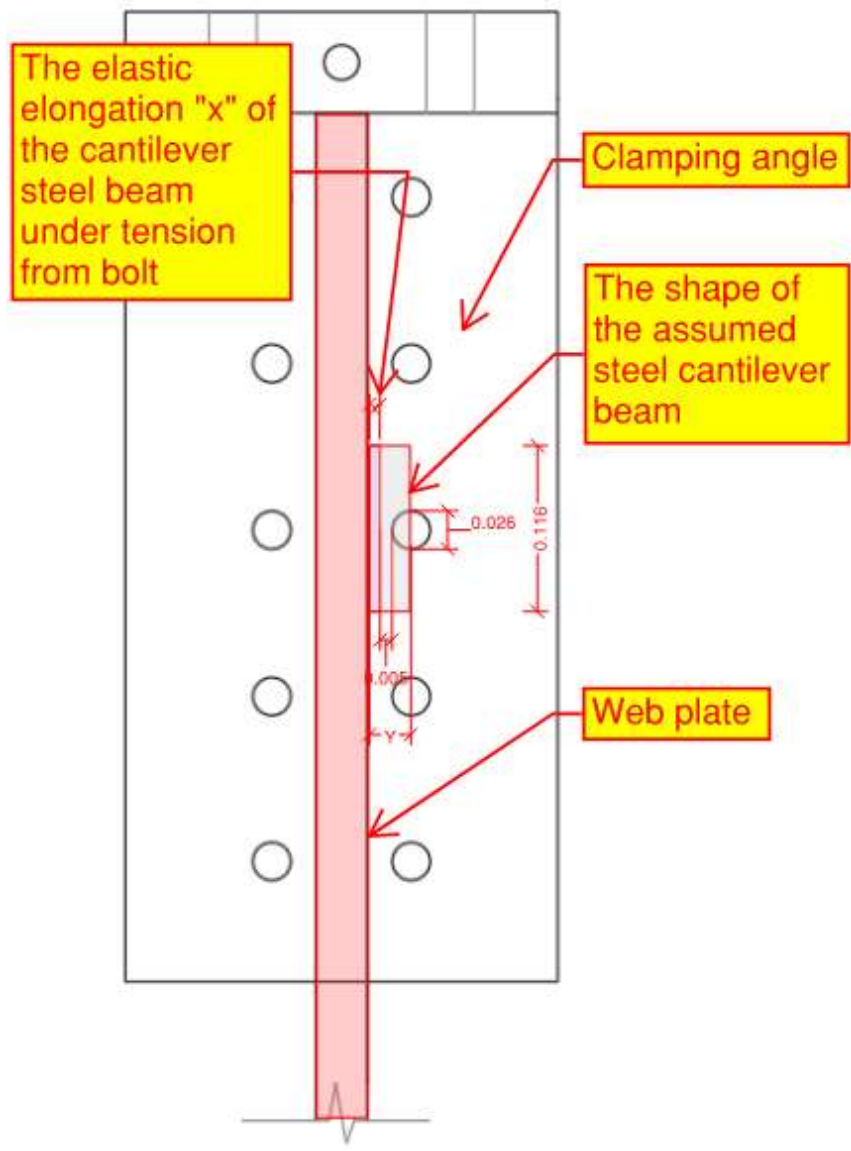


Figure 22: Dimensions for the steel cantilever part in calculation-front view

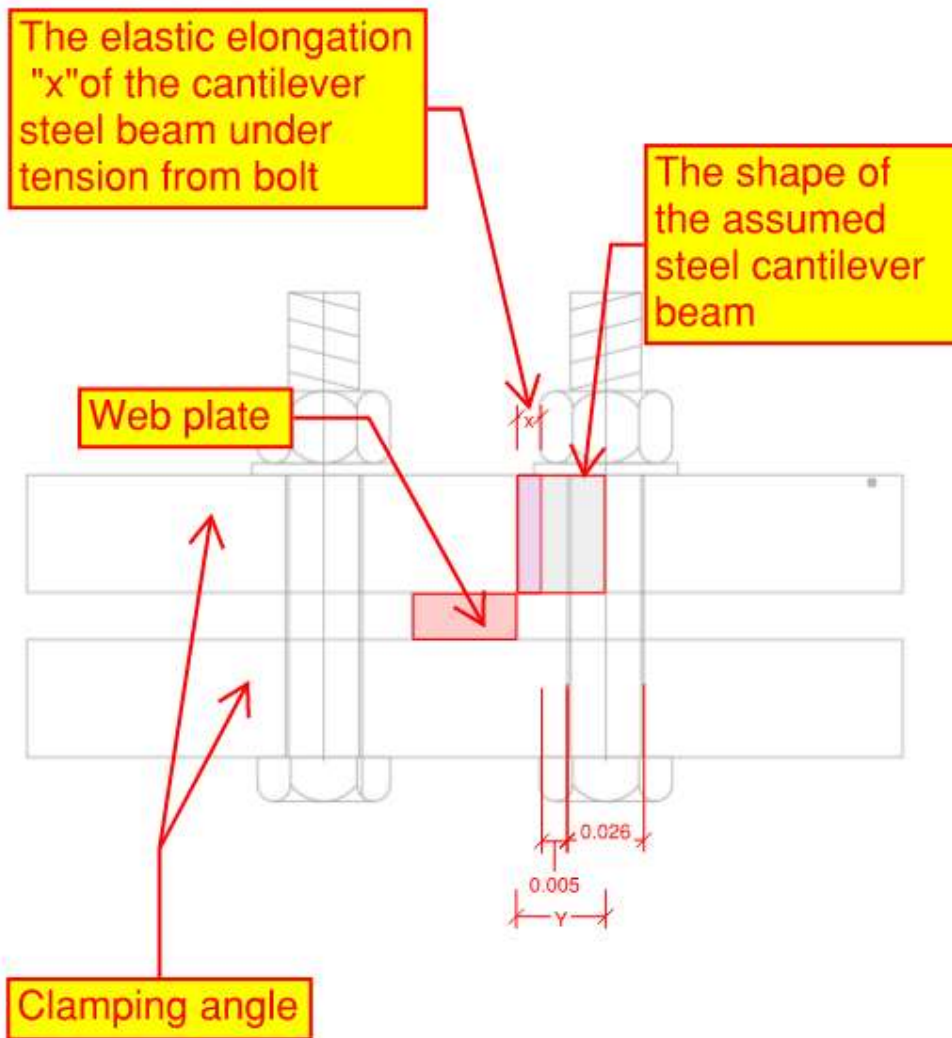


Figure 23: Dimensions for the steel cantilever part in calculation-inside view

Bending moment induced stress:

$$f_y = 230 \text{ (G250 steel)}$$

Y: the length of the cantilever beam which from the edge of the web plate to the centre of the M24 bolt

x: the elastic elongation of the cantilever steel beam under tension force.

0.005mm: the distance from web plate to bolt hole (edge to edge)

0.026mm: the bolt hole diameter

$1.25f_y$: yield capacity for yield area

210kN: tension stress for M24 structural 8.8 bolt

200kN: tension stress for M20 structural 10.9 bolt

For:

When the stem is 60mm, the linear equation in two unknowns is as below:

$$Y = x + 0.005 + 0.026 \div 2$$

$$116 \times x \times 1.25 \times f_y = 210$$

The result of x and y:

$$x = 0.0058\text{mm} \approx 0.006\text{mm}$$

$$Y = 0.024\text{mm}$$

When the stem is up to 80mm, the linear equation in two unknowns is as below:

$$Y = x + 0.005 + 0.016$$

$$116 \times x \times 1.25 \times f_y = 200$$

The result of x and y:

$$x = 0.005\text{mm}$$

$$Y = 0.026\text{mm}$$

Case 1: when b is full size neglecting bolt hole:

Treat every bolt as 115mm wide, 24mm length cantilever beams.

$$Z_e = b \times \frac{d^2}{6} = 0.115 \times \frac{0.04^2}{6} = 3.07 \times 10^{-5}$$

Equation 7: The effective section modulus calculation

Elastic bending moment capacity for each:

$$\begin{aligned} \phi M_s &= \phi \times f_y \times Z_e = 0.9 \times 230 \div 1000 \times 3.07 \times 10^{-5} \times 1000 \times 1000 \\ &= 6.36\text{kN.m} \end{aligned}$$

Equation 8: Normal section moment capacity in NZS3404

$$M^* = \phi N_{tf} \times L = 210 \text{ (M24 Full tension)} \times 0.024 = 5.04\text{kN.m}$$

$$M^* = \phi N_{tf} \times L = 200 \text{ (M20 Full tension)} \times 0.026 =$$

$$5.2\text{kN.m} \text{ (Assume the stem is 80mm)}$$

$$\phi M_s > M^* \text{ ok}$$

ϕM_s : section moment capacity

Z_e : the effective section modulus (elastic)

M^* : the design bending moment of the plate

L: force lever arm

ϕN_{tf} : axial tension capacity according to NZS3404: Part1: 1997, Table 15.2.5.1, fully tensioned.

Case 2: when b is including the bolt hole loss of area:

Treat every bolt as 115mm wide, 24mm length cantilever beams.

$$b = 115 - 26 = 89\text{mm}, d = 40\text{mm}$$

$$Z_e = b \times \frac{d^2}{6} = 0.089 \times \frac{0.04^2}{6} = 2.37 \times 10^{-5}$$

Elastic bending moment capacity for each:

$$\begin{aligned}\phi M_s &= \phi \times f_y \times Z_e = 0.9 \times 230 \div 1000 \times 2.37 \times 10^{-5} \times 1000 \times 1000 \\ &= 4.9\text{kN.m}\end{aligned}$$

$$M^* = \phi N_{tf} \times L = 210 \text{ (M24 Full tension)} \times 0.024 = 5.04\text{kN.m}$$

$$M^* = \phi N_{tf} \times L = 200 \text{ (M20, 10.9 Full tension)} \times 0.026 = 5.2\text{kN.m}$$

$\phi M_s < M^*$ Not ok, but still close

Case 3: when b is including the bolt hole loss of area and using plastic mode:

$$b = 115 - 26 = 89\text{mm}, d = 40\text{mm}$$

$$Z_e = b \times \frac{d^2}{4} = 0.089 \times \frac{0.04^2}{4} = 3.56 \times 10^{-5}$$

Elastic bending moment capacity for each:

$$\begin{aligned}\phi M_s &= \phi \times f_y \times Z_e = 0.9 \times 230 \div 1000 \times 3.56 \times 10^{-5} \times 1000 \times 1000 \\ &= 7.36\text{kN.m}\end{aligned}$$

$$M^* = \phi N_{tf} \times L = 210 \text{ (M24 Full tension)} \times 0.024 = 5.04\text{kN.m}$$

$$M^* = \phi N_{tf} \times L = 200 \text{ (M20 Full tension)} \times 0.026 = 5.2\text{kN.m}$$

$\phi M_s > M^*$ ok

Check combined shear and bending to NZS3404, clause 5.12.2:

From the results above, $\phi M_s = 4.9\text{kN.m}$ is the worst case but still very close to $M^* = 5.04\text{kN.m}$. Use $\phi M_s = 5.04\text{kN.m}$ for checking:

For $0.75\phi M_s \ll M^* \ll \phi M_s$

$$V_{vm} = V_v \times \left[2.2 - \left(\frac{1.6 \times M^*}{\phi M_s} \right) \right] = 244\text{kN} > 210\text{kN Ok}$$

Equation 9: Calculation of nominal web shear capacity in the presence of bending moment in NZS3404

Shear strength of each:

According to NZS3404, clause 5.11.3:

For

$$V_{vn} = \frac{2V_{vu}}{0.9 + \left(\frac{f_{vm}^*}{f_{va}^*}\right)} \ll V_{vu}$$

Equation 10: Calculation of nominal shear capacity of a flat plate with non-uniform shear stress distribution in NZS3404

$$\frac{f_{vm}^*}{f_{va}^*} = 1.5$$

$$\begin{aligned} V_{vu} &= 0.6 \times f_y \times A_W = 0.6 \times 230 \div 1000 \times 0.116 \times 1000 \times 0.04 \times 1000 \\ &= 640.32\text{kN} \end{aligned}$$

$$\text{So: } V_{vn} = \frac{2V_{vu}}{0.9 + \left(\frac{f_{vm}^*}{f_{va}^*}\right)} = 0.83V_{vu} = 531.47\text{kN} \quad \text{Ok!}$$

V_{vu} = the nominal shear capacity of the flat plate calculated assuming a uniform shear stress distribution, from 5.11.2

f_{vm}^*, f_{va}^* = the maximum and average design shear stresses in the web determined by a rational elastic analysis.

V_{vn} = nominal shear capacity of a flat plate with non-uniform shear stress distribution (5.11.3)

f_y : yield stress.

A_W : gross sectional area of the web.(Use net area for conservative purpose here.)

2.3.2.2.4 Bearing check (In case of developing bearing):

The clamping angles bearing capacity (Shahab Ramhormozian, 2020a):

$$\begin{aligned} \phi V_b &= \phi \times 3.2 \times f_{up} \times d_f \times t_p = 0.9 \times 3.2 \times 370(250 \text{ Grade form}) \div 1000 \times \\ &(2 \times 0.024 \times 1000) \times (0.04 \times 1000) \times 2 = 4092\text{kN, ok} \end{aligned}$$

Equation 11: Steel ply in a bolted connection in bearing in NZS3404

1500kN dynamic actuator's factored load <

4866.05kN Bearing failure will not occur

d_f : diameter of the bolt

t_p : thickness of the ply

Tear-out check (In case of developing):

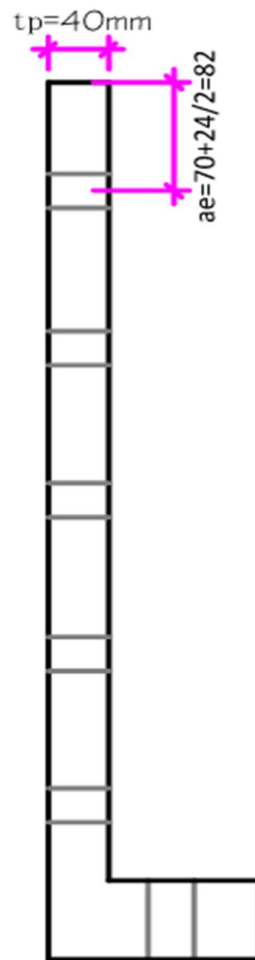


Figure 24: Clamping angle a_e , t_p dimension

The clamping angle tear-out capacity:

$$\phi V_b = \phi \times a_e \times t_p \times f_{up} \times 2 = 0.9 \times (0.083) \times 1000 \times (0.04 \times 1000) \times 370 \div 1000 \times 2 \times 2 = 4422.24 \text{ kN} \quad \text{ok}$$

Equation 12: Steel ply in a bolted connection in tearout in NZS3404

1500kN dynamic actuator's factored load < 4422.24kN

Clamping plate tearout fracture will not occur

a_e : minimum distance from the edge of a hole to the edge of a ply + half the bolt diameter.

2.3.2.2.5 Tensile yield capacity underfriction mode at the critical cross section:

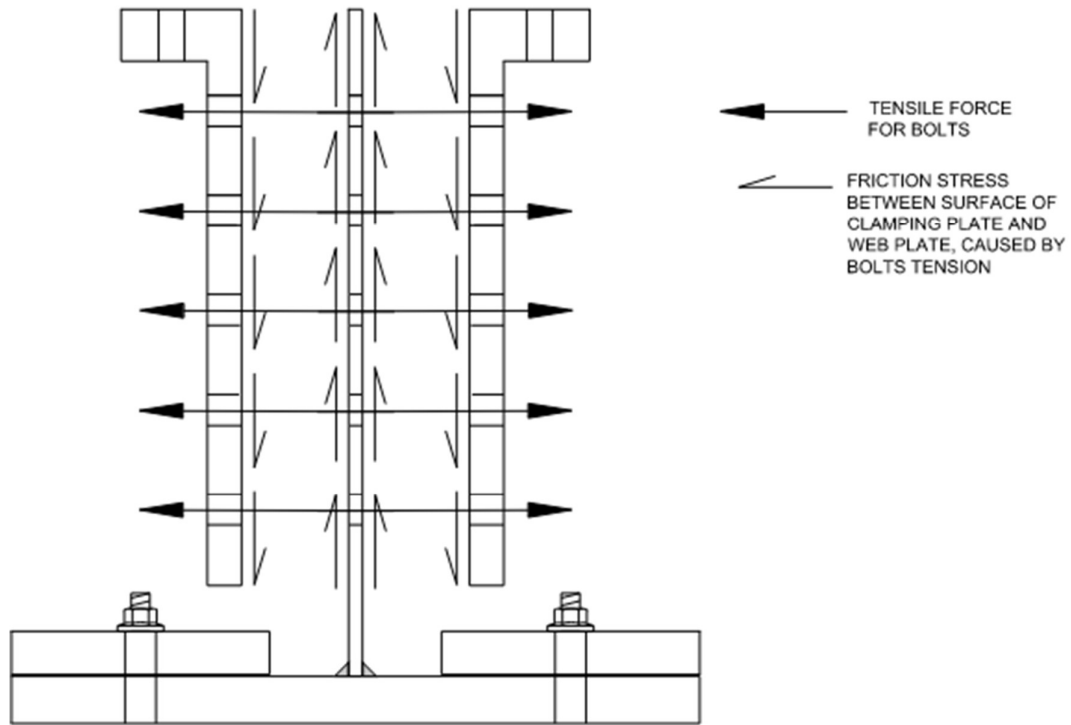


Figure 25: Clamping angle under tension-friction mode

Maximum friction force:

$$F = 0.3 \times n \times 2 \times T = 0.3 \times 10 \times 2 \times 210 = 1260\text{kN}$$

0.3: assumed coefficient of friction

n: number of bolts

T: minimum tension of the fully tensioned bolts

$$F = 1260\text{kN} > \text{Maximum strength: } F_{w16} = 391.28\text{kN}$$

Using 1000kN dynamic actuator capacity for Uniformly Distributed Friction force.

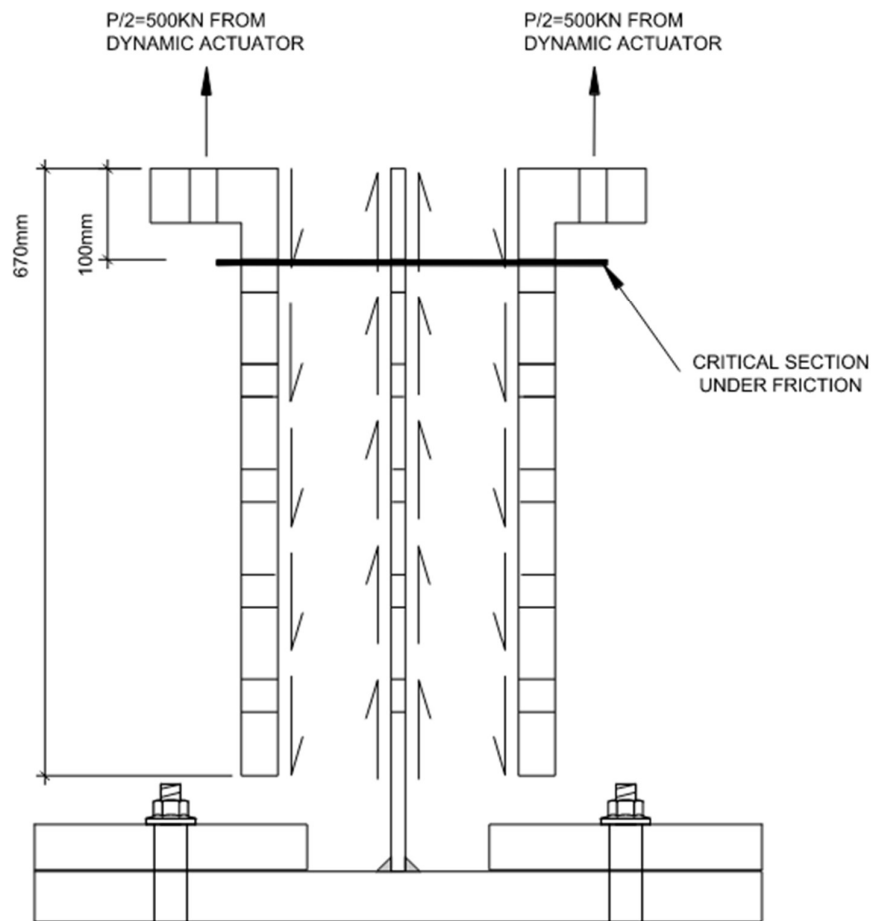


Figure 26: Critical section of clamping angle under tension-friction mode

Maximum design friction force on clamping angle (see Figure 26):

$$F = (P - \text{Friction force above the critical cross section}) \div 2 = (1000 - 1000 \div (100 \times 670)) \div 2 = 425.38\text{kN}$$

The average stress in clamping angle caused by friction at the critical cross section:

$$\sigma_{ave} = \frac{F}{A_n} = 425.38 \div (0.298 \times 0.04 - 2 \times 0.026 \times 0.04) \div 1000 =$$

$$43.23\text{MPa} < 230\text{MPa steel yield strength} \quad \text{OK}$$

The maximum stress in clamping angle caused by friction at the critical cross section:

$$\sigma_{max} = 3 \times 43.23 = 129.69\text{MPa} < 230\text{MPa steel yield strength} \quad \text{OK}$$

3: assumed maximum stress distributing number

2.3.2.2.6 Clamping angle's short leg connected to the actuator:

Shear strength of each:

According to NZS3404, clause 5.11.3:

For

$$V_{vn} = \frac{2V_{vu}}{0.9 + \left(\frac{f_{vm}^*}{f_{va}^*}\right)} < V_{vu}$$

$$\frac{f_{vm}^*}{f_{va}^*} = 1.5$$

$$\begin{aligned} V_{vu} &= 0.6 \times f_y \times A_W \\ &= 0.6 \times 230 \div 1000 \times (0.298 - 0.033 \times 2) \times 1000 \times 0.07 \times 1000 \\ &= 1920.96 \text{ kN} \end{aligned}$$

$$\text{So: } V_{vn} = \frac{2V_{vu}}{0.9 + \left(\frac{f_{vm}^*}{f_{va}^*}\right)} = 0.83V_{vu} = 1594.40 \text{ kN Ok!}$$

V_{vu} = the nominal shear capacity of the flat plate calculated assuming a uniform shear stress distribution, from 5.11.2

f_{vm}^*, f_{va}^* = the maximum and average design shear stresses in the web determined by a rational elastic analysis.

V_{vn} = nominal shear capacity of a flat plate with non-uniform shear stress distribution (5.11.3)

f_y : yield stress.

A_W : gross sectional area of the web. (Use net area for conservative purpose here.)

Bending moment induced stress:

$$Z_e = b \times \frac{d^2}{6} = 0.298 \times \frac{0.07^2}{6} = 24.34 \times 10^{-5}$$

Elastic bending moment capacity for each:

$$\begin{aligned} \Phi M_s &= \Phi \times f_y \times Z_e = 0.9 \times 230 \div 1000 \times 24.34 \times 10^{-5} \times 1000 \times 1000 \\ &= 48.32 \text{ kN.m} \end{aligned}$$

Maximum expected bending moment during the test for each:

$$M^* = 750 \times L = 750 \times (0.14 - 0.058 - 0.04/2) = 46.5 \text{ kN.m}$$

$$\Phi M_s = 48.32 \text{ kN.m} > M^* = 46.5 \text{ kN.m OK}$$

ΦM_s : section moment capacity

Z_e : the effective section modulus (elastic)

M^* : the design bending moment of the plate.

$L1$: the distance from the bolt centre to the centreline of the long leg as Figure 27 shows.

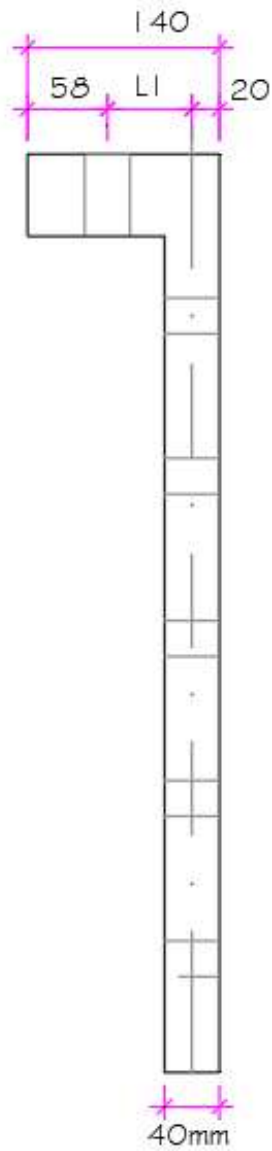


Figure 27: Dimension $L1$

Tension capacity of the 4 M30 bolts connecting clamping angles to the actuator:

$4 \times M30$ (Proof load: $\phi N_{tf} = 373\text{kN}$):

$$4 \times \phi N_{tf} = 4 \times 373 = 1492\text{kN}$$

$> 1500\text{kN}$ dynamic actuator capacity within 1% OK

ϕN_{tf} : axial tension capacity of a bolt

2.3.2.3.7 Clamping angle capacity conclusions:

Normal section design tensile capacity= 4934.88 kN > Net design tensile

capacity=4629.47kN > Tear-out strength=4422.24 kN > Bearing capacity=4092kN

Average bearing tensile stress around the critical bolt hole: 37.71Mpa < 230MPa

Maximum bearing tensile stress around the critical bolt hole: 113.13Mpa < 230MPa

Average friction tensile stress around the critical bolt hole: 43.23Mpa < 230MPa

Maximum friction tensile stress around the critical bolt hole: 129.69Mpa < 230MPa

Bending moment capacity: $\emptyset M_s = 48.32 \text{ kN} \cdot \text{m} > M^* = 46.5 \text{ kN} \cdot \text{m}$

Bolts tension capacity between clamping angle and actuator endplate: 1492kN

Hence the clamping angles remain elastic under any conditions and the bolts are always loaded below their capacities.

2.3.2.3 Cover Plate:

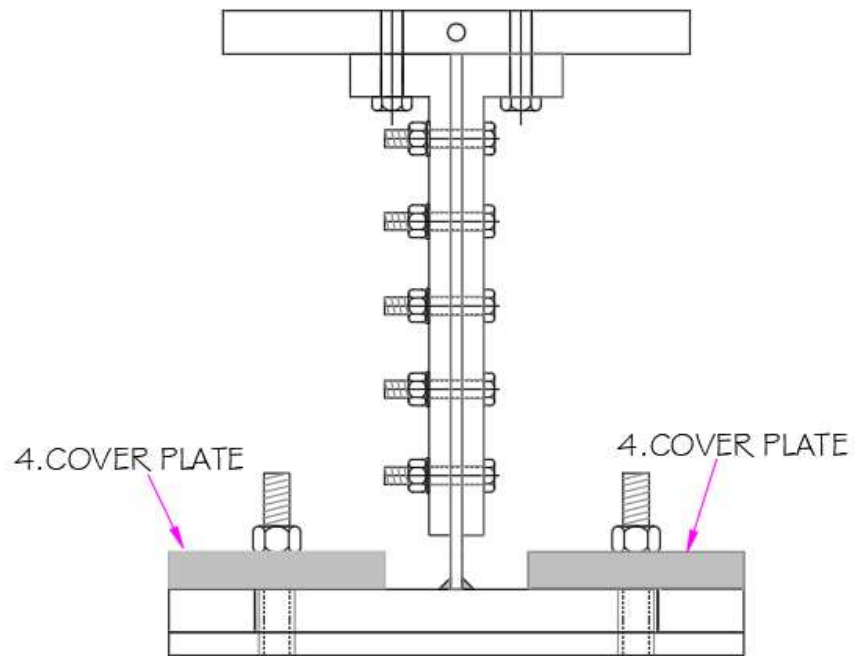


Figure 28: Cover plate

Bolts:

Tension capacity of 4×M36 bolts on cover plate:

4 × M36(from table 9.1.3; $\phi N_{tf} = 541\text{kN}$):

$4 \times \phi N_{tf} = 4 \times 541 = 2164\text{kN} > 1000\text{kN}$ dynamic actuator capacity OK

ϕN_{tf} : axial tension capacity

Cover plate bolts capacity conclusion:

Tensile capacity from bolts=2164kN >1000kN dynamic actuator capacity

2.3.2.4 Out of plane capacity based on yieldline theory

2.3.2.4.1 Checking cover plate elastic and plastic strength based on yieldline theory

(Civil 313 Yieldline Theory and Application: 2016):

Case 1 complete Tee stud yielding checking:

Yieldline theory equation for case 1:

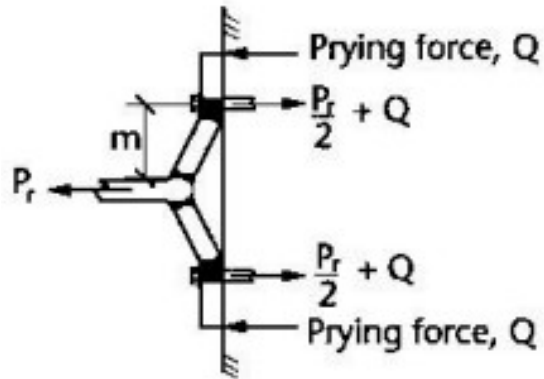


Figure 29: Yieldline theory case 1: Complete Tee stud yielding

$$m_p = t_p^2 \times f_{yp} / (6 \text{ or } 4) \text{ (elastic or plastic moment per unit width)}$$

$$P_r = m_p \times 4b \div m$$

m : distance from bolt centre to 20% distance into column or end plate weld

Yieldline theory strength checking:

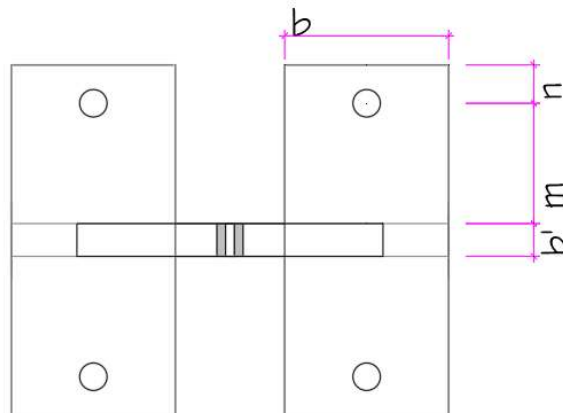


Figure 30: Cover plate yieldline theory dimension

$$m = (0.64 - 0.06) \div 2 - 0.07 = 0.22m$$

m : the distance from bolt center to 20% distance into column root or end plate weld

$$m_p = t_p^2 \times f_{yp} \div 6 = 0.05 \times 0.05 \times 300 \times 1000/6 = 125 \text{ kN.m} \text{ – elastic}$$

$$m_p = t_p^2 \times f_{yp} \div 4 = 0.05 \times 0.05 \times 300 \times 1000/4 = 187.5 \text{ kN.m} \text{ – plastic}$$

m_p : bending moment per unit length.

$$P_r = m_p \times 4 \times \frac{b}{m} = 2 \times 125 \times 4 \times (0.18 + 0.03) \div 0.22 =$$

$$954.54 \text{ kN (2 cover plates)} > F_{w16} = 391.28 \text{ kN} \text{ OK}$$

Case 2 bolt stretching with flange yielding checking:

Yieldline theory equation for case 2

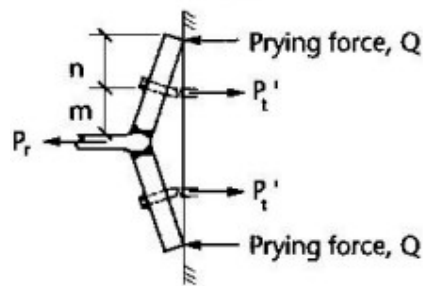


Figure 31: Yieldline theory case 2: Bolt stretching with flange yielding

$$M_p = m_p \times L_{\text{eff}}$$

M_p : elastic or plastic capacity

L_{eff} : effective length of yield line in equivalent T – stub

$$P_r = \frac{(2 \times m_p \times b + n \times \sum p_t)}{n + m}$$

Yieldline theory strength checking:

$$n = 0.07 \text{ m}$$

n : the effective edge distance

$$b = 0.24 \text{ m}$$

b : the yield line length

$$2 \times \frac{(2 \times m_p \times b + n \times \sum p_t)}{n + m} = 2 \times (2 \times 125 \times 0.24 + 0.07 \times 541) \div (0.07 + 0.22) =$$

$$623.24 \text{ kN (2 cover plate)} > F_{w16} = 391.28 \text{ kN} \text{ OK}$$

Case 3 bolt stretching with no flange yielding:

4 bolts tension capacity is checked already.

2.3.2.4.2 Flange base plate strength based on yieldline theory (G300):

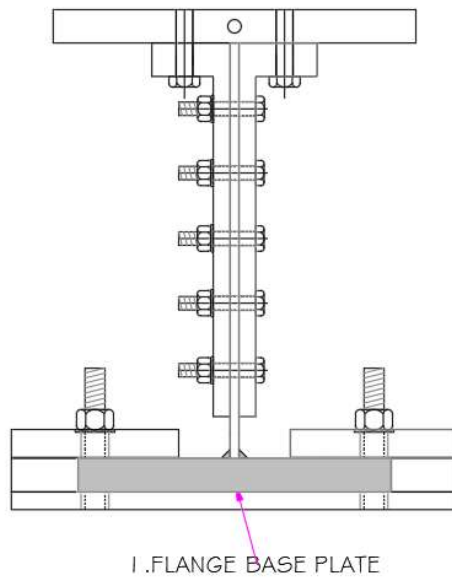


Figure 32: Flange base plate

Case 1: complete Tee stub yielding check:

(Girao Coelho, 2006) presents the same Tee stub yielding check as illustrated in the figure below in the article.

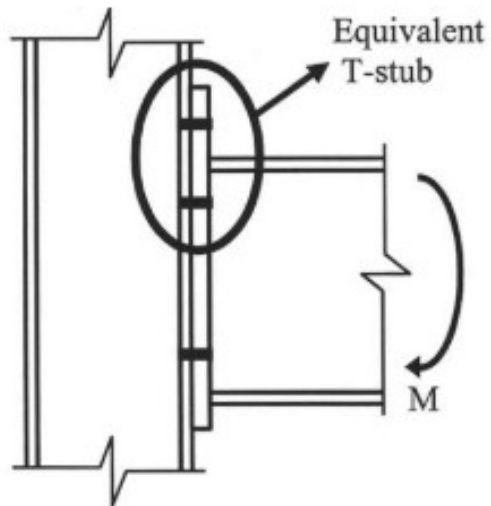


Figure 33: T-stub identification and orientation (Girao Coelho, 2006)

The same principle applies to these dimensions related to the yielding check, as illustrated in Figure 34 below.

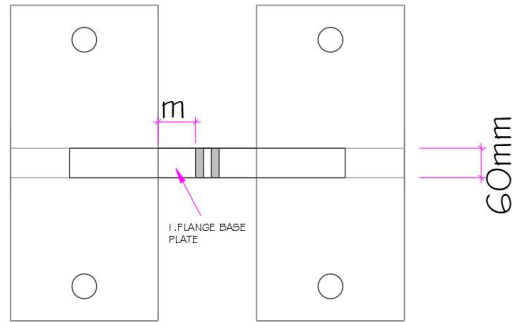


Figure 34: Flange base plate yieldline theory dimension

$$m = (0.8 - 0.016 - 0.016 \times 2) \div 2 - 0.3 = 0.076m$$

$$m_p = tp^2 \times f_{yp} \div 6 = 0.060 \times 0.060 \times 300 \times 1000 / 6 = 179.70 \text{ kN.m}$$

$$m_p \times 4 \times \frac{b}{m} = 179.70 \times 4 \times 0.06 \div 0.076 = 567.66 \text{ kN} > F_{w16}$$

$$= 391.28 \text{ kN OK}$$

2.3.2.4.3 Clamping angle strength based on yieldline theory (G250):

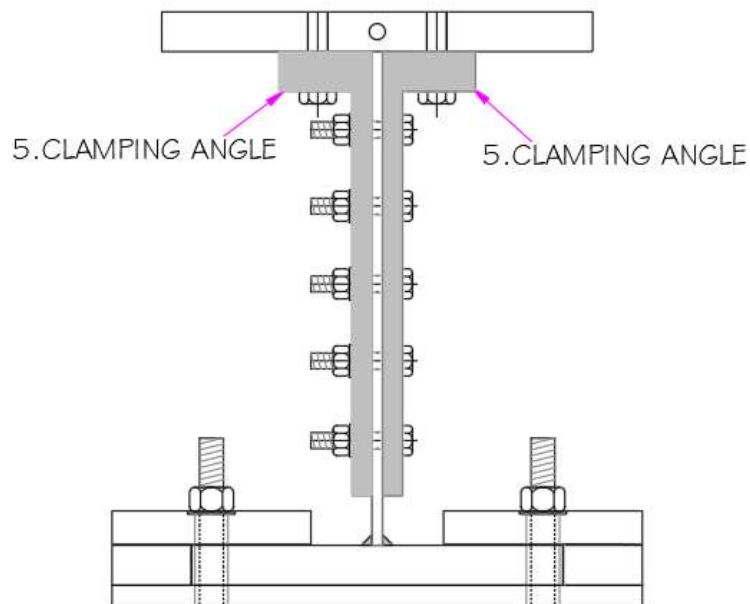


Figure 35: Clamping angle

Case 1 complete Tee stub yielding:

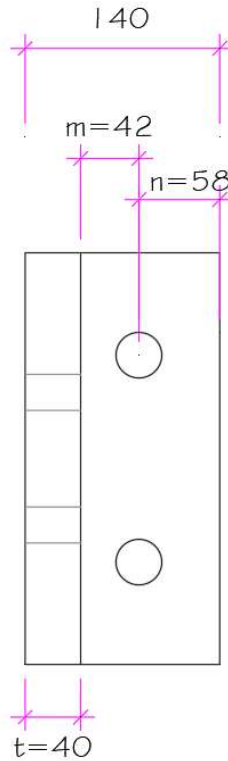


Figure 36: Dimensions of the clamping angle base plate in yieldline theory

$$m = 0.14 - 0.058 - 0.04 = 0.042m$$

$$b = 0.298m$$

m: the distance from bolt center to 20% distance into column root or end plate weld

$$m_p = tp^2 \times f_{yp} \div 6 = 0.07 \times 0.07 \times 230 \times \frac{1000}{6} = 187.83 \text{ kN.m for elastic}$$

m_p : bending moment per unit length.

$$P_r = m_p \times 4 \times \frac{b}{m} = 187.83 \times 4 \times 0.298 \div 0.042 = 5330.88kN >$$

1500kN dynamic actuator OK

Case 2 bolt stretching with flange yielding checking:

$$n = 0.058m$$

n: the effective edge distance

$$b = 0.298m$$

b: the yield line length

$$\Sigma p_t = \text{Total tension capacity for all the bolts in the groups}$$

$$\frac{(2 \times m_p \times b + n \times \Sigma p_t)}{n+m} = (2 \times 187.83 \times 0.298 + 0.058 \times 335 (\text{M30 bolt tension capacity}) \times 2) \div (0.058 + 0.042) = 1508.07 \text{ kN} > 1500 \text{ kN dynamic actuator capacity OK}$$

Case 3 bolt stretching with no flange yielding:

4 bolts tension capacity is checked already.

Clamping angle strength based on beam theory:

$$\text{Design bending moment: } M^* = P \div 2 \times (m + t) = 1500 \div 2 \times 0.082 = 31.5 \text{ kN.m}$$

("t" here stand for the thickness of the stem of the clamping angle)

$$\text{Bending capacity under elastic: } \emptyset M = \emptyset f_y \times b \times \frac{d^2}{6} = 0.8 \times 230 \times 0.298 \times 0.07 \times$$

$$0.07 \div 6 \times 1000 = 44.78 \text{ kN.m}$$

$$\emptyset M_s = 44.78 \text{ kN.m} > M^* = 31.5 \text{ kN.m Ok!}$$

$$\text{Bending capacity under elastic: } \emptyset M = \emptyset f_y \times b \times \frac{d^2}{6} = 0.8 \times 230 \times 0.274 \times 0.07 \times$$

$$0.07 \div 6 \times 1000 = 41.17 \text{ kN.m}$$

$$\emptyset M = 41.17 \text{ kN.m} > M^* = 41 \text{ kN.m}$$

Very close.

2.3.2.4.4 Clamping angle restraint against specimen buckling:

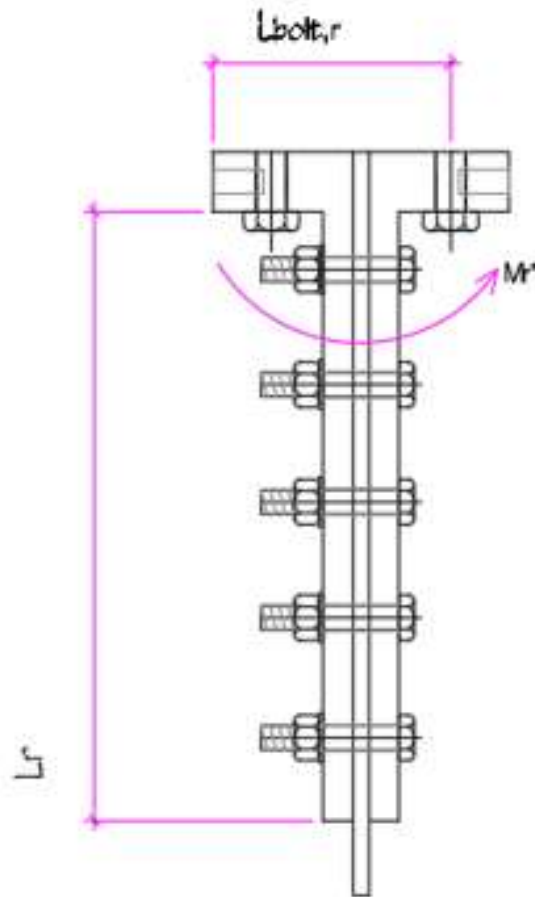


Figure 37: Clamping angle restraint against specimen buckling

$$L_r = 670 - 70 = 600\text{mm (Conservative)}$$

L_r : the length of the lever arm is 0.6m

The lateral holding strength needs to be 25% of normal strength to prevent buckling.
(New Zealand Standard, 1997).

$$M_r^* = 1000 \times 0.25 \times 0.6(L_r) = 15\text{kN.m}$$

Equation 13: Holding moment for lateral moment in NZS:3404

Check the additional force on M30 bolts (Tension)

$$N_{bolts,bottom}^* = \frac{15}{L_{bolt,r}} = \frac{15}{0.238} = 63\text{kN (on 2 bolts)}$$

$$L_{bolt,r} = 140 + 16 + 82 = 238\text{mm as per Figure 38}$$

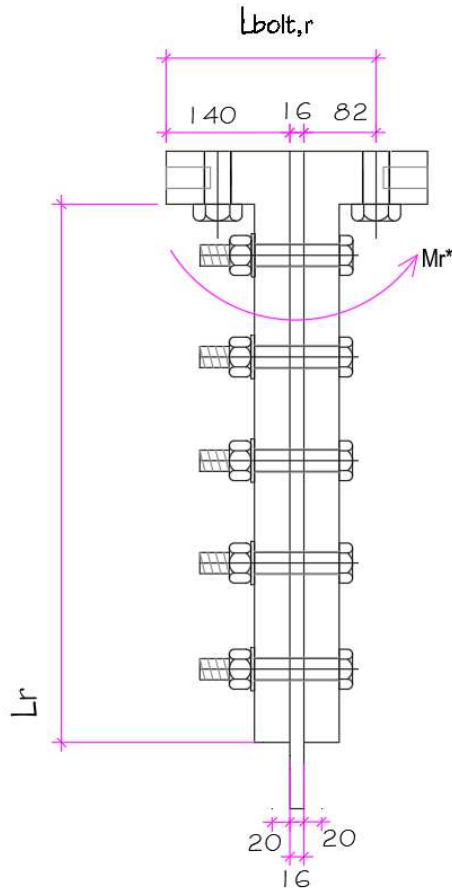


Figure 38: Dimensions used in the calculation.

However, this restraint applies when load in compression and in that direction, there is no external applied force on the bolts. The bolts will not go into tension due to restraint action.

Check long leg under restraint induces axial force:

$$N_{LL}^* = 15 / [(40/2 + 16 + 40/2) \times 10^{-3}] = 267.33 \text{ kN (Tension)}$$

$40/2$ is half of the thickness of the long leg clamping angle as Figure 38 shows.

16 is the thickness of the web plate as Figure 38 shows.

N_{LL}^* represents the force exerted on the long leg due to M_r^* ,

When N_{LL}^* is tension force, the compression force from the actuator will be diminished by this tensile force.

However, $N_{comp}^* = 500 \text{ kN/long leg (unfactored)}$

So adequate strength provided.

2.3.2.5 Check Web plate subject to compression(G300) (Shahab Ramhormozian, 2020b)

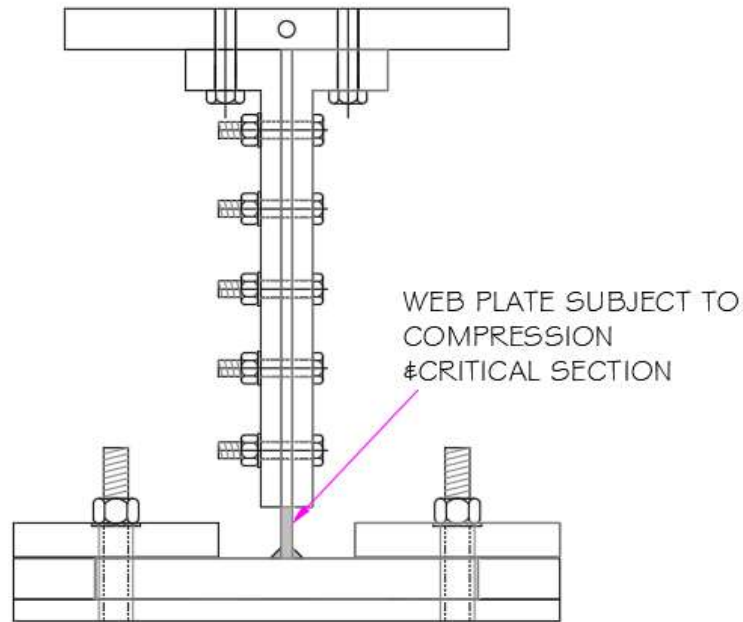


Figure 39: Web plate subject to compression (G300)

Step 1. Determining the effective length, L_e , for each axis of buckling for member design;

According to (Shahab Ramhormozian, 2020b)

$$L_y=75\text{mm}, L_{ey} = 0.7 \times 75 = 52.5\text{mm}$$

Equation 14: Effective length in NZS3404

L_e : effective length of a compression member.

L_y : member actual length about minor principal y – axis

Step 2. Calculate the slenderness ratio, L_e/r , for each axis of buckling where: $r^2 = I/A$

$$r_y^2 = \frac{I}{A} = \frac{60 \times 16^3 \div 12}{60 \times 16} = 21.33\text{mm}^2$$

Equation 15: Radius of gyration for y-axis in NZS3404

$$\frac{L_{ey}}{r_y} = 52.5 \div \sqrt{21.33} = 11.36$$

Equation 16: Slenderness ratio in NZS3404

Where:

r: radius of gyration

I: second moment of area of a (bare steel member) cross section

I_y: I about the cross section minor principal y-axis

Step 3. Assume the form factor:

$k_f = 1.0$ (The plate will not undergo local buckling prior to buckling out of plane.)

Where:

k_f : form factor for members subject to axial compression

Step 4. Calculate section capacity

$$N_s = k_f A_n \sigma_y = 1.0 \times (0.06 \times 1000) \times (0.016 \times 1000) \times 300 \div 1000 = 288kN$$

Equation 17: Nominal section capacity in NZS3404

Where:

N_s: nominal section capacity of a compression member

A_n: net area of a cross section at the connection

σ_y: yield strength

Step 5. Calculate modified slenderness ratio

$$\lambda_{ny} = \frac{L_{ey}}{r_y} \sqrt{k_f} \sqrt{\frac{f_y}{250}} = 11.36 \times \sqrt{1} \times \sqrt{\frac{300}{250}} = 12.45 \text{ (for buckling about y-axis = in x direction)}$$

Equation 18: Modified compression member slenderness in NZS3404

Where:

λ_n: modified compression member slenderness

Step 6. Select the member section constant, α_b

$k_f = 1.0, \alpha_b = 0$ (The default value for any compression member not covered by NZS3404: Table 6.3.3(1).)

Where:

α_b : compression member section constant

Step 7. Obtain the slenderness reduction factor α_c

From Table 6.3.3(2):

10 1.000

15 0.995

When $\lambda_{ny} = 12.45 \alpha_{cy} = 0.9976$

α_c : compression member slenderness reduction factor

Step 8. Calculate the nominal member axial force capacities

$$N_{cy} = \alpha_{cy} N_s = 0.9976 \times 288 = 287.31 \text{ kN}$$

Equation 19: Calculation for member axial force capacity in NZS3404

N_c : nominal member capacity in compression

The minimum, nominal member capacity, $N_c = 287.31 \text{ kN}$

Step 9. Check that $N^* \leq \phi N_s$, and $N^* \leq \phi N_c$

$N^* = 288 \text{ kN}$ (Web plate yield strength)

$$N^* = \phi N_s = 288$$

$$N^* \geq \phi N_c = 0.9 \times 287.31 = 258.58 \text{ kN}$$

$$\phi N_c = 258.58 \text{ kN is critical.}$$

Where:

$$\phi = 0.9$$

N^* : design axial force, compressive or tensile

N_s : nominal section capacity of a compression member

N_c : nominal member capacity in compression

Conclusion:**The test setup members (without web plate):**

Expected modes of failure of the experiments based on the structural design.

All parts of the test setup, except the web plate and/or fillet welds, which are the testing samples, remain elastic and/or below their capacities (latter is for bolts) even if the maximum actuator's load of 1000kN is imposed either in tension or compression.

Web-plate:

- Under tension:

The net design tensile capacity of 259.2kN governs with the critical section passing through the bottom hole.

Considering $F_{w16} = 399.32\text{kN} > F_{w12} = 299.27\text{kN} > F_{w10} = 249.39\text{kN} > F_{w8} = 199.52\text{kN}$

The design tensile capacity of the Web-plate (259.2kN) is between design capacity of the 10mm and 12mm fillet welds according to current provisions of NZS3404.

- Under compression:

Web-plate design compression capacity=258.58kN

If there is no gap between the web plate and the base plate, there will be no internal action generated in the welds. If there is a gap, the welds will be loaded under compression too, and in that case the design compressive capacity of the web plate is between design capacity of the 10mm and 12mm fillet welds according to current provisions of NZS3404.

It is worth noting that the above design capacities are valid until the stem (i.e. web plate) is in the elastic range. After the stem is yielded, the tangent elastic modulus will significantly reduce, hence buckling of the free part of the stem in compression will be unavoidable, hence the necessity of using anti-buckling restraints (holding plate) shown in Figure 40 for overall stability of the setup.

2.4 The setup and specimen (i.e. testing sample) drawings

(Note the full drawings are included in Appendix A.)

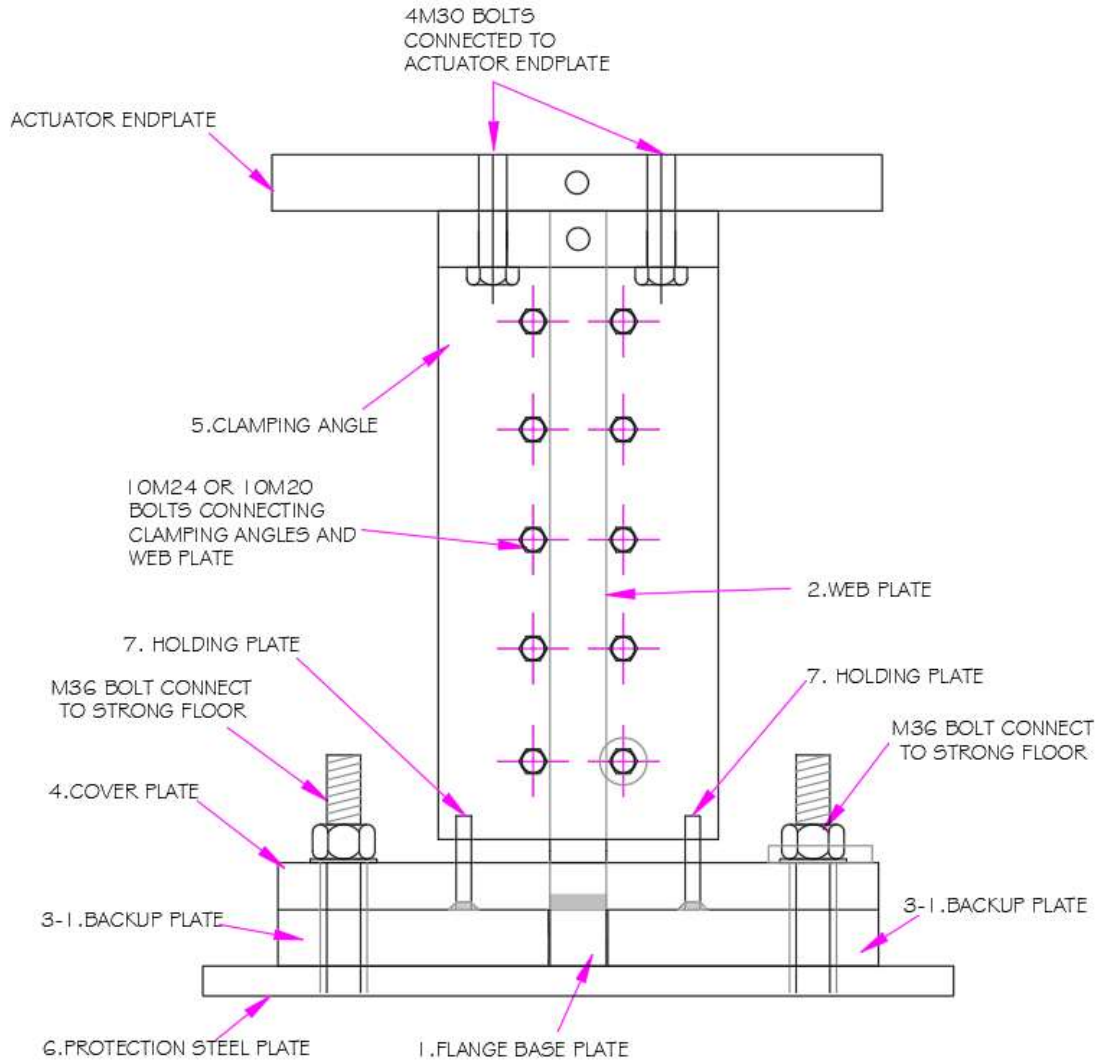


Figure 40: Front view of the test setup and test sample

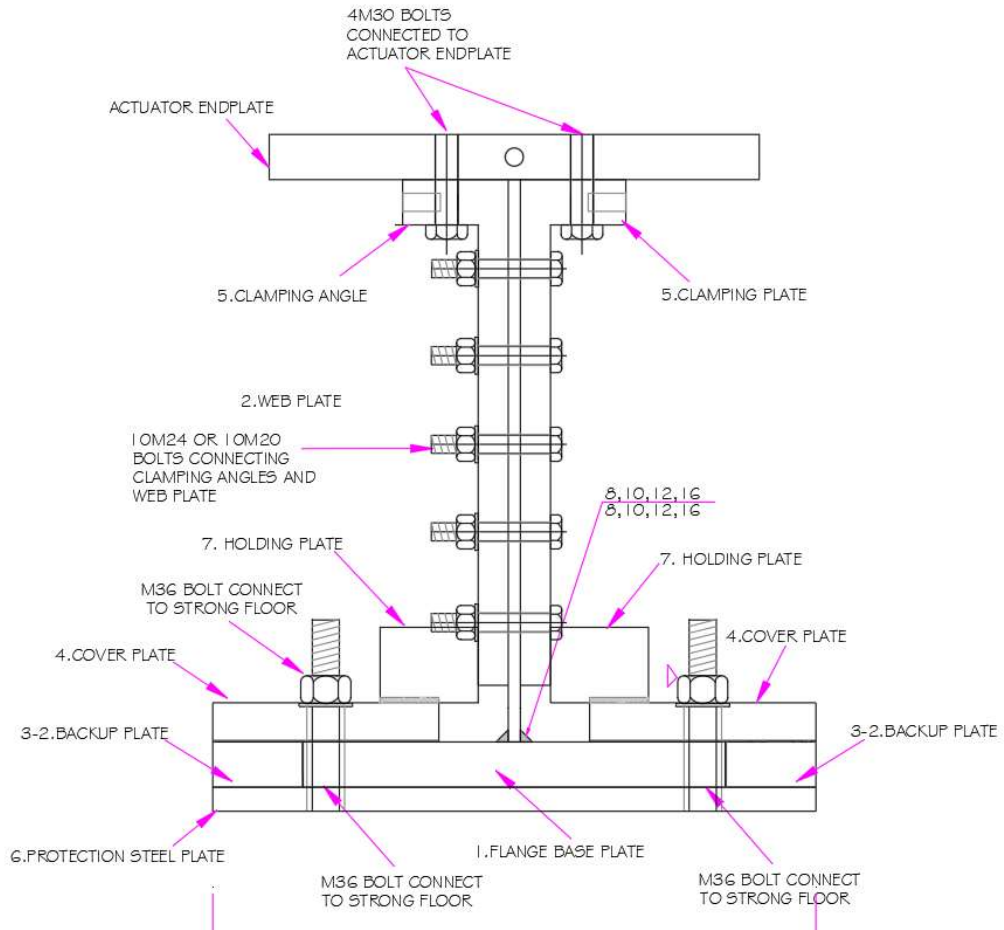


Figure 41: Side view for test sample

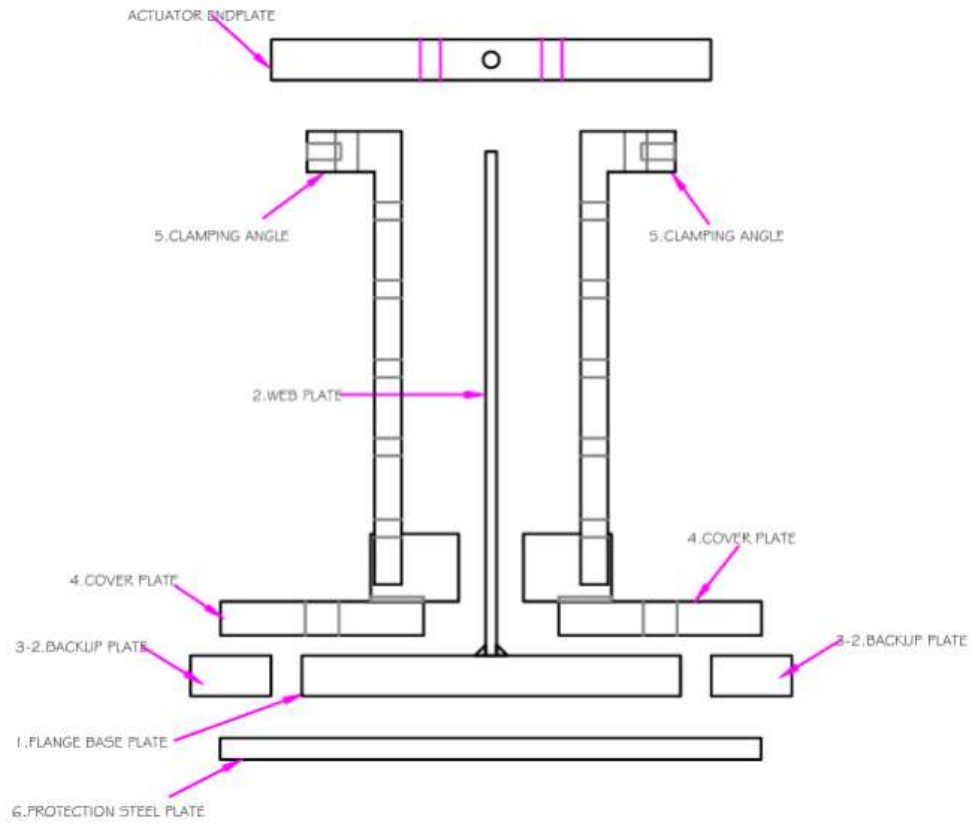


Figure 42: Separated parts for test sample

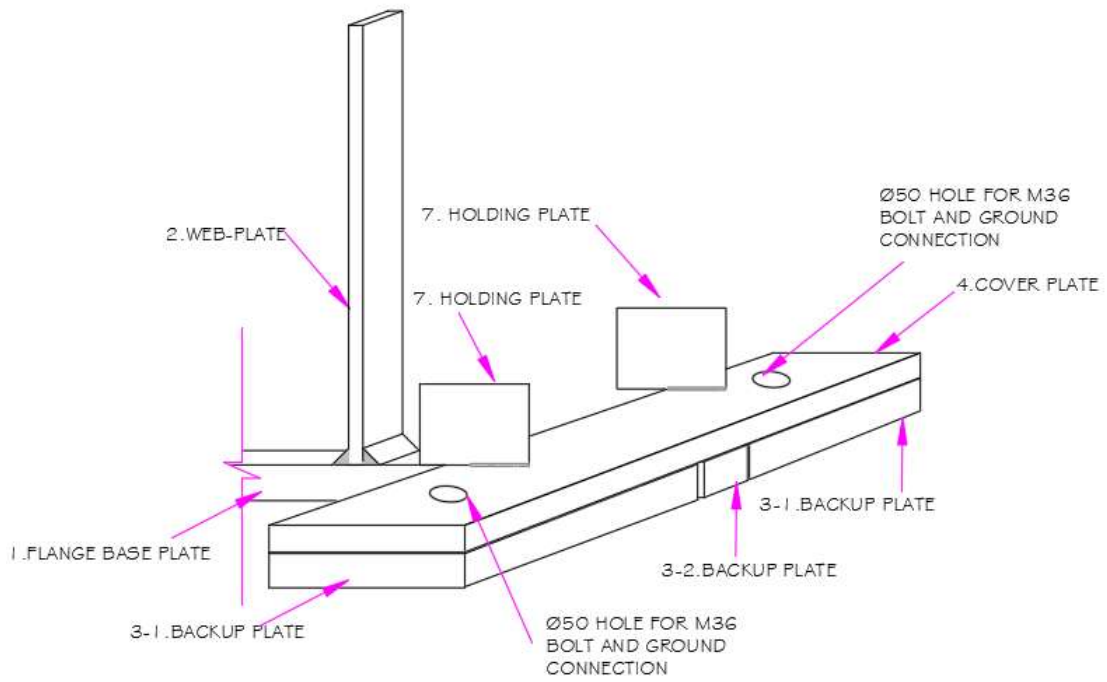


Figure 43: 3D view of the sample

3.0 Experiments procedure:

3.1 Introduction of the Loading regime:

The selection of an appropriate loading regime is a crucial consideration in this test to represent the realistic conditions.

A loading regime refers to the combination of types, magnitudes, and durations of various loads that a structure is to endure during the test.

In this test, the chosen loading regime aims to replicate the severe seismic events and beyond. This allows us to better understand the response and behaviour of the system under earthquake conditions.

The loading regime adopted for the tests is derived from AISC 2016 Seismic Provisions for Structural Steel Buildings, with the modifications made to fit the purpose. Specifically, it falls under the section titled "Prequalification and Cyclic Qualification Testing Provisions," more specifically in "Cyclic Tests for Qualification of Beam-to-Column and Link-to-Column Connections," under "Loading Sequence for Beam-to-Column Moment Connections." The specific reference in the document is section K-K2-4b on page 148. It is very similar to the Figure 44 in (Venture, 1997) as below.



Figure 44: The Figure E-1 in SAC steel project: Report No. SAC/BD-97/02

The inter-storey drift angle refers to the relative displacement between two consecutive floors of a building divided by the height between those floors, expressed as an angle. In the following pages, calculations are provided to convert drift deformation into axial displacement.

The LVDTs, strain gauges, and load cells will be used to record data and monitor the performance of the test samples. A modification has to be implemented in the loading regime ensuring the specimens were not pushed below their initial location. The stem was pulled and then pushed back to its original position, ensuring that the loading history does not have any values below the starting point.

To simulate the connection in a real structure, the stem, which is 16mm thick, can be considered equivalent to the flange of a 460UB82.1 steel beam, which also has a thickness of 16mm. The detailed dimensions of the 460UB82.1 steel beam are shown in Figure 45:

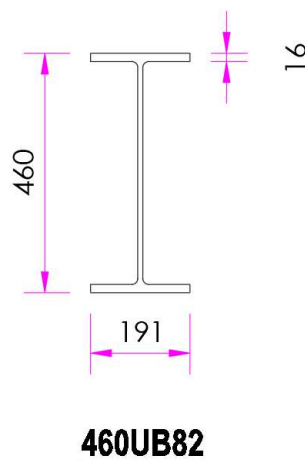


Figure 45: Detail dimensions of the 460UB82.1

3.2 Converting the drift deformation to axial displacement

The calculations described in this paragraph involve transferring drift deformation to axial displacement control. These calculations and trial tests revealed that the stem will experience plastic deformation even at the initial load step, where the peak drift deformation is 0.00375. To assess the stem's performance in the elastic and post-elastic ranges, five smaller drift angles (0.00046875, 0.0009375, 0.001875, 0.0025, and 0.003 radian) are incorporated into the loading regime before reaching 0.00375 radian. By

editing the loading regime in this manner, we can comprehensively evaluate the stem's behaviour across the entire range, from elastic to post-elastic and plastic deformation. Based on a trial test in the elastic range, the flexibility of the whole system (reaction frame, actuator, and the test setup) was identified to specify the displacement to be defined for the control system in order to achieve a required displacement at the specimen level. The trial test included loading a sample up to 200kN of load and unloading to zero. The displacement magnification factor was identified as 30.68.

The loading protocol outlined in (AISC, 2016) involves a multiple-step test-loading history. In this protocol, the deformation θ is defined as drift (note that this θ is a different from the θ mentioned in Section 1.2.4). The drift angle θ must be converted into the axial elongation of the stem. Subsequently, the simultaneous displacement of the actuator can be determined, and this displacement becomes the transferred loading regime derived from the drift angle θ . The calculation process is as follows and uses the first line of loading regime from (3.2 Table 1) as an example:

1. Find the real end drift from the peak deformation θ by 0.8 factor (assuming 80% of the drift is attributed to the beam end deformation):

$$f \times \theta' = \theta$$

2. Find the elongation of the stem from θ by considering half of effective depth from the assuming steel beam 460UB82.1 (assuming the point of rotation being center of the beam cross section):

$$\theta \times \frac{d}{2} = l$$

3. Find the strain of the stem at the drift θ from the elongation dividing by the plastic hinge length:

$$l_p = \frac{d}{2} + 78$$

$$l \div l_p = s$$

4. Find the stem's free part's elongation (representing beam flange) from the strain:

$$s \times l_s = l_{en}$$

5. Find the actuator displacement from the stem's free part's elongation by the magnification factor:

$$f_m \times l_{en} = l_a$$

θ' : peak drift deformation or story drift angle from (AISC, 2016)

f: factor 0.8 (Eom, Park, & Lee, 2013)

θ : real drift angle at the plastic hinge

d: half of effective depth of steel beam for example, 460UB82.1 in this test

l: End beam flange elongation

l_p : plastic hinge length = 222 + 78(Fenwick & Dhakal, 2007)

s: Strain at beam end flange, also at the stem's free part

l_{en} : Stem's free part's elongation

f_m : Displacement magnification factor between actuator displacement and stem elongation = 30.86 from the trail test

l_a : Actuator displacement

The calculation example is the given as below from the first line of loading regime form (3.2 Table 1)

$$f \times \theta' = 0.00046875 \times 0.8 = 0.000375 = \theta$$

$$\theta \times \frac{d}{2} = 0.000375 \times [(460 - 16) \div 2] = 0.08325 = l$$

$$l_p = \frac{d}{2} + 78 = 222 + 78 = 300\text{mm} \div l_p = 0.008325 \div 300 = 0.0002775 = s$$

$$s \times l_s = 0.0002775 \times 80 = 0.0222\text{mm} = l_{en}$$

$$f_m \times l_{en} = 30.68 \times 0.0222 = 0.681096 = l_a$$

Based on the information provided earlier, the loading regime form is structured as follows:

Table 2: Loading regime values:

Load step	Story drift angle	Beam end rotation at the plastic hinge	No of cycle, (n)	End beam flange elongation (mm)	Strain at beam end flange, also at the stem's free part	Stem's free part's elongation (mm)	Actuator displacement (mm)	Stress in stem (Mpa)	Actuator load (kN)			Loading frequency (Hz)
									Test sample width (62.2mm)	Sample width (70mm)	Sample width (80mm)	
									1	0.00046875	0.000375	
2	0.0009375	0.00075	6	0.1665	0.000555	0.0444	1.362192	111	110.467	124.32	142.08	0.1
3	0.001875	0.0015	6	0.333	0.00111	0.0888	2.724384	222	220.934	248.64	284.16	0.1
4	0.0025	0.002	6	0.444	0.00148	0.1184	3.632512	296	294.579	331.52	378.88	0.1
5	0.003	0.0024	6	0.5328	0.001776	0.14208	4.3590144	355.2	353.495	397.824	454.656	0.0667
6	0.00375	0.003	6	0.666	0.00222	0.1776	5.448768					0.0667
7	0.005	0.004	4	0.888	0.00296	0.2368	7.265024					0.0667
8	0.0075	0.006	4	1.332	0.00444	0.3552	10.897536					0.0667
9	0.01	0.008	2	1.776	0.00592	0.4736	14.530048					0.0667
10	0.015	0.012	2	2.664	0.00888	0.7104	21.795072					0.0667
11	0.02	0.016	2	3.552	0.01184	0.9472	29.060096					0.0667
12	0.03	0.024	2	5.328	0.01776	1.4208	43.590144					0.0667
13	0.04	0.032	2	7.104	0.02368	1.8944	58.120192					0.0667

3.3 The facilities used in AUT labs:

3.3.1 the equipment used in the cyclic/dynamic tests and general procedure:

HPU : The hydraulic power unit (HPU) is responsible for supplying high-pressure hydraulic fluid to system components to facilitate system operation (see figures 45 and 46). In the AUT lab, the HPU used is the SilentFlo 515 model, equipped with 6 pump modules, enabling it to handle multiple actuators or shake tables simultaneously. For this specific test, 3-4 modules were utilized to activate the 1000kN dynamic MTS hydraulic actuator.

To ensure balanced utilization of the pump modules and prevent overuse of specific ones, it is advisable to alternate the enabled modules for each test, effectively distributing the workload between the pumps.

Before commencing the test, it is crucial to inspect the pipes and valves connected to the flowing oil to confirm that all valves are in the open position and there are no oil leaks in the vicinity (see figure 47). The oil will be pumped to the Hydraulic Service Manifold (HSM), which, in turn, will distribute the hydraulic fluid pressure as per the tester's requirements and manipulations (see figures 48 and 49). This careful and diligent setup allows for proper dynamic output during the test, ensuring smooth and controlled operations throughout the testing process.



Figure 46: HPU in AUT labs



Figure 47: HPU's pumps (photo taken from inside of the hood)

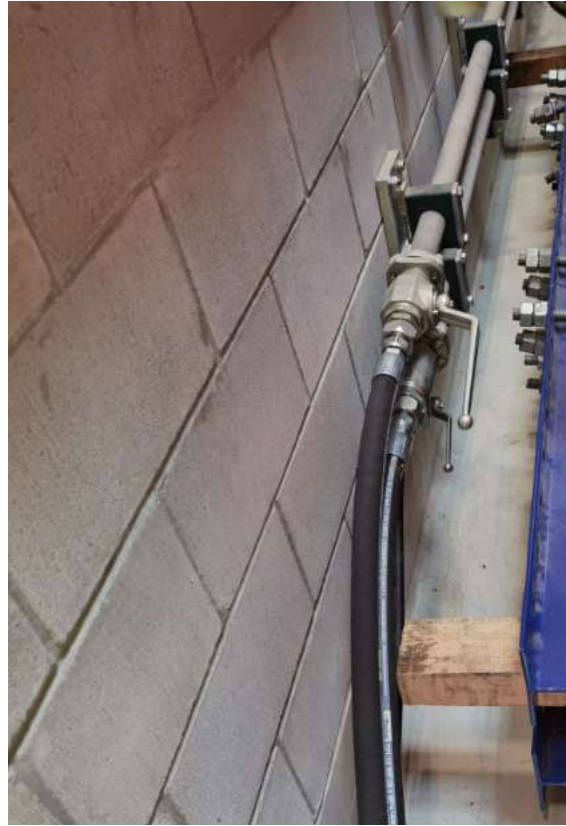


Figure 48: The pipes and valves for delivering the hydraulic fluid

HSM : The Hydraulic Service Manifold (HSM) is responsible for managing the distribution of hydraulic fluid pressure. When the hydraulic fluid is received from the hydraulic power unit and channelled towards the actuator, the fluid stress can be monitored and read from the gauge on the hydraulic service manifold.

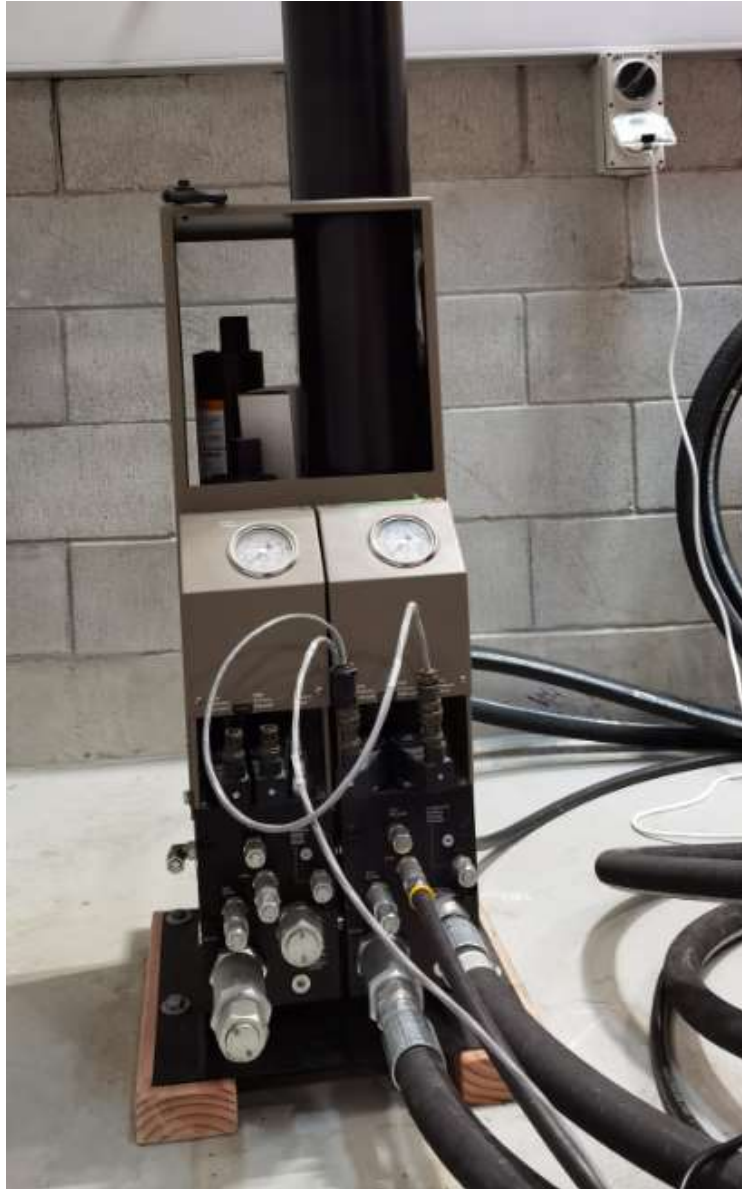


Figure 49: An HSM in AUT labs



Figure 50: The pressure gauges of an HSM in AUT labs

Actuator: An actuator serves as a device or component that transforms an input signal or energy into physical motion or action, finding widespread use in various systems and applications to control and manipulate mechanisms, objects, or processes. These essential components play a critical role across diverse fields, including engineering, automation, robotics, aerospace, automotive, and more, enabling precise control and operation of mechanical systems.

Actuators can be categorized into four main types based on their operational principles: electric actuators, hydraulic actuators, pneumatic actuators, and mechanical actuators. For the current test, the actuator in use is the MTS244_HydraulicActuator model, which utilizes hydraulic fluid pressure provided by the Hydraulic Power Unit (HPU) to generate both force and motion. It boasts a displacement capacity of 500mm for extension or retraction from the static/dynamic stroke, and simultaneously, it has a remarkable 1000kN allowed load capacity.

The actuator is connected and fixed at one end to red strong reaction frame and attached to red strong plate using 4M30 high strength bolts at the other end, through a built-in Swivel end (see figure 50). The actuator has built-in displacement gauge as well as load cell.

An LVDT (Linear Variable Differential Transformer) is incorporated within the actuator to accurately measure and record its displacement, providing crucial data that needs to be collected during the test. This information plays a significant role in analysing the actuator's performance and overall test results.

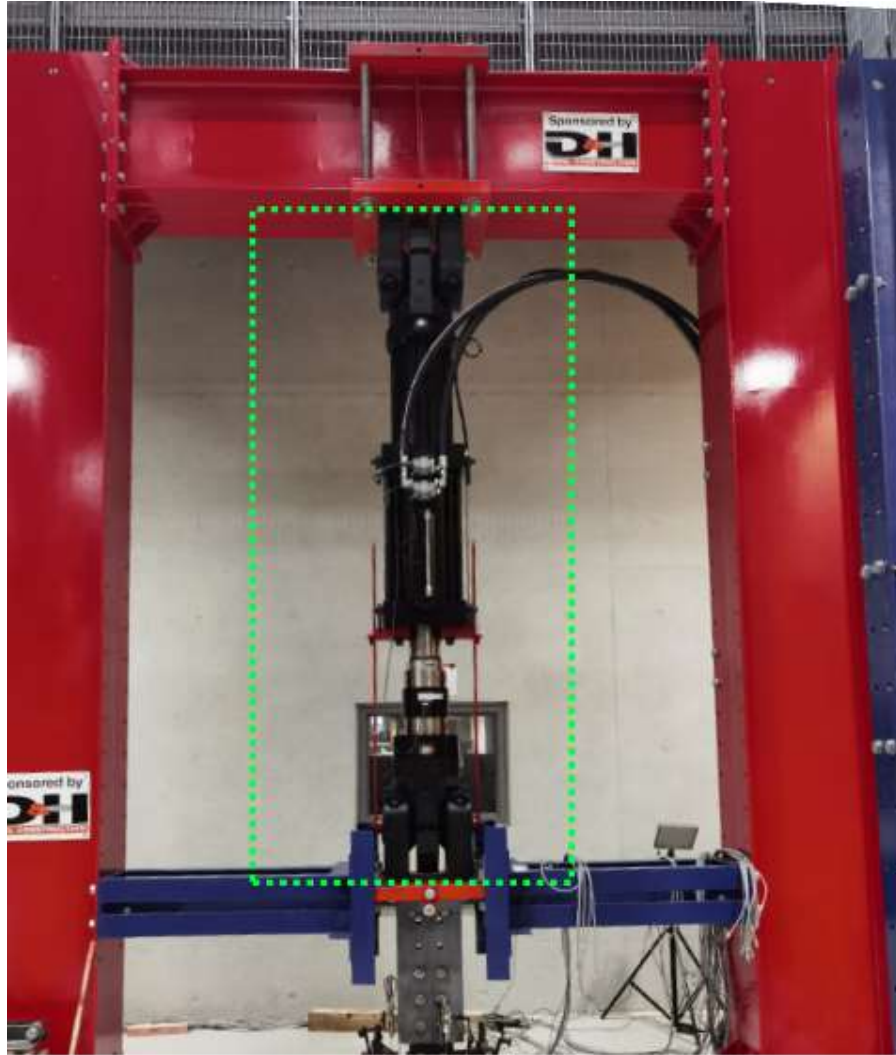


Figure 51: The actuator and its reaction frame in AUT labs

3.2.2 The instrumentation used in the test:

The strain gauge: A strain gauge is a measuring tool or device used to determine the strain experienced by an object it is attached to. Strain here refers to the deformation of the steel surface when subjected to a load from the actuator.

In this research, the strain gauges being utilized are purchased from Bestech Sensor&Teaching Equipment (Bestech Australia Pty Ltd). The specific type of strain gauge being used is Tokyo Measuring Instruments Lab's FLAB-6-11-1-1LJC-F, with a strain limit of 5% at room temperature. In the type of code, "6" indicates a gauge length of 6mm, "11" refers to the material used for temperature compensation, which

is mild steel, and "1LJC-F" denotes a 1-meter length and an integral lead wire with CE compliance.

The dimensions of the strain gauge are 6mmx2.2mm, with a backing size of 11mmx4.3mm.

Using the strain gauge requires some external equipment, including:

1. Wheatstone Bridge: To measure the resistance changing in the strain gauge accurately.
2. Instrumentation Amplifier: This amplifies the output voltage from the bridge, which is typically in the millivolt range, to obtain a precise value of strain.
3. Microcontroller Integration: An ADC (Analog-to-Digital Converter) converts the output into a digital value, which is then displayed on the LCD display, allowing for easy reading and interpretation of the data obtained from the strain gauge.



Figure 52: The details on the package of strain gauge from Bestech Australia Pty Ltd

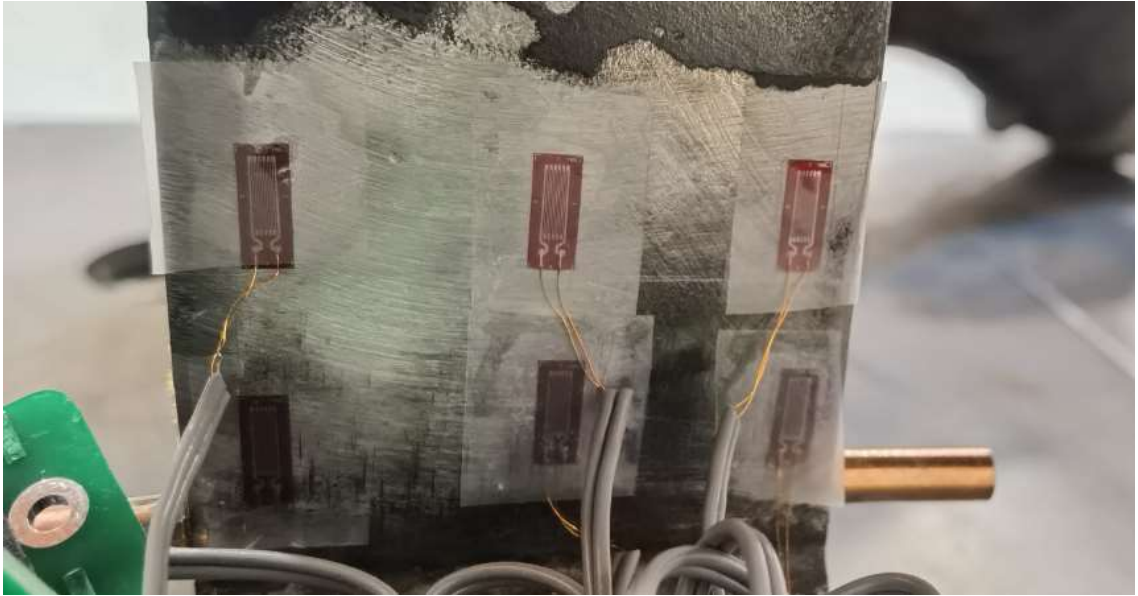


Figure 53: The strain gauges on trial test sample

LVDT:

The LVDT, short for Linear Variable Differential Transformer, is an electromechanical transducer renowned for its ability to accurately measure linear displacement or position. This device consists of a primary coil, a secondary coil, and a cylindrical ferromagnetic core. To operate, the LVDT is excited by an alternating current (AC) signal applied to the primary coil, which, in turn, induces voltages in the secondary coils. The ferromagnetic core is mechanically linked to the object whose position requires measurement.

As the ferromagnetic core moves linearly within the LVDT, it brings about a change in the magnetic coupling between the primary and secondary coils, thereby resulting in a differential output voltage. This output voltage is directly proportional to the displacement or position of the core within the LVDT. By carefully assessing the magnitude and phase of the output voltage, the precise position of the object can be determined with accuracy (see figure 53).

LVDTs are highly valued in industrial settings where precise position sensing is of utmost importance. Their remarkable advantages include high accuracy, exceptional linearity, and long-term stability, making them the preferred choice for a wide range of precision measurement tasks.

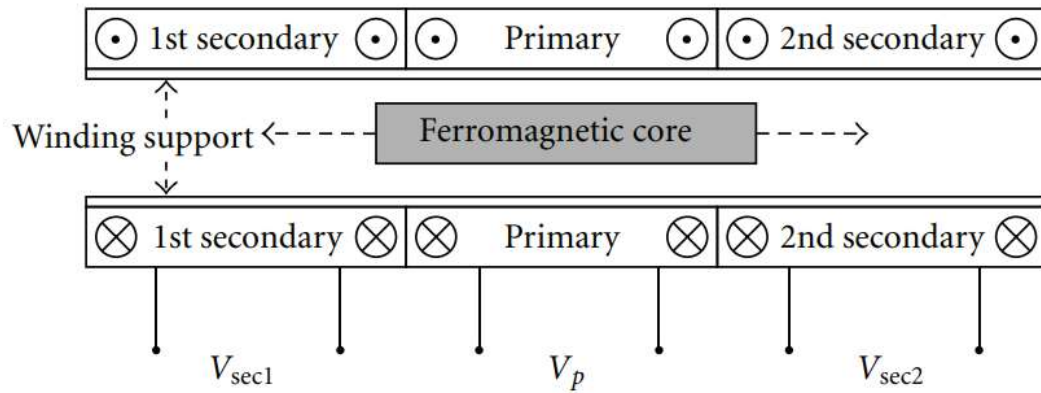


Figure 54: Typical LVDT layout and working principle (Masi, Danisi, Losito, Martino, & Spiezia, 2011)



Figure 55: The type of LVDT used in these tests from AUT labs

3.2.3 Data recording tools and software - Data Acquisition (DAQ)

Systems and the controllers/commanders:

Flexlogger: FlexLogger is a software application developed by National Instruments (now part of Keysight Technologies) for data logging and acquisition in various testing and measurement applications. It is designed to simplify the process of configuring, logging, and visualizing data from a wide range of sensors and instruments.

FlexLogger offers engineers and technicians a user-friendly interface to set up data logging tasks effortlessly, without the need for extensive programming knowledge. It is compatible with various hardware devices, including data acquisition (DAQ) devices, sensors, cameras, and more. The real-time data monitoring feature allows users to observe acquired data during the logging process and testing. With FlexLogger, users can easily visualize measurements, monitor signals, and ensure the quality of the acquired data. Before the tests start, it is needed to calibrate and/or insert calibration factors of the measurement tools such as strain gauge and LVDT.

During this study, FlexLogger logs data from multiple channels concurrently, enabling simultaneous data acquisition. Once the test is completed, the collected data is outputted in CSV (Comma-Separated Values) format.

Station manager: it provides station servo control based on a control source provided by a test application or station manager controls. After starting the HPU, the station manager can be run on computer by clicking on the associated icon. The software will start to run after around half a minute of loading. Then one needs to select the configuration file, in this research named “SB-ACT”, which is set for the test from the menu bar. Then the control panel will open, and at this stage we need to check that the starting data including displacement and force should be the same or fairly close to these starting data from flexlogger. If these data are close enough, the station manager window can be minimized, and Multipurpose elite can now be run.

Multipurpose elite: it is a secondary software to overcontrol the configuration file “SB-ACT” from station manager and collect test data. The name HSS T-stub cyclic testing was given to the programme to run the tests in this study, which is over control the “SB-ACT” running from station manager. For each test, we can establish sub-file with identical name under programme “HSS T-stub cyclic testing” for clear recording reason. Before running the actuator, it needs to double confirm that the M24 bolts,

which hold the actuator from gravity-induced elongation, are loose. Also, it needs to check if the flexlogger starts recording the data which means the communication between flexlogger and multipurpose elite is established and running ok. Then we need to click off the interlock, and power the HPU and HSM from lower power to full power. After power the HPY/HSM, it needs to check around the power pipes and valves making sure there are no oil leaking, and if so, it is needed to turn off the power from full power to lower power and report to lab manager immediately. If no issue is observed, the test can be started by click the start button.

3.2.4 The common tools used in the test preparation

Grinder: An electric grinder is a power tool widely used for grinding, sanding, or polishing various materials such as metal, wood, or plastic. It uses an electric motor to rotate an abrasive wheel or disc, allowing for precision shaping, smoothing, or removing material from the workpiece. The grinder was frequently used in this study specially in etching test, surface preparation and the installation of strain gauges. The two model types of grinders used in this research at AUT labs are shown in figures 55 and 56.



Figure 56: AG125-15DB Corded angle grinder



Figure 57: AG 125-A22 Cordless angle grinder

Standard podger spanner: the podger spanner also known as a podger wrench or podger bar, is a specialized hand tool primarily used in construction and steelwork industries. It is designed for aligning and tightening steel bolts and nuts in various applications, particularly in the erection of steel structures such as scaffolding, frameworks, and formwork.

According to the NZS3404 requirements for snug-tight connections, the standard podger spanner used for M20 bolts has dimensions of 30x32 and a length of approximately 400mm. Similarly, for M24 bolts, the standard podger spanner is sized 32x36 and has a length of around 450mm (see figures 57 and 58).

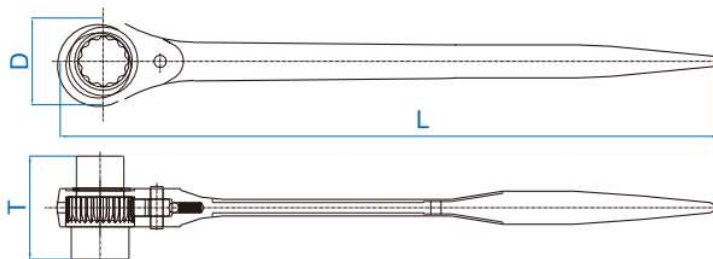


Figure 58: Shown plan for the size of podger spanner (*Podger Ratchet Wrench-KING TONY-1500*)



*Figure 59: The dimension of the standard podger spanner
(<http://www.wrenchmm.com/English/Product/7026814542.html>)*

Torque wrench: A torque wrench is a precise hand tool utilized for applying a specific amount of rotational force, known as torque, to fasteners like bolts and nuts. For the tests, the TOPTUL CHES2408 Reversible Ratchet torque wrench was used (see figure 59), which features an adjustable tube handle with a length range from 500mm to 800mm. During the test, we considered the 500mm handle length to be equivalent in effort to using a standard podger spanner for snug tightening. However, when connecting the clamping angles and the red plate, we employed the 800mm handle length with a person exerting full effort to properly tighten the M30 high strength bolts.



Figure 60: The torque wrench used in AUT labs

3.3 Installation of strain gauges:

Initially before installing any strain gauges, the sample must be prepared to facilitate the installation of the strain gauge, which will measure strain during the test and record the resulting data for further processing. The designated locations for installing the strain gauges can be found in the drawing provided in figure 61.

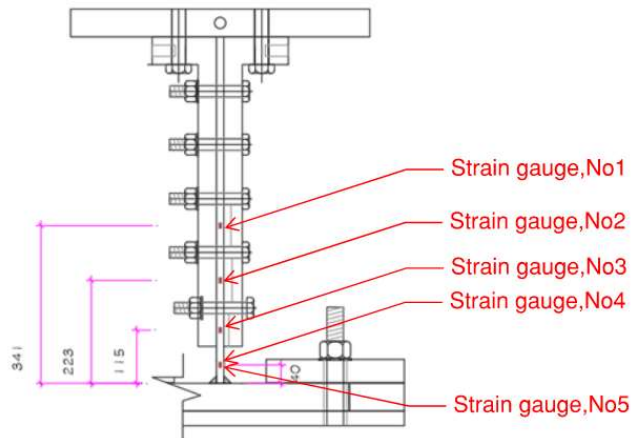


Figure 61: The drawing for the strain gauges positions on samples

The installation of the strain gauge holds significant importance as it is a highly sensitive instrument. During the strain gauge installation process, specific spots need to be ground for the strain gauges to be located and glued. For this purpose, a grinder and the orange disc 100 x 16mm Rapid Strip Disc Norton Blaze were utilized, as shown in Figure 62.

The disc 100 x 16mm Rapid Strip Disc Norton Blaze (Figure 62) serves the purpose of removing paint or coating from the steel surface and also eliminates rust without causing damage to or scratching the metal. It is essential to avoid using very fine or smooth strip discs for the strain gauge installation, as an excessively smooth surface can adversely affect the strain gauge's performance. The proper finished steel surface should look like the spots shown in Figure 63. Once the steel surface is ground and thoroughly cleaned with a clean cloth, a shiny and smooth metal surface is achieved, ensuring a proper surface for installation of the strain gauge.



Figure 62: The disc 100 x 16mm Rapid Strip Disc Norton Blaze

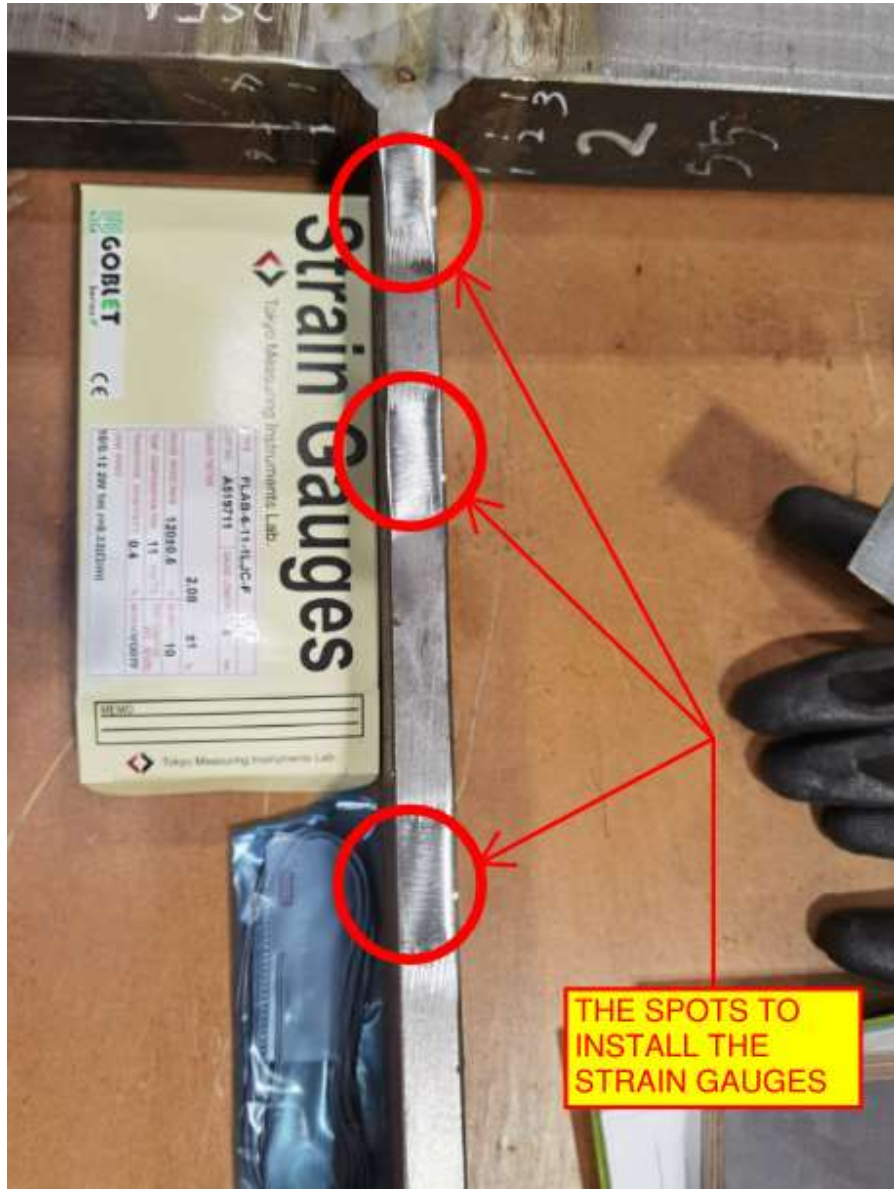


Figure 63: The finished steel surface preparation work for strain gauge installation

The procedure for strain gauge installation is as follows:

1. Begin by placing a drop of adhesive on the backing (opposite side of the gauge). Use the adhesive nozzle to spread it thinly and evenly across the backing surface.
2. Position the gauge carefully, ensuring it is placed as straight as possible. It is essential to mention that the strain gauge used in this setup is uniaxial, meaning it has a single grid for measuring strain in the grid direction. During the installation of the strain gauge, utmost care should be taken to ensure it is

positioned as straight as possible on the sample stem. Any misalignment could lead to additional errors in the measurements.

3. Next, lay a polyethylene sheet over the gauge and apply thumb pressure for at least 1 minute to allow the adhesive to cure.
4. Connect the lead wire to the circuit board at the quarter bridge connection as shown on Figure 64.



Figure 64: The circuit board for quarter bridge connection

5. As the lead wire from the strain gauge can be easily detached, it is essential to secure and protect it from any accidental forces during the test. After positioning the strain gauge, fix the lead wire in place using either glue or tape for safety reasons. For this purpose, Selleys Araldite 5-Minute Epoxy Adhesive super glue (see Figure 65) was used.



Figure 65: The super glue for the wire fixing

6. At this point, the installation of the strain gauge is completed, as illustrated in Figure 66.



Figure 66: The sample with strain gauges installed

3.4 Test sample assembling:

As the whole assembly (Figure 67) shown, the actuator is connected to the red frame as well as to the test sample via a red plate. To prevent horizontal movement, lateral restraints secure the red plate from both sides.

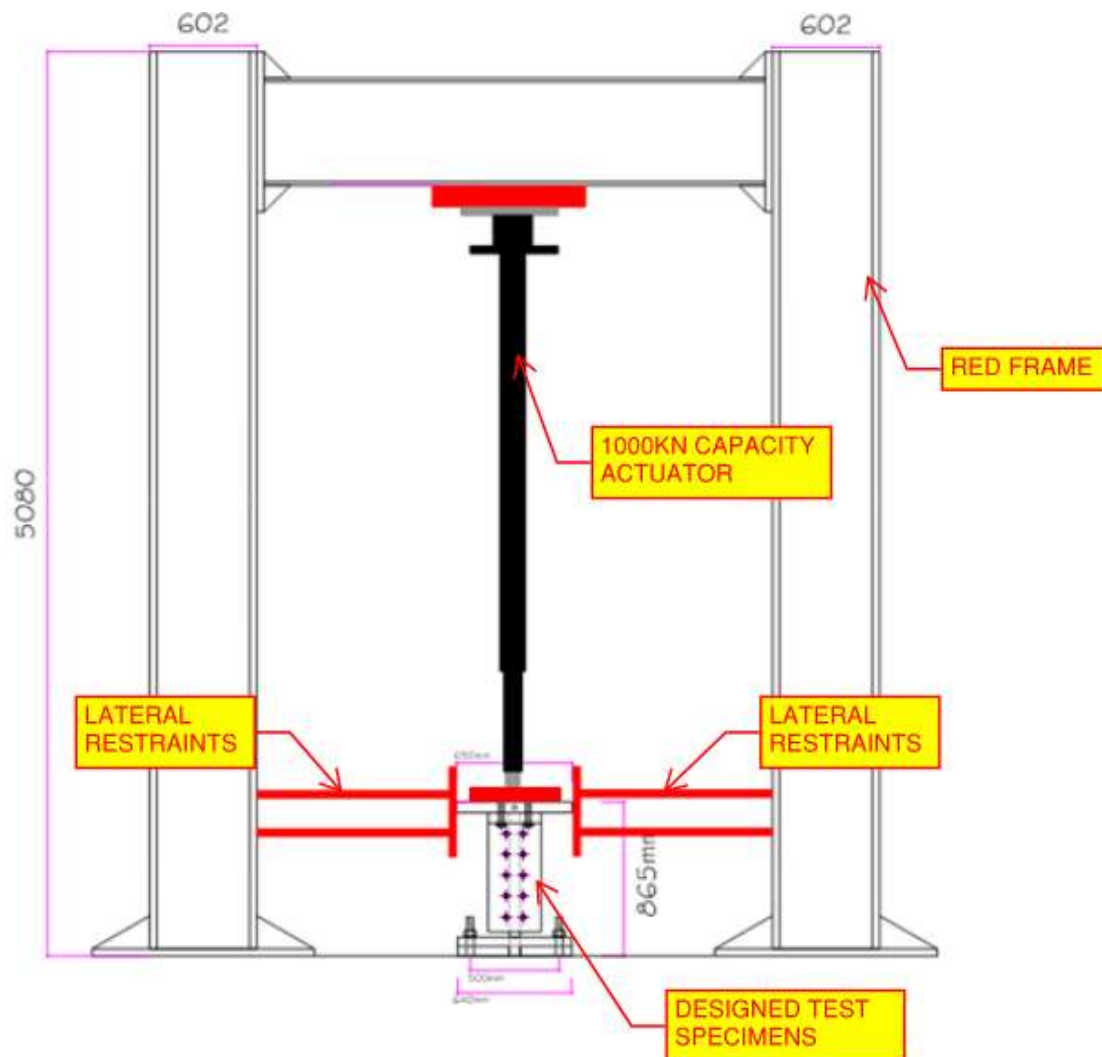


Figure 67: The outline of the test structure

The assembling steps for the test sample (designed test specimens) under the red plate is as below:

1. First, it is crucial to centre the test sample and equipment to minimize additional stress resulting from misalignments. To achieve this, geometry central lines will

be carefully marked on the clamping angle, ground protection plate, and the T-joint which is the weld-together sample of the web plate and flange base plate, as illustrated in Figure 68.



Figure 68: Marked up central lines on the clamping angle and ground protection plate for alignment purpose

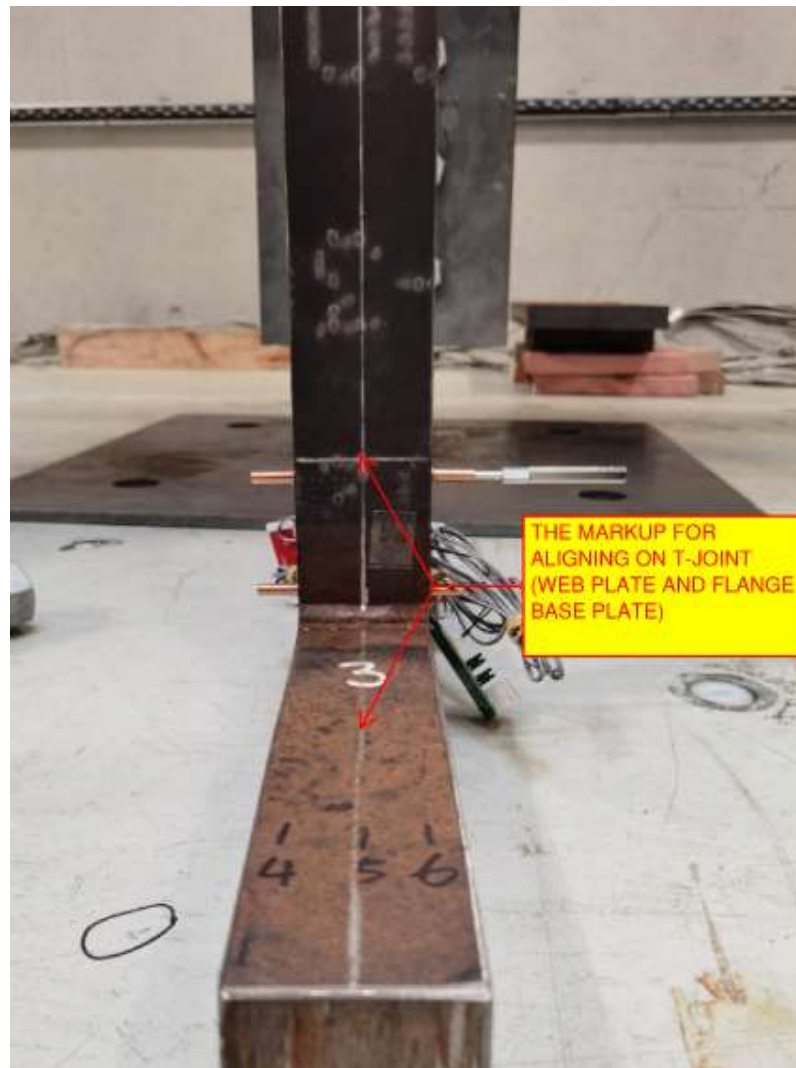


Figure 69: Marked up central lines on the T-joint for alignment purpose

2. The ground protection plate will be placed on the ground first, serving as the base for assembling the test sample and to protect the concrete surface of the strong floor. On top of the ground protection plate, position the T-joint sample, which comprises the weld-together sample of the stem plate and flange base plate, along with the backup plate.
3. Begin by installing one of the clamping angles to the red plate using 2 M30 bolts.
4. Carefully position the T-joint from the side of the clamping angle. Then, install the other clamping angle and connect the two clamping angles firmly using 10 M24 8.8 grade or M20 10.9 grade bolts to secure the test sample T-joint in the middle.



Figure 70: Placing the test sample in a position close to one of the clamping angles.

5. In the end, place the cover plates on top of the flange base plate of the T-joint. These cover plates will secure the T-joint, by firmly pressing it to the strong floor using 4M36 PC8.8 threaded rods. Furthermore, by utilizing the holding (anti-buckling restraining) plate on the cover plate, the cover plate prevents lateral out of plane movements of the bottom of the clamping angles.



Figure 71: Placing the cover plates on the test sample (flange base plate)

3.5 Bolts installation for the sample's assembling:

First, it is essential to conduct a thorough inspection of the bolts and bolt/nut/washer assemblies intended for use in the test. The bolts must be visually examined to identify any potential damage to the threads and/or coating. Additionally, a free-turn-of-nut test should be conducted to ensure the bolts' high quality.

During the free-turn-of-nut test, the nuts should run freely when part of a bolt/nut assembly. This can be verified by manually running the nut along the bolt's threads for the full length of the thread before using it in a connection. Only bolt/nut assemblies that pass this test should be deemed suitable for use. Once a bolt/nut assembly has been

subjected to this test, neither component should be substituted with others. All these processes, including snug-tightening, must strictly adhere to the instructions provided by (Shahab Ramhormozian, Clifton, & Cowie, 2016).

The connection between the red plate and the clamping angle:

The connection between the red plate and the clamping angle is achieved using 4M30 PC8.8 bolts inserted through the thread holes. To securely fasten them, a Toptul ratchet extended to 800mm was used based on full effort of a person.

The connection between the clamping angles clamping the T-join sample:

The test utilized G8.8 HSFG M24 structural bolts that have passed the Free turn-of-nut test. The tightening pattern involved starting the snug-tightening first and further tightening after the snug-tightening.

The bolts were snug-tightened from the top (stiffest part) to the bottom (free edge). To achieve this, snug-tightening was undertaken on the bolts using an impact wrench or a 500mm ratchet, equivalent to a standard podger spanner.

Once snug-tightened, the bolts were further tightened to a specific degree using an electric torque wrench to reach the proof load of 210kN (Shahab Ramhormozian et al., 2016). The AUT labs' electric torque wrench (gun) utilized in this process was a V-RAD 16, shown in Figure 72.



Figure 72: The electric torque wrench (torque gun) type: V-RAD 16

The torque calibration chart for the torque wrench, manufactured by New World Technologies Incorporation (supplier) is provided as shown in Figure 73.

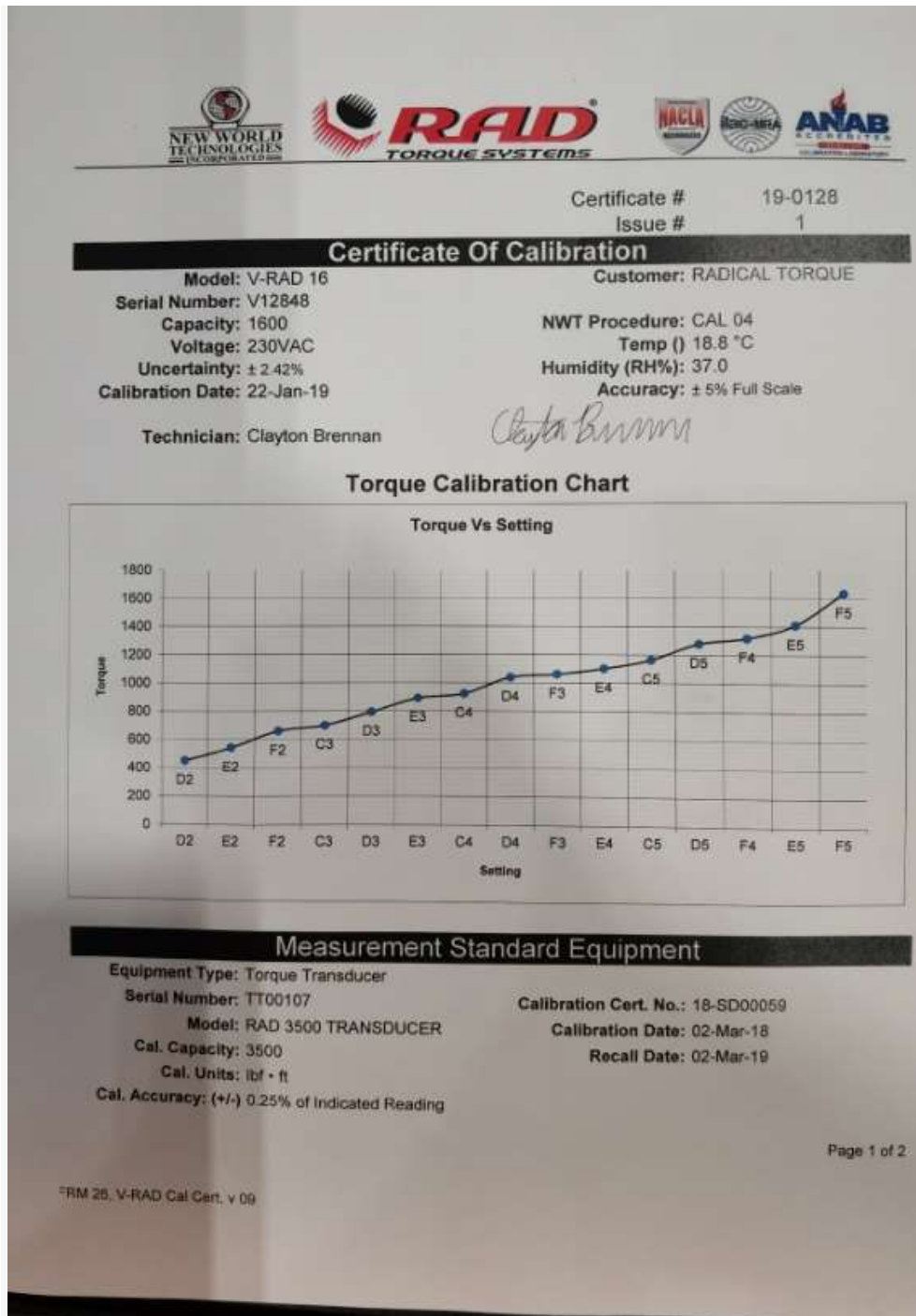


Figure 73: The torque calibration chart for electric torque wrench type: V-RAD 16

Calibration Value Table	
Units:	LBF • FT
Setting	Torque
D2	448
E2	540
F2	656
C3	696
D3	791
E3	889
C4	922
D4	1038
F3	1060
E4	1101
C5	1163
D5	1278
F4	1318
E5	1410
F5	1631

Certificate # 19-0128

Customer Address:
 RADICAL TORQUE SOLUTIONS PTY LTD
 7 MAB EASTERN PROMENADE
 TONSLEY,
 Australia
 5042

Figure 74: The calibration values table for electric torque wrench type: V-RAD 16

Before using the torque gun, adjustments were made by turning the button above the torque gun to set a torque as a safety measure, not to overtighten the bolts. It is worth noting that the bolts in these experiments were not tightened considering torque values but turn of nut. The calculation used to make the decision about setting the torque is outlined below:

$$T = (K \times D \times P) \div 12$$

Equation 20: Calculation for required torque (From: Determining Torque: The Facts About Required Torque, Tension and Clamp Loads (mudgefasteners.com))

T = Torque (ft.-lbs.)

D = Nominal Diameter (inches)

P = Desired Clamp Load Tension (lbs.)

K = Coefficient of Friction

The K factor can vary depending on the condition of the threaded fasteners.

Commonly used factors range

Lubricated with wax, oil or other coating = 0.10

Plain, uncoated = 0.20

Galvanized = 0.30

Dirty or Rusty = 0.30+

The T (torque) is what need to know. D (nominal diameter) is the diameter of the bolt rod M24 which is 0.95 inch. P is the proof load of M24 bolts that is 47209lbs (210kN). 0.3 is K value.

$$T = (K \times D \times P) \div 12 = (0.3 \times 0.95 \times 47209) \div 12 = 1121 \text{ (ft. lbs)}$$

From the torque calibration chart by comparing the calculation result, 1121(ft. Lbs) is in the D4 range and set the adjustment at D4

Preloading 210kN tension force onto M24 8.8G bolts after snug tight:

Before proceeding, it is crucial to establish location marks to indicate the relative position of the nut and the socket on the torque wrench during operation. Additionally, determining the required rotation degree to reach the proof load of 210kN for M24 bolts is essential.

Based on AS/NZS1252 specifications, the bolt shank measures 71mm, and the total thickness to be clamped is 105.2mm, encompassing two clamping angles ($2 \times 40mm$), the web plate ($1 \times 16mm$), and two washers ($2 \times 4.6mm$). In addition to accounting for the clamping length, we must also consider the nuts, which measure 36.6mm each, along with a specific pitch part length. Consequently, the total length of the M24 bolts we ordered from the manufacturer is 140mm. As a result, the loaded threaded part covers a length of 29mm, providing more than 9 threads in the loaded section. The calculation is as follows (S Ramhormozian, Clifton, Nguyen, & Cowle, 2015):

$$K_{bolt} = \frac{AE}{L}$$

Equation 21: Calculation for longitudinal elastic stiffness of the bolt

$$\Delta_e = \frac{N}{K_{bolt}} = \frac{NL}{AE} \quad (2)$$

Equation 22: Calculation for elongation of the bolt due to the preload

$$R = \frac{\Delta_e}{P} \times 2\pi \quad (3)$$

Equation 23: Calculation for rotation of the nut for M24 bolts in radians

K_{bolt} = longitudinal elastic stiffness of the bolt;

A=effective cross-sectional area of the bolt. This can be considered as a weighted average of the bolt shank and thread cross sectional areas with respect to their length.

E=elastic modulus of the bolt material.

Δ_e =elongation of the bolt due to the preload N;

R=amount of rotation of the nut in radians to reach the bolt to the preload N from the point at which the bolt tension is just zero.

P=pitch of the bolt threads.

L=effective length of the bolt; this is the summation of the shank length (l_s) and length of the loaded part of the thread (l_t) and can be assumed approximately as the joint grip length i.e., thickness of the plies to be clamped.

Equation 21 can also be re-calculated more precisely as Equation 24, which considers the bolt shank and threaded part as two springs in series(S Ramhormozian et al., 2015):

$$K_{bolt} = \frac{A_s A_t E}{l_s A_t + l_t A_s}$$

Equation 24: Calculation for longitudinal elastic stiffness of the bolt

where A_s =shank cross sectional area,

A_t =thread cross sectional area

After the calculation is result is as below:

$$K_{bolt} = \frac{A_s A_t E}{l_s A_t + l_t A_s}$$

$$R = \frac{NL}{AEP} \times 2\pi = \frac{210 \times 10^3 \times 100}{353 \times 210 \times 10^3 \times 3} \times 2 \times \pi = 0.65$$

Equation 25: Calculation for rotation of the nut for M24 bolts in radians

$$0.65 \times 180 = 117^\circ$$

To achieve the proof load of 210kN, all bolts must be further rotated by 120 degrees, if the initial tension in the bolt is zero (which is not the case for a snug tightened bolt). This has been also checked against table 15.2.5.2 of NZS3404 in which the required part-turn to fully tension the bolts is specified. However, in this study given the bolts were intended to be reused for more than one test, the amount of rotation was carefully selected to preferably just achieve the proof load and not beyond that, so that the bolts can be re-used for few repeats before being disposed. To impose the required turn following snug tight condition, a point was marked on the socket of the torque gun and two points, each spaced 120 degrees apart, on the clamping angle near the nut. Prior to running the torque wrench, the starting point on the socket with the mark close to the nut was aligned. As the torque wrench is operated, the nut rotates until the mark on the socket aligns with the other mark near the bolt, indicating that the nut has been rotated by 120 degrees and is now preloaded close to 210kN. During imposing the rotation, the

bolt's head was fixed in place by another spanner, ensuring the imposed rotation is applied only on nut and not the whole bolt/nut assembly.

Preloading 180kN tension force onto M20 PC10.9 bolts after snug tight:

For certain samples the stem size was wider than 70mm. Due to the limited space between the two bolts rows on the clamping angle, smaller i.e. M20 bolts needed to be used for those samples. To enhance tension friction between the bolts and clamping angles, Belleville springs were also employed instead of ordinary hardened washers. The Belleville springs were same as those used by Ramhormozian and Clifton et al (Shahab Ramhormozian, Clifton, MacRae, Davet, & Khoo, 2019)

For tests utilizing M20 10.9 bolts with 140mm in length, all tightening steps are similar to those used in experiments with M24 8.8 bolts, with the exception of the following items:

1. Instead of using a single hardened washer, two Belleville springs are used for each bolt, one at the head side and another at the nut side.
2. The snug-tight process remains similar to that of the M24 bolts, but for the M20 bolts, more rotation is necessary to achieve the snug-tight condition. The wrench will be turned considerably more during this process.
3. Following the tightening of each M20 10.9 bolt on the clamping angle, a second nut should be manually tightened as a safety precaution in case the first nut experiences excessive load from the actuator.
4. By following this procedure, each bolt is likely to achieve a tension of approximately 180kN. This tension should be sufficient for the test requirements.
5. The amount of nut turns after snug-tight is determined using the following equation. This is adopted from Ramhormozian 2018 (Ramhormozian, 2018) .

$$0.1 + \left(0.45 \times \frac{1.7}{pitch}\right) + \left(0.05 \times \frac{2.5}{pitch}\right)$$

Equation 26: Calculation for rotation of the nut for M20 bolts in radians

The pitch of the M20 10.9 bolts utilized in the test is measured on-site as shown in Figure 75 and confirmed to be 2.5mm by the manufacturer.



Figure 75: Confirm the pitch size of M20 10.9 bolt

Then the calculation is

$$0.1 + \left(0.45 \times \frac{1.7}{2.5}\right) + \left(0.05 \times \frac{2.5}{2.5}\right) = 0.456 \text{ (Turn)}$$

A rotation of 0.456 turns is equivalent to 164 degrees. This means that after snug-tightening, the M20 10.9 bolts required a further rotation of 164 degrees, not 120 degrees as used for M24 bolts, to reach the desired tension.

Cover plate connecting the ground with 4M36 8.8 threaded rods

After connecting the clamping angle to the red plate and clamping the stem using the clamping angles, the cover plates needed to be secured via post tensioned rods connected to the strong floor using 4M36 8.8 threaded rods. For reusability and also according to the strong floor threaded holes specifications, the pretension load should

be set at 80% of the proof load of the M36 PC8.8 threaded rods, which is approximately 400kN (80% of 490kN). However, since this high pretension load exceeds the capacity of the electric torque wrench available in the lab, the EZIJAC socket type model: B3S-L5 and hydraulic pump were employed to install these M36 threaded rods.

Initially, the M36 threaded rods need to extend over the cover plate by 75mm to ensure a proper fit with the socket, enabling sufficient threads to hold the tension force from the EZIJAC and prevent any damage. This setup allows for the reuse of the M36 threaded rods throughout the experiments.



Figure 76: The EZIJAC socket type model: B3S-L5

4.0 Dimensions and observations on samples:

The information about the welding procedures and the steel samples is as follows:

The welding procedure specification follows the AS/NZS 1554.1:2014 standard, with the details as follows:

Weld Category: GP & SP

Material Spec/Grade/Type: Steel Type 1 & 4

Process: FCAW(C)

Type: Semi-automatic

The welding consumables are as follows:

Specification (Root): AS/NZS ISO 17632-B

Classification (Root): T492T1-1 CAU H10

Flow Rate: 18 l/min to 25 l/min

Weld Wire: E71T-12M H4

Shielding Gas: Welding-grade CO₂

More information can be found in Appendix D.

Upon receiving the samples, it was essential to document their details, including the dimensions of the T-joint and the size of the weld. Additionally, a thorough inspection of the surface condition was required to prepare the samples for testing.

To measure the dimensions of the T-joint, tools such as the steel ruler and Digital Vernier Caliper Gauge were utilized. As an example, the measurement results for the sample FW10G0R1N3S2 (excluding weld dimensions) are shown in Figure 77:

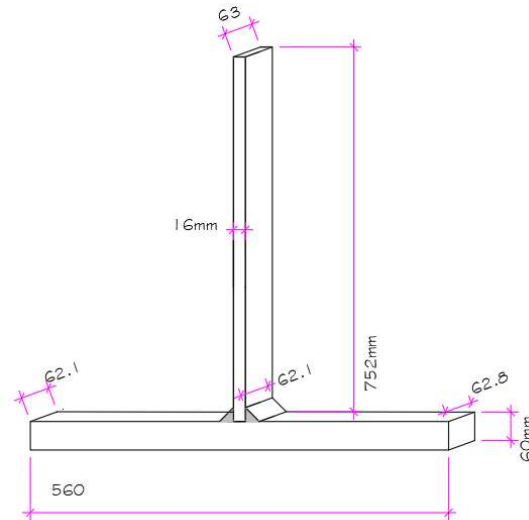


Figure 77: The documented size of the sample FW10G0R1N3S2

To document the weld dimensions, data is gathered from measurements of leg length, root length, and throat, each comprising six points' readings. These points are positioned 10mm from each edge of the weld, with one additional point at the centre of the weld. The measurement points on the web plate for the leg length are indicated in Figure 78, while the measurement points on the flange base plate for the root length are shown in Figure 79. The section illustrating the leg length, root length, and throat can be found in Figure 80.

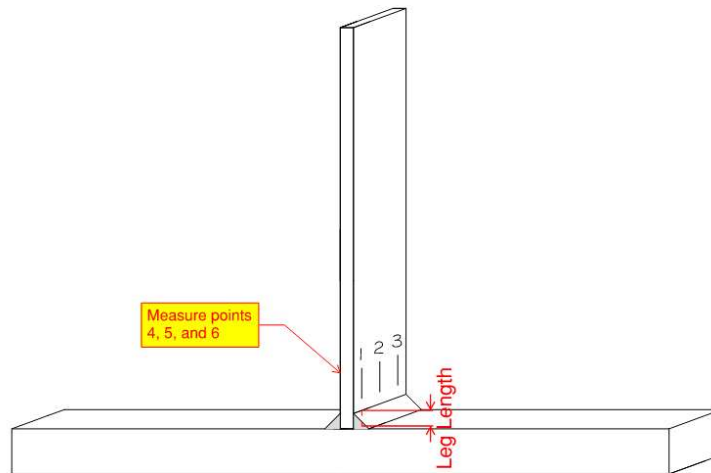


Figure 78: the 6 points on the web plate to measure leg length(3D view)

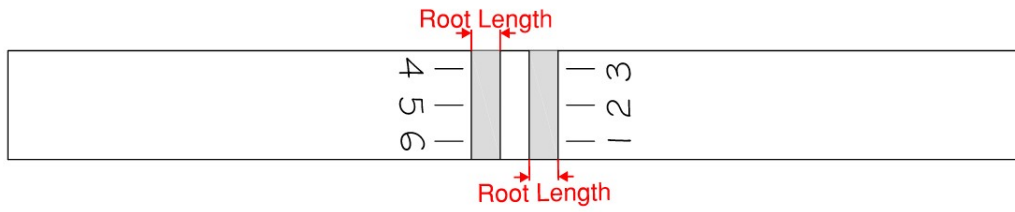


Figure 79: the 6 points on the flange base plate to measure root length (plan view)

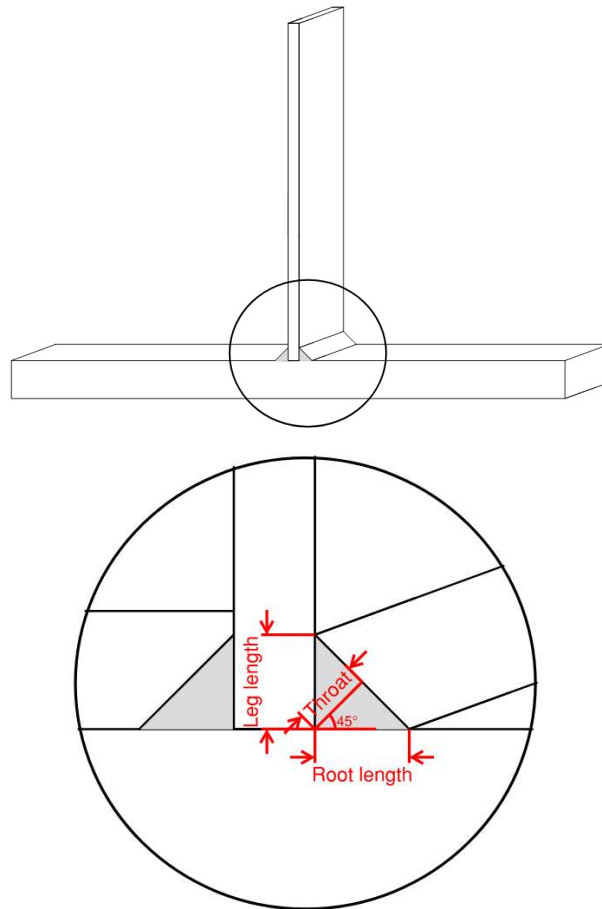


Figure 80: The illustration of leg length, throat, and root length

A fully recorded sample measurement, exemplified by FW10G0R1N3S2, is presented in the following Table 3. It includes data for leg length, root length, and throat, each

with measurements from 6 points. In the analysis, we will employ the average value for the analysis.

Table 3: Table of the dimension of sampleFW10G0R1N3S2 – dimensions are all in mm.

Measured size for specimens

		1	2	3	4	5	6	Average value(mm)
No1-20230321- FW10G0R1N3S2	Leg	10.1	10.2	10.3	9.6	9.9	10.5	10.1
	Root	12.5	13.1	12.8	12.5	12.2	12.2	12.55
	Throat	9.2	9.2	9.2	10.4	10.1	11.5	9.93

To accomplish this, a Cam Type Gauge (see Figure 81), also known as a welding gauge or fillet weld gauge, was unutilized, which could measure both the leg dimension and throat thickness of the weld.



Figure 81: Cam Type Gauge

Steps to Measure Weld Leg Length with a Cam Gauge:

1. Select the Correct Scale on the Cam Gauge:
 - o Identify the scale on the cam gauge that corresponds to the leg length measurement. Most cam gauges have multiple scales and indicators for different measurements.
2. Position the Cam Gauge:

- Place the cam gauge against the weld so that it is perpendicular to the surface of the base metal. The gauge should be aligned with one of the legs of the fillet weld.
- 3. Adjust the Cam Gauge:
 - Slide or rotate the adjustable component of the cam gauge until it touches the toe of the weld leg you are measuring. Ensure that the gauge is in full contact with the surface to avoid any measurement errors.
- 4. Read the Measurement:
 - Look at the scale on the cam gauge to read the weld leg length. This is the distance from the weld toe to the point where the gauge meets the weld root.
- 5. Repeat for the Other Leg:
 - To measure the other leg length of the fillet weld, reposition the cam gauge perpendicular to the other leg and repeat the process.

Steps to Measure Weld Throat Thickness with a Cam Gauge:

1. Select the Correct Scale on the Cam Gauge:
 - Identify the scale or indicator on the cam gauge that corresponds to throat thickness measurement. Different cam gauges might have specific features for this measurement.
2. Position the Cam Gauge:
 - Place the base of the cam gauge against one leg of the weld, ensuring it is perpendicular to the base metal surface.
3. Adjust the Gauge:
 - Adjust the sliding or rotating components of the cam gauge so that one end touches the weld face (the highest point of the fillet weld) while the other end contacts the weld root (the point where the two metal pieces meet).
4. Measure the Effective Throat:
 - Ensure the gauge is positioned correctly to measure the effective throat, which is the shortest distance from the root to the face of the weld. This distance is crucial as it determines the strength of the weld.
5. Read the Measurement:
 - Read the scale on the cam gauge that shows the throat thickness measurement. This will usually be indicated by a marked point on the gauge.

The sizes of the six points of the weld are collected for each sample, for example the dimensions of sample FW10G0R1N3S2 are shown in table 3. The complete record of the weld dimensions can be found in Appendix B.

Samples surface preparation:

During the manufacturing process at the factory, some sharp edges and spurs may be present on the surface of the samples, as shown in Figure 82 and Figure 83.



Figure 82: Unfinished steel surface with spur on the flange base plate



Figure 83: Unfinished steel surface with spur on the stem web plate

Before conducting the test, it is crucial to perform surface preparation works to ensure the safety of the testers and prevent any damage to the equipment caused by the coarse surfaces of the samples.

The electrical power grinder HILTI AG 125-15DB and hard disc A Rhodius RS28 125x7,0(Figure 84) were used for cutting of the metal spurs from the sample's surface.

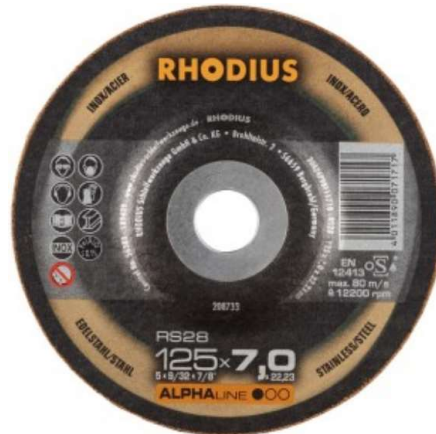


Figure 84: hard disc type: A Rhodius RS28 125x7,0

After cutting off the spurs, a handle grinder and Brumby Zirconia Flap Discs 80G disc were used to smooth out the coarse surface and sharp edges of the samples. Once the sample preparation work is complete, the samples are safe for manual handling by testers. Additionally, clamping the equipment and test setup together with these prepared samples will not cause damage or leave cutting marks during the test.

5.0 Etching test:

A total of thirty-two samples were used in the etching and subsequent testing. These included 5 samples with 8mm fillet welds, 6 samples with 10mm fillet welds, 5 samples with 10mm fillet welds and a 1.5mm gap, 5 samples with 12mm fillet welds, 6 samples with 12mm fillet welds and a 3mm gap, and 5 samples with 16mm fillet welds.

The etching test primarily follows the guidelines from ISO/TR16060(ISO): Destructive tests on welds in metallic materials — Etchants for macroscopic and microscopic examination with inputs from experts and chemistry technicians at the AUT labs.

When choosing the appropriate etchant, it is essential to prioritize the use of less hazardous chemicals over more dangerous ones. Additionally, consideration must be given to the large size of the samples and the existing equipment in the lab. Cuprochloric is a suitable choice for the etching test as it is a less hazardous material and does not require a fume hood during operation or using a wash tank to clean up the residual chemical after the test.

The selected etchant, as described in table 4 of this thesis, which is tableA.9 from ISO/TR16060, consists of 30ml H₂O, 25ml ethyl alcohol, 40ml HCL, and 5g CuCl₂.

The steps involved in the etching test are summarized as follows:

1. Initially, the surface of the sample must be ground to prepare it for the etching test. The grinding process will adhere to the guidelines outlined in Table A.9 of ISO/TR16060, which specifies that the surface preparation should be at least 1,000 grit or finer.

Table 4: Table of etching test solution

Table A.9 — Cuprochloric solution 1

Type of etchant: Macroscopic etchant
Composition in volume and in order of mixing: 30 ml water (H ₂ O) 25 ml ethyl alcohol (C ₂ H ₅ OH) 40 ml hydrochloric acid (HCl) 5 g copper (II) chloride (CuCl ₂)
Safe shelf life: 2 h
Surface preparation: 1 000 grit or finer
Etching temperature: Ambient
Etching time: 10 s to 20 s
Additional precautions/requirements: After the etching, the specimen should be washed in order to remove copper deposits. Usual precautions for handling and disposal of acids.
Comments: Reveals cold working strain lines.

1.1 The grinding process begins with an 80-grit disc to prepare the specific area of the surface required for the etching test. The grinding machine used is AG125-15DB Corded angle grinder. It is recommended to grind perpendicularly to the existing veins of the steel for better results. The outcome, depicted in (Figure 85), marks the completion of the initial grinding step.



Figure 85: Finished steel surface after 80-grit grind

1.2 Following the initial grind with the 80-grit disc, a step-by-step approach will be taken using progressively finer grit discs (120, 240, 500, and 1000) to achieve a very fine and mirror-like finish on the steel surface. It is crucial to maintain a perpendicular grinding direction to the previous step. The Makita Cordless Sander Wood Grinder, as shown in Figure 86, along with the corresponding grit discs, were utilized for these grinding stages.

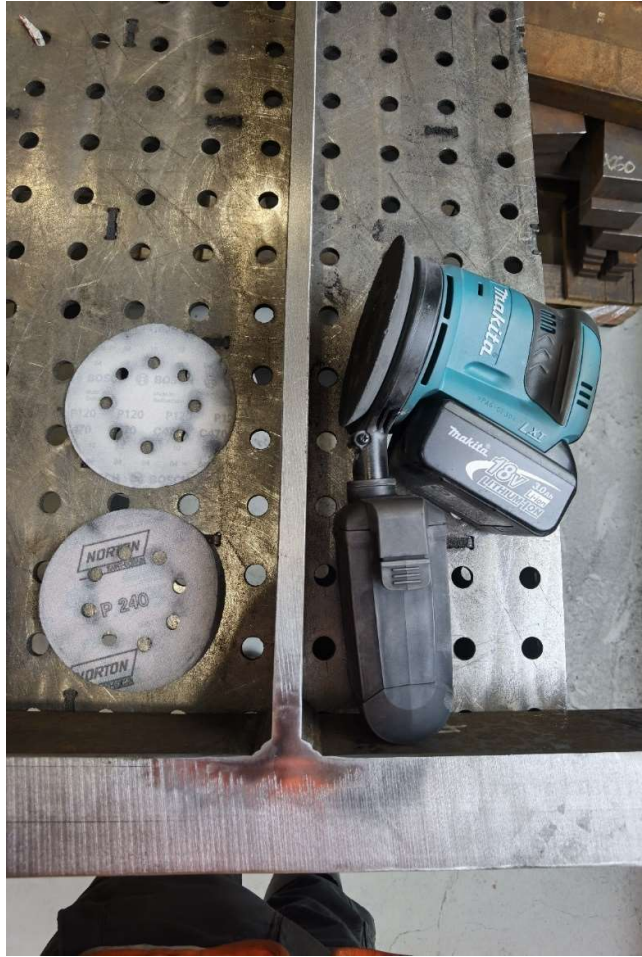


Figure 86: Finished steel surface after 120 and 240 grit grind



Figure 87: Finished steel surface ready for etching test

2. It is essential to blow away any dust and iron scurf using an air gun. Failure to remove these particles may result in undesirable interactions with the etchant, potentially compromising the quality of the etching surface.
3. Place the sample on the table with appropriate support, as the size of the sample is too large for any available container to place them in. The samples during the test are as shown in Figure 88.



Figure 88: the processing of the etching test

By supporting the sample on the table, the etchant can flow off the surface and also drain away from the gaps. It is crucial to properly support and hang the samples during the cleaning and washing process. If not supported correctly, small amounts of etchant could be trapped in gaps and react with the steel surface again, potentially leading to damage and ruining the etched surface.

4. Apply the etchant evenly on the steel surface, and if needed, add more to cover any areas where it may flow out from the sides or gaps. Wait patiently until the desired etching result is achieved, and then stop the etching process. The duration of etching in this test is approximately ten minutes.
5. After achieving the desired etched weld shape, proceed with the washing and cleaning steps as follows.

- 5.1 Gently tilt the sample to allow the etching fluid to flow out from the surface, and simultaneously, wash the sample from the top to ensure even and complete cleaning.
 - 5.2 Avoid blowing water directly onto the etched surface, as it may mix with the etchant and lead to uneven reactions on the steel surface, resulting in a messy appearance with different colours and marks.
 - 5.3 Thoroughly wash the gaps and concave areas with ample water to completely remove any remaining etchant. Small amounts of etchant hiding in these areas could react with the steel.
 - 5.4 If necessary, use a blow gun with gentle pressure to volatilize the surface water. Avoid blowing forcefully, as it may cause water capillaries to appear on the surface. The purpose of volatilizing the surface water is to minimize or reduce the lingering effects of the etchant on the steel.
 - 5.5 In some cases, when quick drying of the surface is required, gently dab the water with a tissue instead of wiping it off completely.
6. Immediately after completing the test, place paper or angle rulers and the corresponding series number on the sample, and promptly take a photo to capture the current condition before any further actions take place. As an illustration, the completed sample, FW8G0R0N4S3, is depicted in Figure 89 below.



Figure 89: record a sample after the etching test

6.0 Results and analysis:

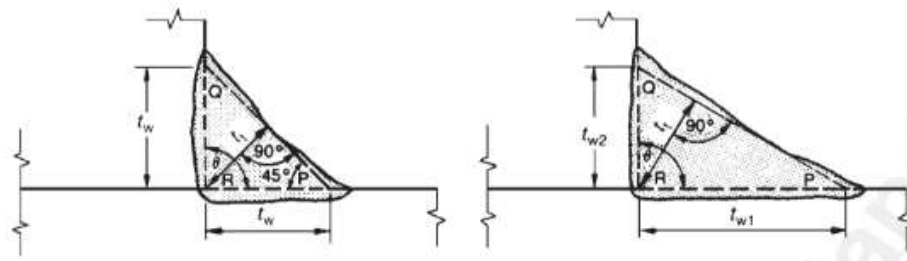
6.1 General goal:

The primary goal of this research is to either validate or compare the test results with the fillet weld design method outlined in section 9.7.3.10.3 of NZS3404:1997. The failure theory employed in Eq. 9.7.3.10 of NZS3404:1997 is based on Von Mises failure/yield criteria, which is suitable to be used for ductile material (the factor 0.6 in the NZS3404 weld design equation is close to the factor $(\frac{1}{\sqrt{3}} = 0.577$ in von Mises equation). During the tests, the loading was cyclic and increasingly continued until the samples reached the fracture range (or termination of the test).

6.2 Determination of the throat thickness of the samples:

The determination of throat thickness is a crucial aspect of weld-related research and weld design. In this research, two methods have been employed to determine the throat thickness of the samples, one based on physical dimension measurements and the other one based on the photos taken from the etched surface of the welds.

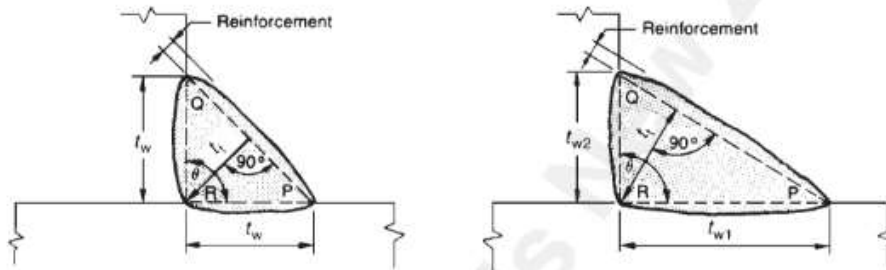
According to NZS3404:1997, section 9.7.3.4.1 and figure 9.7.3.1 as below, the throat thickness can be determined based on the physical measured weld leg length.



Equal leg fillet weld

Unequal leg fillet weld

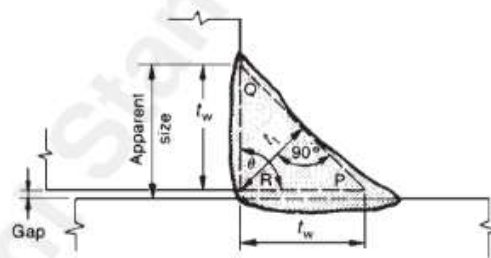
(a) Concave fillet welds



Equal leg fillet weld

Unequal leg fillet weld

(b) Convex fillet welds



(c) Fillet weld with root gap

Figure 90: The fillet weld size in NZS3404:1997

Furthermore, the AS/NZS 1554.1:2014 standard (AS/NZS, 1996b) provides an example (Figure 91, shown below) for determining the design throat thickness of compound welds with incomplete penetration welds.

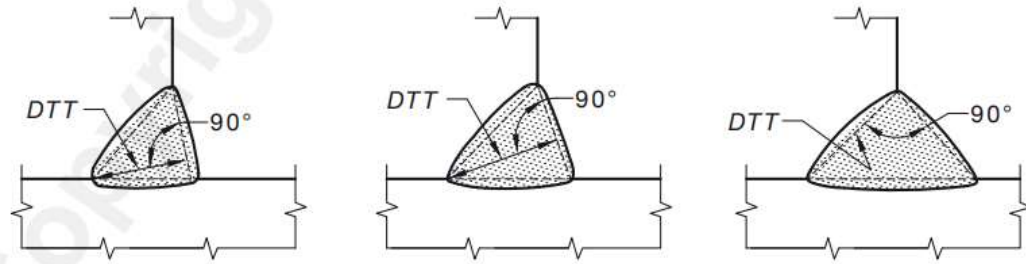


Figure 91: design throat thickness of compound welds with incomplete penetration welds

A key concept used in both processes is the "triangle inscribed within the cross section of the weld," which is essential for defining the weld capacity and geometry in weld design. However, the standard does not provide detailed instructions on how to precisely define these inscribed triangles.

For weld sizes of 8mm and 10mm, where only one weld path is used, determining the inscribed triangle is relatively straightforward since the weld shapes are mostly convex. However, for larger weld sizes like 12mm and 16mm, which may require three or more weld paths to complete, concavity on the weld edge can occur, leading to uncertainty in defining the inscribed triangle. To address this challenge, the experts from HERA, UOA, and AUT conducted collaborative group meetings and specified and agreed on a reasonable method to define the throat thickness and the finalized method is described in section 6.2.1.

6.2.1 Determination of the throat thickness from the etching test

The etching test offers several advantages. Through this test, we can evaluate critical aspects such as the size of Weld Penetration, Heat-Affected Zone (HAZ), and the boundary between the weld and parent metals. Additionally, the etching test serves as a valuable tool for identifying defects within the weld.

Furthermore, the etching test results aid in defining the "triangle inscribed within the cross section of the weld" (New Zealand Standard, 1997) even when dealing with irregularly shaped welds. This information is crucial for accurate assessment and welding design purposes.

The following steps outline the process of determining the throat thickness of a weld from the results of an etching test:

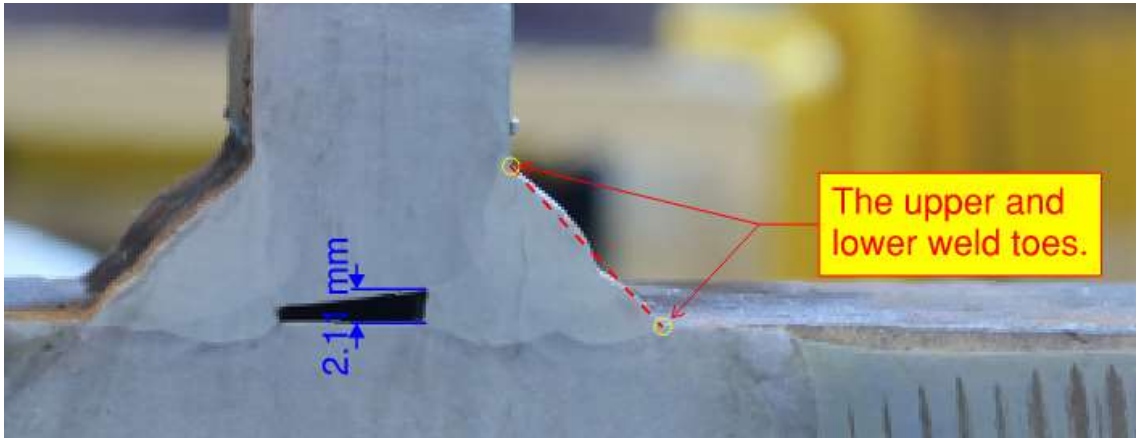


Figure 92: Two weld toes located

Step 1: locate two weld toes (see Figure 92) and then draw a line connecting the points of intersection between the upper and lower weld toes in the weld metal.

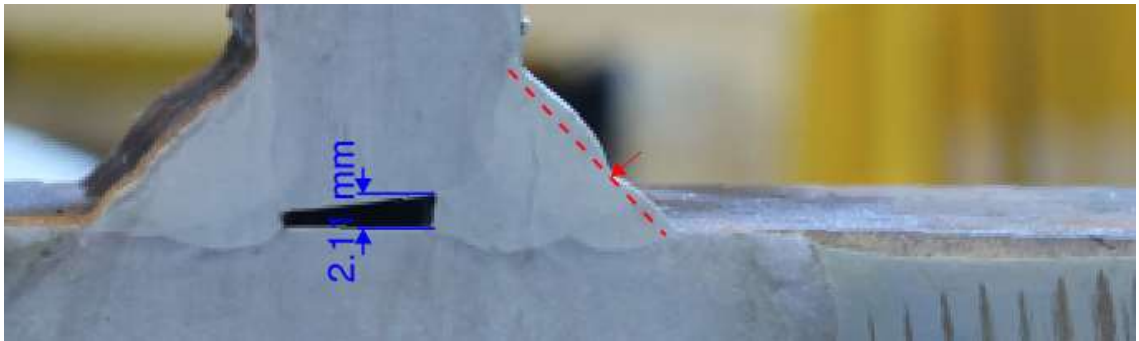


Figure 93: The line excluding concavity

Step 2: Next, draw another line parallel to it, excluding any concavity (underfill) present in the weld (see Figure 93).

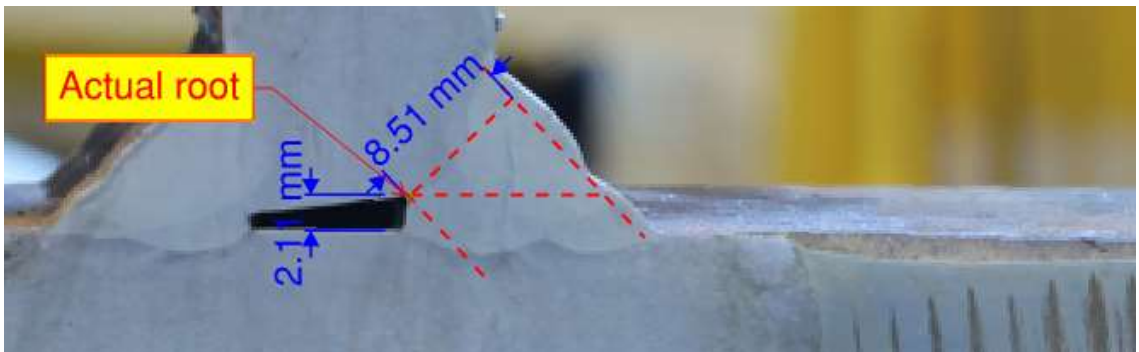


Figure 94: Find the throat thickness from the actual root

Step 3: Locate the actual root, which should be the shortest distance from the edge of the gap to the line drawn in Step 2 (see figure 93).

Step 4: The line starting from the actual root and perpendicular to the line in step 2 represents the throat line.

Two important assumptions must be noted for this method to be acceptable:

1. The throat line may intersect with the parent metal since both the weld and parent metals are capable of handling stress.
2. The actual root will be determined from the intersection of the weld and the horizontal leg. This emphasizes the significance and importance of the horizontal leg over the vertical leg.
3. After determining the throat thickness for each side, the values will be summed and then divided by four to obtain the average throat thickness for static analysis.

6.2.2 The physical measurements of the critical throat thickness

In an alternate scenario, when the fracture happened in the weld and forms an angle θ , or generally when the physical measurements of the weld are available with an assumed fracture angle of θ , we can employ a triangle-based calculation to ascertain the length of the critical thickness, as outlined below.

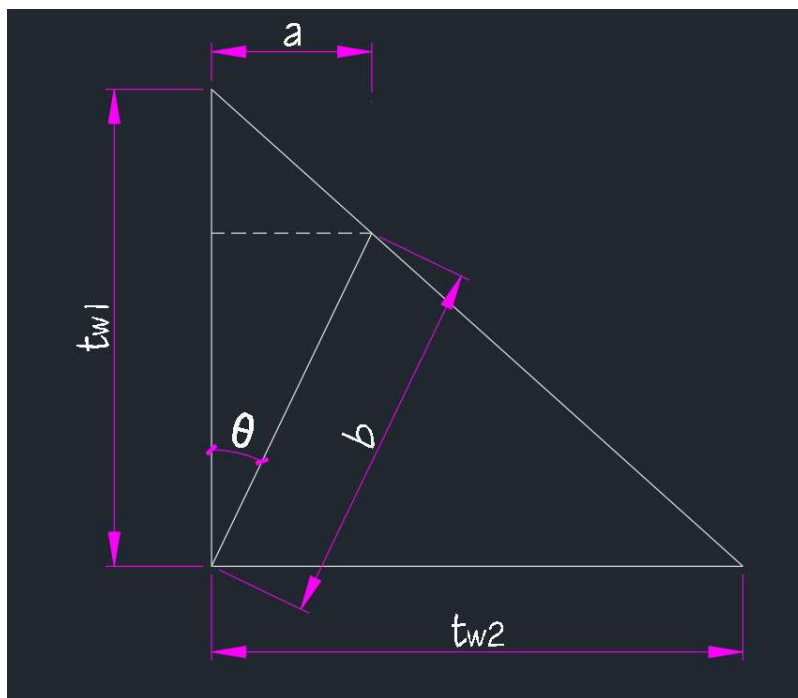


Figure 95: Finding the throat thickness from the weld legs (without gap)

t_{w1} : the leg of the fillet weld from the measurement

t_{w2} : the root of the fillet weld from the measurement

b : the fractured critical thickness.

b_1 : the fractured critical thickness of a weld sample with gaps

b_2 : the assistance line starting from root and parallel to b_1

θ : the fracture angle in weld from the measurement

a : assistance dash line which is parallel to t_{w2}

From the triangle, the following equation is valid.

$$\frac{b \times \sin \theta}{t_{w2}} = \frac{t_{w1} - b \times \cos \theta}{t_{w1}}$$

Hence b will be calculated as:

$$b = \frac{t_{w1} \times t_{w2}}{t_{w1} \times \sin \theta + t_{w2} \times \cos \theta}$$

Equation 27: Calculating the throat length using the leg dimensions and angle

For the case with gap in between parent metal, finding the length of the throat thickness

b_1 is explained below.

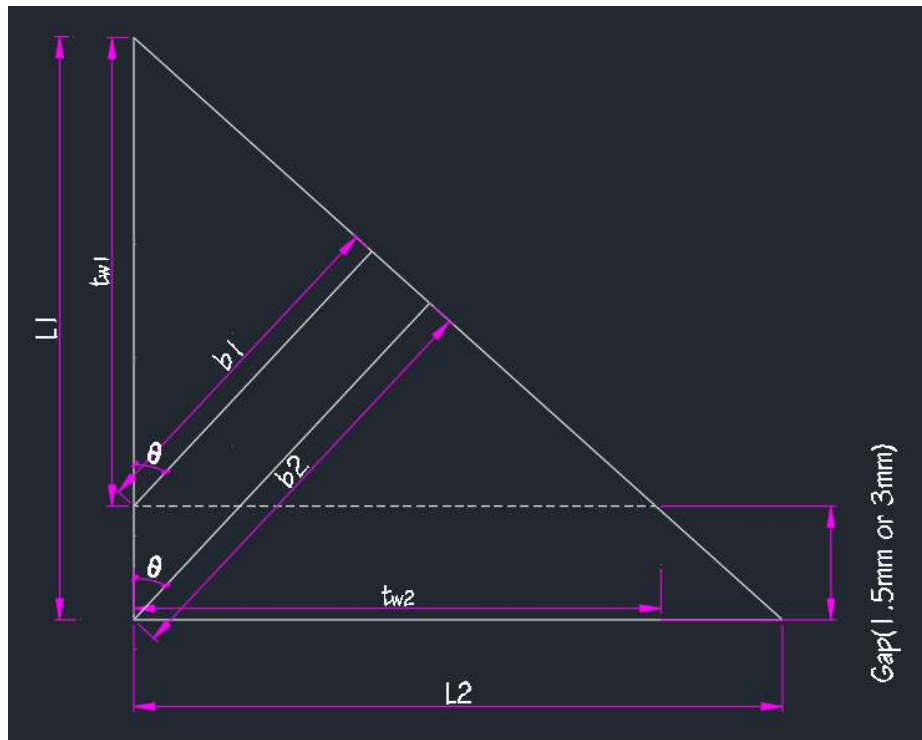


Figure 96: Finding the throat thickness from the L_1 and L_2 (with gap)

Because:

$$\frac{t_{w1}}{L_1} = \frac{b_1}{b_2} \text{ and } b_2 = \frac{L_1 \times L_2}{L_1 \times \sin \theta + L_2 \times \cos \theta}$$

$$\text{So } \frac{L_1 - \text{Gap}}{L_1} = \frac{b_1}{\frac{L_1 \times L_2}{L_1 \times \sin \theta + L_2 \times \cos \theta}}$$

$$b_1 = \frac{(L_1 - Gap) \times L_2}{L_1 \times \sin \theta + L_2 \times \cos \theta}$$

Equation 28: Calculating the throat thickness based on the weld dimensions L1 and L2, as well as the angle, for weld samples with a gap

6.3 Failure mode results and preliminary statistical analysis:

Based on the test results of the samples, three typical failure/test termination modes were observed:

1. Failure occurred due to fracture in the weld.
2. Failure occurred due to fracture in the web.
3. Termination of the test due to sample slipping. The summarized test results in terms of failure mode are as follows.

Table 5: The summary of the test failure mode

Sample type	Failure mode
FW12G0N1	1 fractured on stem (N1S1) and 4 failed in slip
FW10G3N2	5 fractured on stem and 1 failed in slip(N2S2)
FW10G0N3	4 fractured on weld(N3S1, N3S3,N3S5,N3S6) 1 failed in slip and 1 failed in buckling(N3S2 Trail test)
FW8G0N4	3 fractured on weld(N4S2,N4S3, N4S4) and 2 failed in slip
FW10G1.5N5	2 fractured on weld(N5S2,N5S5) and 3 failed in slip
FW16G0N6	1 fractured on stem(N6S1) and 4 failed in slip

An observation from the fractured test samples is that the fracture planes do not align with the code-specified weld throat, which is supposed to be the shortest weld throat according to NZS3404. Typically, test samples with smaller throat thickness is more prone to failure at the weld. It is evident that the actual throat thickness is larger than the theoretical throat thickness calculated from the design leg length.

6.3.1 Tested samples fractured in weld.

The weld stress capacity is calculated by dividing the maximum recorded load during the test by the critical plane, which is the product of the throat thickness and the weld length. To determine the actual weld capacity, the maximum actual weld demand during the test was divided by the critical plane, which is the throat thickness multiplied by the weld length. The stress capacity analysis takes into account three different throat

thickness obtained from the measurement methods of Cam Type Gage, etching test, and the failure plane of the weld.

Due to bending and twisting occurred during the test (partly due to post-elastic buckling of the stem) resulting in the weld failure, the fracture angles are not consistent along the length of the weld. The analysis utilizes the average angle of the four angles on each side of the fractured sample. For instance, in the tested sample FW10G0R1N3S1, as shown in the Figure 97 below, the average angle of the four is calculated as $(43.63^\circ + 16.47^\circ + 26.22^\circ + 31.02^\circ) \div 4 = 29.34^\circ$

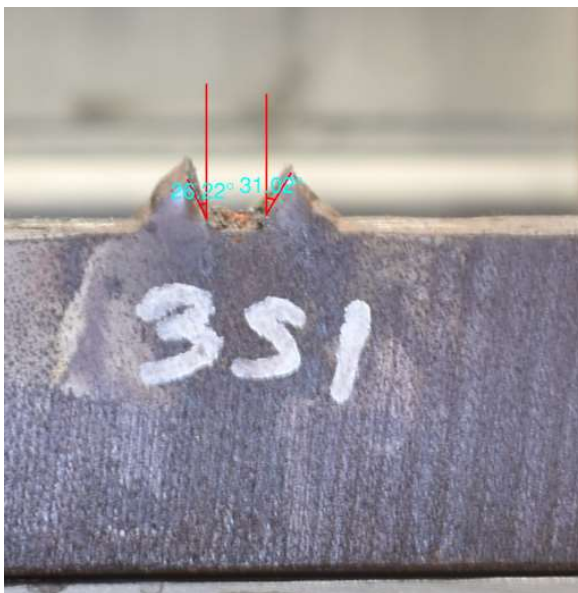


Figure 97: The measured angles from fractured sample

Table 6: The summary for tested samples fractured on weld (Note: the analysis includes both side of the fillet weld.)

Tested samples fractured on weld

Sample	Stem's top width (mm)	Stem's Bottom width (mm)	Theoretical throat Length-both sides-45° (mm)	Throat Length-both sides(mm)			Max actual weld total demand (kN)	Average angle of fracture on weld	Theoretical weld design force-both side-capacity (kN/mm)	Actual weld force-both side-capacity (kN/mm)			Ratio of actual capacity/theoretical force		
				Cam Scale (45°)	Etching Test	Failure plane (Actual degree)				Cam Scale	Etching Test	Fracture plane	Cam Scale	Etching Test	Fracture plane
FW8G0N4S2(M24)	70	68.2	11.31	13.92	15.71	15.60	493.88	14.99	2.66	5.89	5.22	6.06	2.21	1.96	2.28
FW8G0N4S3(M24)	69.1	69.4	11.31	14.21	15.03	15.43	506.37	17.44	2.66	5.81	5.49	6.03	2.18	2.06	2.27
FW8G0N4S4(M20)	72.3	74.3	11.31	14.62	14.86	16.65	533.02	13.06	2.66	5.55	5.46	5.74	2.09	2.05	2.16
FW10G0N3S1(M24)	60.3	61	14.14	14.30	15.59	15.47	453.15	29.34	3.33	7.35	6.74	5.64	2.21	2.03	1.70
FW10G0N3S3(M24)	61.9	60.3	14.14	13.62	15.99	12.71	444.86	29.84	3.33	7.66	6.53	6.80	2.30	1.96	2.05
FW10G0N3S5(M24)	63.3	60.4	14.14	14.30	16.53	14.82	416.44	32.78	3.33	6.82	5.90	5.39	2.05	1.77	1.62
FW10G0N3S5(M24)	63	63.3	14.14	13.54	16.20	14.16	447.89	28.16	3.33	7.39	6.18	5.91	2.22	1.86	1.78
FW10G1.5N5S2(M24)	69.4	68.7	12.02	16.90	17.30	17.25	503.14	26.03	2.83	5.21	5.09	5.08	1.84	1.80	1.80
FW10G1.5N5S5(M24)	68.7	71.8	12.02	16.54	17.69	17.43	528.66	18.91	2.83	5.35	5.00	5.32	1.89	1.77	1.88

The second and third columns show the size of the stem. The “Theoretical Throat Length - Both Sides - 45°” is the theoretical throat length for a certain given weld size, derived from the weld root length using the cosine of 45°. The “Throat Length - Both Sides (mm)” is the throat length results obtained through three different methods: cam scale, etching test, and measurement by failure plane.

The “Max Actual Weld Total Demand” is the maximum load recorded from the actuator during the test, prior to weld failure. The “Average Angle of Fracture on Weld” is the average angle of the failure plane on both sides.

The “Theoretical Weld Design Force” is calculated based on the theoretical weld size. The “Actual Weld Force - Both Sides - Capacity” is calculated as follows:

$$\text{Actual weld force – Both Side – Capacity} = \frac{\text{Max Actual Weld Total Demand}}{\text{Stem's bottom Wid} \times \text{Thr length-both-s from cam scale, etching test or fracture plan}} \times \text{Fillet weld size} \times \sqrt{2}$$

For example, for an 8mm fillet weld on both sides, the fillet weld size is $8\text{mm} \times 2 = 16\text{mm}$.

The last column, “Ratio of Actual Capacity / Theoretical Capacity,” shows ratio of Actual Weld Force - Both Sides - Capacity to the Theoretical Weld Design Force - Both Sides - Capacity.

According to the test records, it is noteworthy that the loading range causing fracture on the weld for these samples falls within 416.44-533.02kN, and it is worth noting that the 8mm weld size exhibits the highest capacity, which is not expected.

All the samples with weld fractures are either equal to or less than 10mm, and there were no instances of fractures in samples with 12mm and 16mm weld sizes.

Upon comparing the ratio of actual capacity to theoretical capacity, it becomes evident that even when fractures occur on the weld, the actual weld capacity remains significantly higher than the theoretical capacity predicted by the weld design in NZS3404:1997.

Furthermore, the fracture surfaces exhibit non-uniform patterns, suggesting the presence of complex stresses within the weld. Consequently, it becomes challenging to compare these stress distributions between each sample.

The chart provided below offers a summary and comparison of various capacities based on three measurements for a tested sample: cam scale, etching test, and fracture plane from the fracture angle. This figure is from the data of the group FW8 in table 6.

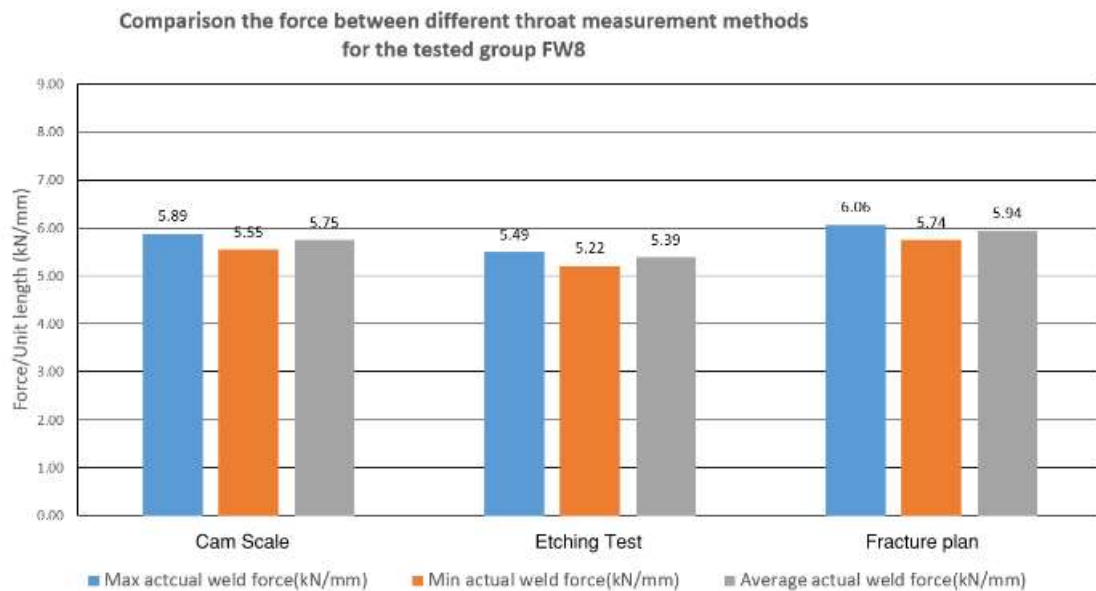


Figure 98: The comparison of the force capacity between different measurement methods for group FW8

From the analysis of the tested samples, certain patterns and regularities have been identified, which differ from previous research findings.

In cases where the samples failed from the weld, the fracture angles were primarily observed to range from 13.06° to 32.78°. This is notably different from the assumed

fracture surface angle used in the current weld design according to NZS3404, which is set at 45°.

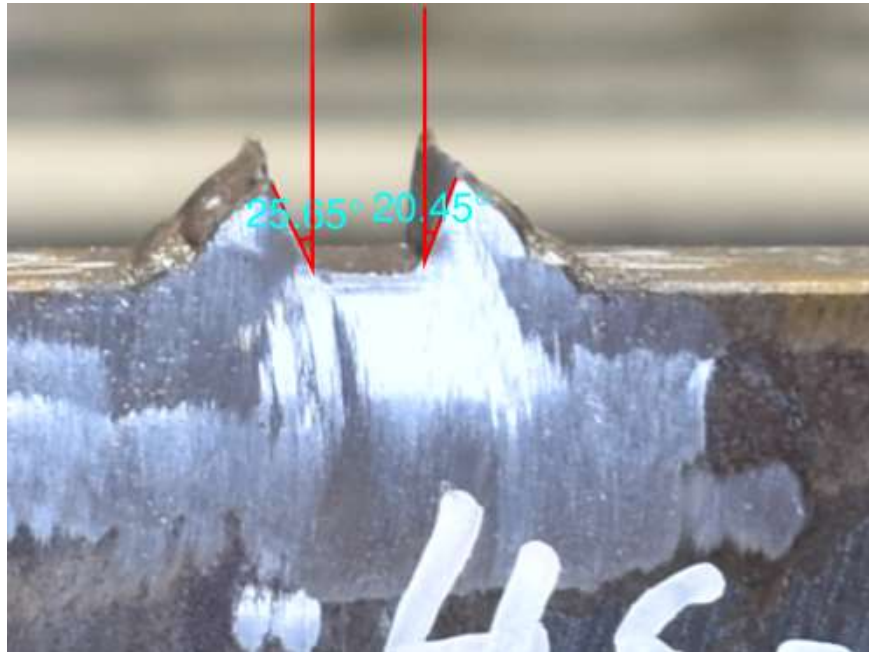


Figure 99: the fracture on weld of the sample FW8G0R1N4S2

6.3.2 Tested samples fractured in stem

In the samples that failed from the stem plate, the fracture paths were predominantly observed to extend from the two weld faces and intersect in the middle of the stem. The angles of this intersection were measured to be approximately 100°, as depicted below.

Table 7: The summary for tested samples fractured in stem. (Note: the analysis includes both side of the fillet weld.)

Tested samples fractured on stem

Sample	Stem's top width (mm)	Stem's Bottom width (mm)	Theoretical throat Length-both sides-45° (mm)	Throat Length-both sides (mm)		Max actual weld total demand (kN)	Load when fracture (kN)	Average angle of fracture on stem	Theoretical weld design force-both side-capacity (kN/mm)	Actual weld demand-both side(kN/mm)		Ratio of actual demand/theoretical demand	
				Cam Scale (45°)	Etching Test					Cam Scale	Etching Test	Cam Scale	Etching Test
FW12G0N1S1(M24)	72.5	73.5	16.97	18.31	18.12	536.78	180.08	99.42	3.99	6.77	6.84	1.70	1.71
FW12G3N2S1(M24)	61.8	62.8	12.73	14.92	19.75	442.37	340.32	97.31	2.99	6.01	4.54	2.01	1.52
FW12G3N2S3(M24)	60.5	61	12.73	15.06	20.46	440.56	358.74	96.48	2.99	6.10	4.49	2.04	1.50
FW12G3N2S4(M24)	61.8	62.4	12.73	15.05	20.28	452.13	352.68	95.04	2.99	6.13	4.55	2.05	1.52
FW12G3N2S5(M24)	57.7	56.8	12.73	16.22	20.23	444.93	237.99	96.42	2.99	6.15	4.93	2.05	1.65
FW12G3N2S6(M24)	60.7	60.7	12.73	14.94	20.39	460.24	278.91	95.36	2.99	6.46	4.73	2.16	1.58
FW16G0N6S1(M24)	73.2	72.6	22.63	24.28	22.94	543.25	222.58	107.96	5.32	6.97	7.38	1.31	1.39

Based on the test records, the loading range that caused fractures on the stem was between 440.56-543.25kN. The actual weld demand was determined to be in the range of 4.54-7.38kN/mm. All the samples that fractured on the stem had weld sizes of 12mm and 16mm. When comparing the ratio of actual demand to theoretical capacity, all sample ratios were over 1.2, except for the 16mm weld size samples, however it is worth noting that given the fracture occurred in stem and not weld, it is not possible to identify precisely the weld fracture load (capacity) of such samples but to conclude they are stronger than the maximum recorded values from the tests. These ratios also demonstrate that the actual capacity of the weld, as determined in this test, is higher than the theoretical capacity calculated from the weld design in NZS3404:1997.



Figure 100: The fracture in stem of the sampleFW12G3R1N2S5

6.3.3 The test failed (terminated) due to slipping.

Table 8: The summary for tested samples failed (terminated) due to slipping (Note: the analysis includes both side of the fillet weld.)

Tested samples slipping in test

Sample	Stem's top width (mm)	Stem's Bottom width(mm)	Theoretical throat Length-both sides-45° (mm)	Throat Length-both sides(mm)		Max actual weld total demand (kN)	Theoretical weld design force-both side-capacity (kN/mm)	Actual weld demand-both side(kN/mm)		Ratio of actual demand/theoretical demand	
				Cam Scale 45°	Etching Test			Cam Scale	Etching Test	Cam Scale	Etching Test
FW8G0N4S1(M20)	76.5	73.8	11.31	14.00	15.47	380.78	2.66	4.17	3.77	1.57	1.42
FW8G0N4S5(M20)	78	77.2	11.31	13.70	15.14	462.96	2.66	4.95	4.48	1.86	1.68
FW10G0N3S4(M24)	62.5	62.1	14.14	13.53	16.37	467.46	3.33	7.87	6.51	2.36	1.96
FW10G1.5N5S1(M24)	73.2	70.7	12.02	17.13	18.15	521.99	2.83	5.18	4.89	1.83	1.73
FW10G1.5N5S3(M20)	77.4	77.4	12.02	17.23	17.51	512.71	2.83	4.62	4.55	1.63	1.61
FW10G1.5N5S4(M20)	74	76.6	12.02	16.77	17.40	469.64	2.83	4.39	4.24	1.55	1.50
FW12G0N1S2(M20)	74.9	76.5	16.97	18.89	18.28	496.75	3.99	5.83	6.03	1.46	1.51
FW12G0N1S3(M20)	77	77.5	16.97	18.92	18.26	432.18	3.99	5.00	5.18	1.25	1.30
FW12G0N1S4(M24)	72.8	68.1	16.97	19.72	17.56	511.76	3.99	6.47	7.26	1.62	1.82
FW12G0N1S5(M24)	69.3	70.6	16.97	18.80	18.52	513.89	3.99	6.57	6.67	1.65	1.67
FW12G3N2S2(M24)	63.2	62.6	12.73	16.02	20.43	427.62	2.99	5.43	4.26	1.81	1.42
FW16G0N6S2(M20)	77.1	77	22.63	23.79	23.33	334.59	5.32	4.13	4.21	0.78	0.79
FW16G0N6S3(M20)	75	74.6	22.63	24.56	23.73	447.85	5.32	5.53	5.73	1.04	1.08
FW16G0N6S4(M24)	71.7	68.4	22.63	24.26	22.97	499.19	5.32	6.81	7.19	1.28	1.35
FW16G0N6S5(M24)	66.4	73.1	22.63	24.94	23.77	523.76	5.32	6.50	6.82	1.22	1.28

Based on the test records, the loading range at which these samples started slipping was between 334.59-523.76kN. The actual weld demand during slipping ranged from 3.77-7.87kN/mm. The slipping may have occurred because the stem began buckling inelastically, and the bottom of the clamping angles experienced horizontal load expanding/separating them while resisting against the inelastic buckling of the stem. In most cases, stem buckling indicates that the stem was loaded beyond its yield capacity. In such tests, the deformations experienced by the samples are expected to be significantly more severe than a weld in a seismic resisting system during a severe earthquake. It is also worth noting that given the tests were terminated due to sliding, it is not possible to identify precisely the weld fracture load (capacity) of such samples but to conclude they are stronger than the maximum recorded values (i.e. sliding force) from the tests.

When comparing the actual weld demand with the theoretical capacity of the weld, the actual weld demand was found to be larger, even with tests being terminated due to sliding, except for three cases: 6-S2, 6-S3, and 6-S5. Additionally, considering the overall test results and the weld size, it is highly probable that the 16mm weld size sample would be strong enough to avoid fracturing in the weld. The ratios of actual demand to theoretical capacity also demonstrate that the actual capacity of the weld is

expected to be significantly higher than the theoretical capacity derived from the weld design in NZS3404:1997.



Figure 101: Failed (terminated) in Slipping of the test sampleFW10G0R0N3S4

6.4 Comparison between the actual capacity and/or demand and theoretical capacity

Table 9: The ratio of the weld actual capacity and/or demand to the theoretical capacity (red: fracture in weld, orange: fracture in stem (i.e. web), green: test terminated due to sliding, and black: the sample used in first trail test)

The ratio of the weld actual capacity and/or demand to theoretical capacity

Sample	Ratio of actual capacity and/or demand to theoretical capacity	
	Cam Scale	Etching Test
FW8G0N4S1(M20)	1.57	1.42
FW8G0N4S2(M24)	2.21	1.96
FW8G0N4S3(M24)	2.18	2.06
FW8G0N4S4(M20)	2.09	2.05
FW8G0N4S5(M20)	1.86	1.68
FW10G0N3S1(M24)	2.21	2.03
FW10G0N3S2(M24)	1.98	1.88
FW10G0N3S3(M24)	2.30	1.96
FW10G0N3S4(M24)	2.36	1.96
FW10G0N3S5(M24)	2.05	1.77
FW10G0N3S6(M24)	2.22	1.86
FW10G1.5N5S1(M24)	1.83	1.73
FW10G1.5N5S2(M24)	1.84	1.80
FW10G1.5N5S3(M20)	1.63	1.61
FW10G1.5N5S4(M20)	1.55	1.50
FW10G1.5N5S5(M24)	1.89	1.77
FW12G0N1S1(M24)	1.70	1.71
FW12G0N1S2(M20)	1.46	1.51
FW12G0N1S3(M20)	1.25	1.30
FW12G0N1S4(M24)	1.62	1.82
FW12G0N1S5(M24)	1.65	1.67
FW12G3N2S1(M24)	2.01	1.52
FW12G3N2S2(M24)	1.81	1.42
FW12G3N2S3(M24)	2.04	1.50
FW12G3N2S4(M24)	2.05	1.52
FW12G3N2S5(M24)	2.05	1.65
FW12G3N2S6(M24)	2.16	1.58
FW16G0N6S1(M24)	1.31	1.39
FW16G0N6S2(M20)	0.78	0.79
FW16G0N6S3(M20)	1.04	1.08
FW16G0N6S4(M24)	1.28	1.35
FW16G0N6S5(M24)	1.22	1.28

6.5 Summary of the experimental results

In this section, the experimental data will be summarized graphically:

Note: The capacity of the stem in these Figures pertain to the stem's elastic capacity per unit millimetre.

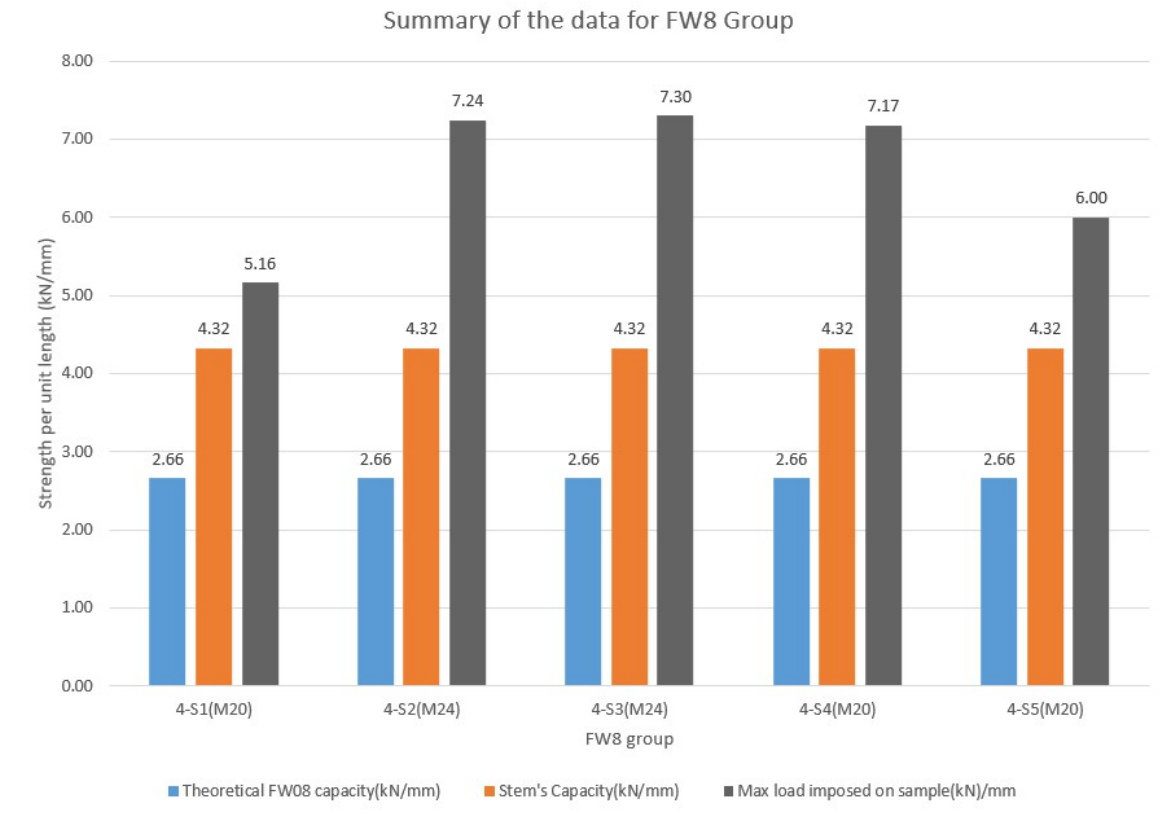


Figure 102: Summary of the data for FW8 Group



Figure 103: Summary of the data for FW10 group

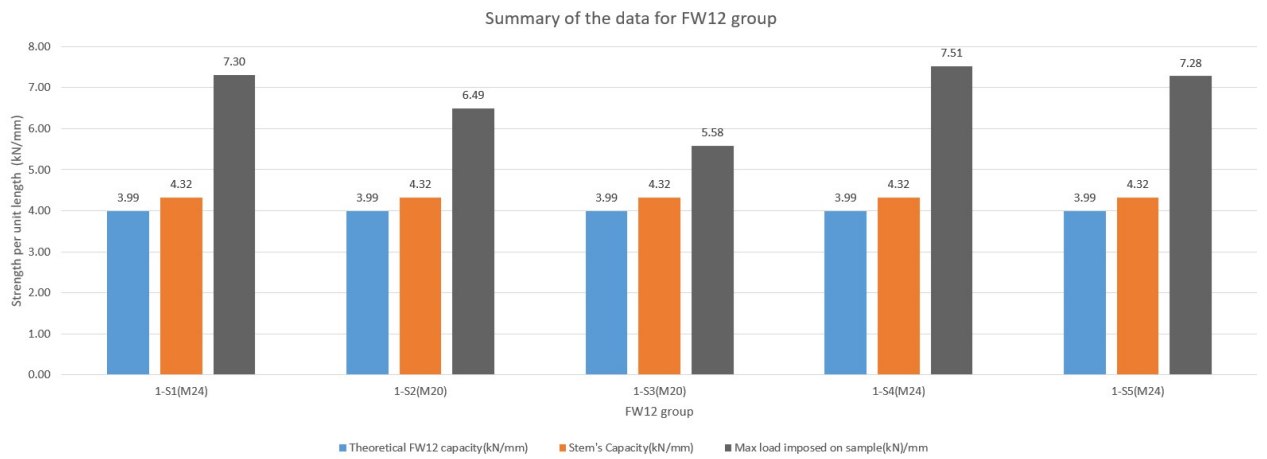


Figure 104: Summary of the data for FW12 group

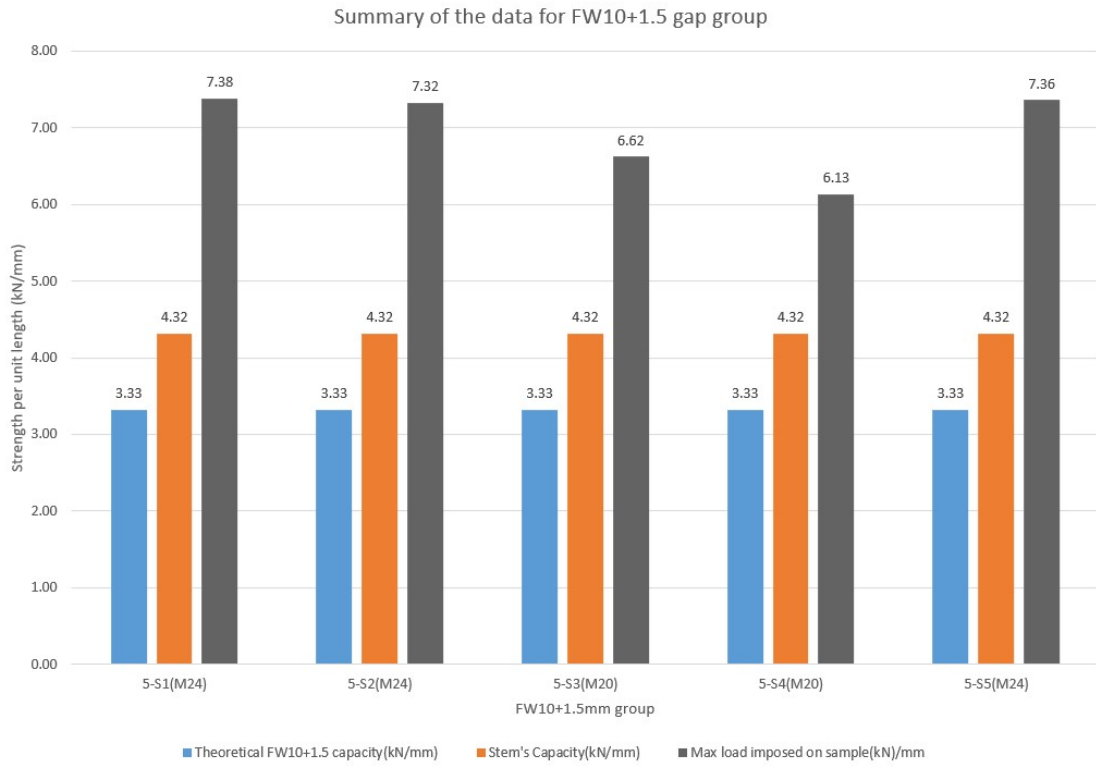


Figure 105: Summary of the data for FW10+1.5 gap group

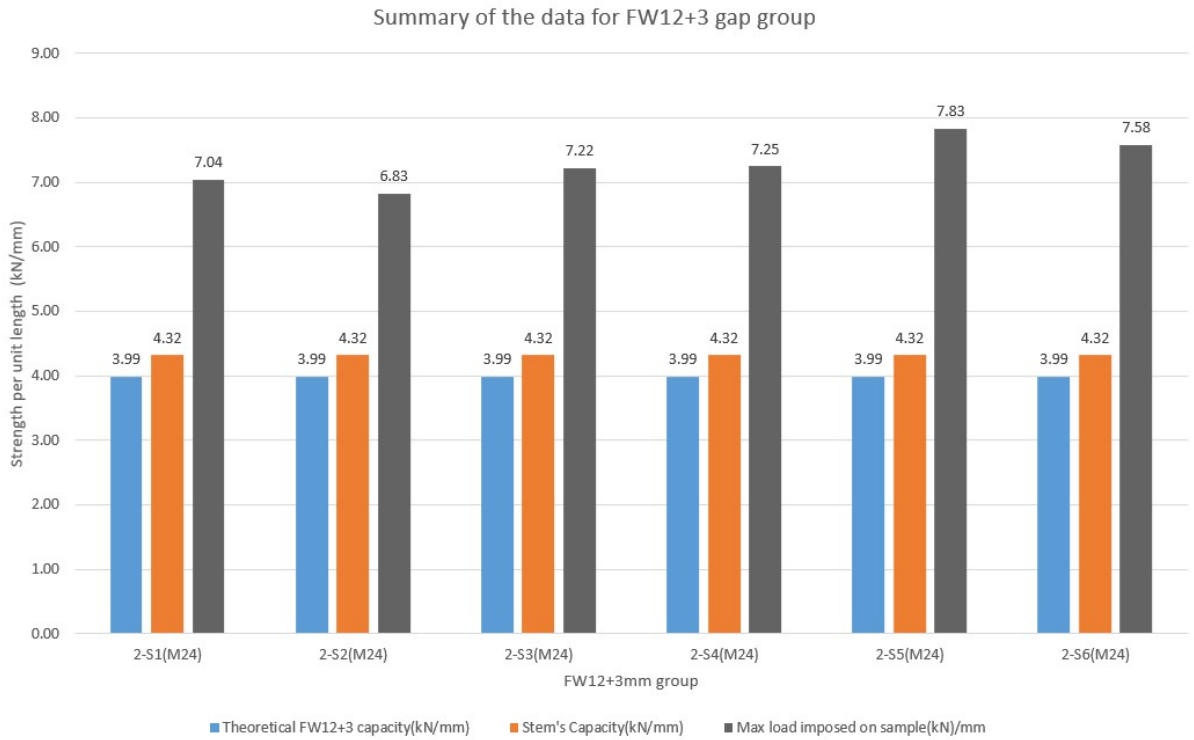


Figure 106: Summary of the data for FW12+3 gap group

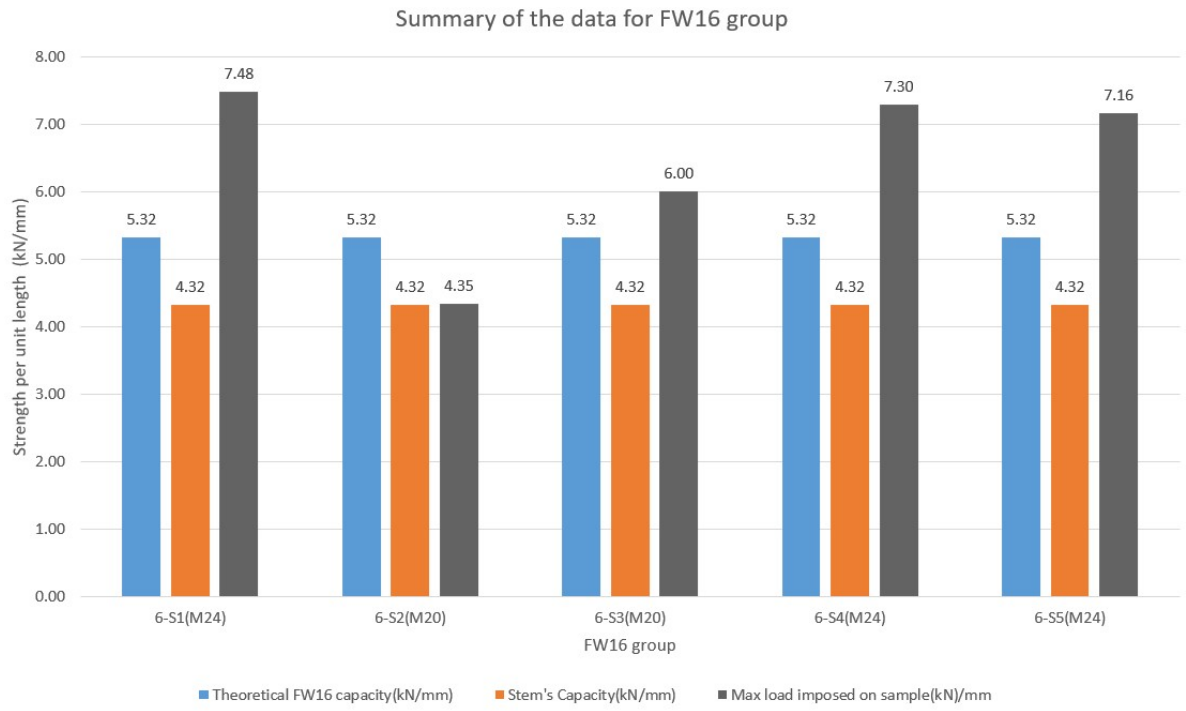


Figure 107: Summary of the data for FW16 group

7.0 Conclusion and recommendations

7.1 Further potential improvements and/or considerations regarding the test setup

Although a conservative friction factor of 0.3 was used to calculate the friction force between the clamping angle and the stem web, slipping still occurred during the test in some cases. This slipping could be attributed to factors such as too small coefficient of friction due to the particular surface profile, and/or stem web's post-elastic in compression resulting in separating the clamping angles and reducing contact between them and the stem. However, the setup design could be enhanced to achieve a better clamping. For instance, incorporating overly strong clamping angles and bolts could lead to improved performance.

Despite using a very strong flange base plate with cross sectional dimensions of 60x60, there is still some relative movement observed when pulling the T-joint sample by the actuator. If the intention is to measure relative displacement, it is recommended to explore the installation of LVDT (Linear Variable Differential Transformer) on the top surface of the flange base plate. Additionally, considering the use of an even larger flange base plate could reduce the out of plane deformations of it.

7.2 Further research

An area of investigation could be the methods used to determine the throat thickness. The shape of the gaps between parent metals and weld can significantly influence the stress distribution in the weld during loading. For instance, if the gaps are triangular or semicircular in shape, the pattern of fractures may differ, and the fractures may not always initiate from the top of the gaps.

Moreover, examining the ratio between weld strength and tensile strength may be valuable. The results indicate that the procedure used in NZS3404 is highly conservative. It may be worth considering adjusting this approach in weld design to allow for a reduction in fillet weld size for a given load while maintaining adequate safety margins.

It is important to note that this research focuses solely on the weld connection, for example of a steel column and beam flange, under seismic loading. To broaden the scope, future research can expand to include the entire beam connection, encompassing the whole beam or the weld group connection. This expansion can provide a more comprehensive understanding of structural behaviour and enhance the overall design practices for beam connections.

7.3 Conclusion

From the test results, it is evident that the weld fracture did not occur in these experiments when the weld size was equal to or greater than 12mm for the 16mm thick stem used in these experiments. All experiments that led to weld fracture suggested significantly higher capacity for the weld compared with that recommended by the NZS3404. There was no experiment suggesting the welds are under designed following NZS3404. Hence, it is highly recommended through this research, to modify the NZS3404 design recommendations making them less conservative and more cost-effective. This can be achieved through analysis of the results for this research reported in this thesis and included in the Masters' research compendium with all details.

8.0 Bibliography

- AISC. (2016). *Seismic provisions for structural steel buildings*.
- AS/NZS. (1996a). AS/NZS 1252: 1996 High-strength steel bolts with associated nuts and washers for structural engineering. In: SNZ Wellington, New Zealand.
- AS/NZS. (1996b). AS/NZS 1554.1:2014: Part 1: Welding of steel structures, Structural steel welding. In: SNZ Wellington, New Zealand.
- European Committee for Standardization. (2005). *EN 1993-1-8:2005: Eurocode 3: Design of steel structures - Part 1-8: Design of joints*. Brussels, Belgium: CEN.
- Cowie, K., & Fussell, A. (2015). Specifying Impact Toughness of Steel Plates for End Plate Connections in Seismic Lateral Resisting Frames.
- Dong, P. (2001). A robust structural stress procedure for characterizing fatigue behavior of welded joints. *SAE transactions*, 89-100.
- Eom, T.-S., Park, H.-G., & Lee, C.-H. (2013). Simplified Method for Estimation of Beam Plastic Rotation Demand in Special Moment-Resisting Steel-Frame Structures. *Journal of Structural Engineering*, 139(11), 1906-1916.
- Fenwick, R., & Dhakal, R. (2007). Material strains and relevance to seismic design.
- Heravi, H. T. (2019). Seismic Evaluation of Welded In *SESOC Confrence 2019- Challenging the Profession 19 & 20 August 2019 SkyCity Convention Centre, Auckland*. Auckland: Auckland University.
- Hyland, C., Cowie, K., & Bird, G. (2010). Structural Steelwork Connections Guide Connection Tables. *SCNZ Report 14.2 2007*.
- ISO, P. TR 16060:(2014). *Destructive tests on welds in metallic materials—Etchants for macroscopic and microscopic examination*.
- Masi, A., Danisi, A., Losito, R., Martino, M., & Spiezia, G. (2011). Study of magnetic interference on an LVDT: FEM modeling and experimental measurements. *Journal of Sensors*, 2011.
- Moynihan, M. C., & Allwood, J. M. (2014). Utilization of structural steel in buildings. *Proceedings of the Royal Society A: Mathematical, Physical and Engineering Sciences*, 470(2168), 20140170.
- Nie, C., & Dong, P. (2012). A traction stress based shear strength definition for fillet welds. *The Journal of Strain Analysis for Engineering Design*, 47(8), 562-575.
- Standards New Zealand. 1997. *NZS 3404:1997: Steel structures standard*. Wellington, New Zealand: Standards New Zealand.
- Ramhormozian, S. (2020a). *Course Notes for ENBU706-2020- Design of Bolted Connections*. (Auckland: Auckland University of Technology.)
- Ramhormozian, S. (2020b). *Course Notes for ENBU706-2020- Members Subject to Compression*. (Auckland: Auckland University of Technology.)
- Ramhormozian, S. (2020c). *Course Notes for ENBU706-2020- Welded Connection Design*. (Auckland: Auckland University of Technology.)
- Ramhormozian, S., Clifton, G., & Cowie, K. (2016). Proposed changes on NZS 3404 specified part-turn method of tensioning high strength friction grip (HSFG) property class 8.8 bolts. *Reducing Risk Raising Resilience*.
- Ramhormozian, S., Clifton, G., Nguyen, H., & Cowle, K. (2015). *Determination of the required part-turn of the nut with respect to the number of free threads under*

the loaded face of the nut in fully tensioned high strength friction grip property class 8.8 bolts. Paper presented at the Proceedings of the Steel Innovations Conference.

- Ramhormozian, S., Clifton, G. C., MacRae, G. A., Davet, G. P., & Khoo, H.-H. (2019). Experimental studies on Belleville springs use in the sliding hinge joint connection. *Journal of Constructional Steel Research*, 159, 81-94.
- Society, A. W. (2007). AWS B4. 0: 2016: standard methods for mechanical testing of welds. In: AWS New York.
- Standard, S. S. (2007). NZS 3404: 1997. *Standards New Zealand, Wellington.*
- Sugitani, D., & MOCHIZUKI, M. (2013). Experimental Study on Effects of Root Gap and Fillet Size of Welds on Joint Strength. *Quarterly Journal of the Japan Welding Society*, 31(4), 104s-108s.
- Venture, S. J. (1997). Protocol for fabrication, inspection, testing, and documentation of beam-column connection tests and other experimental specimens. *Rep. No. SAC/BD-97, 2.*
- Civil 313. (2016). Yieldline Theory and Application. [Class material].

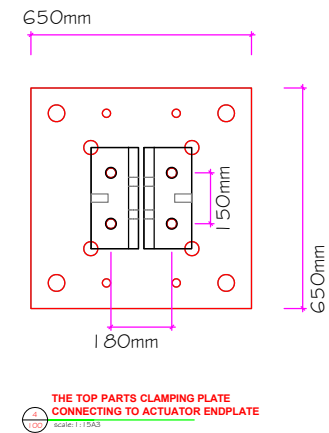
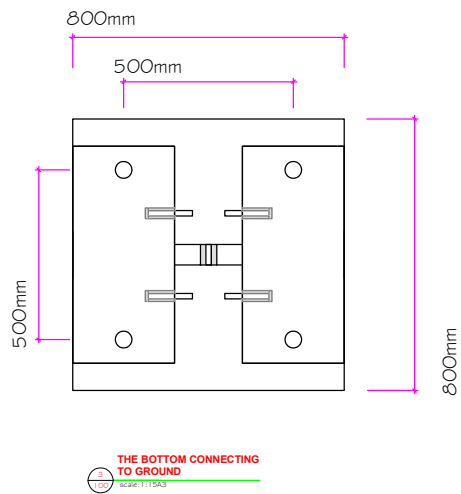
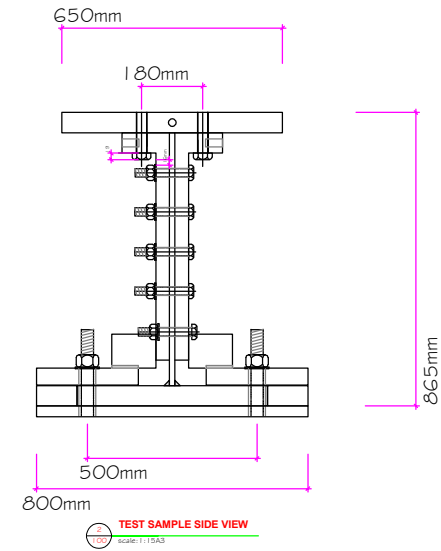
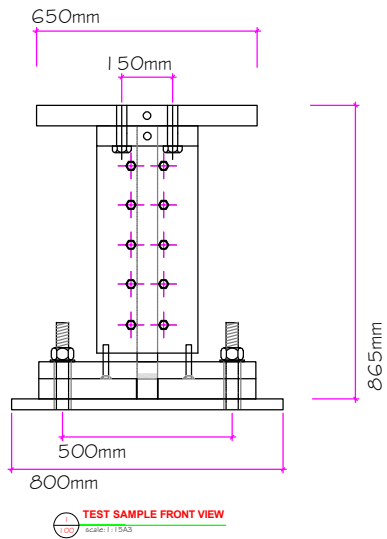
Appendix A - Specimens Design Drawing

SPECIMENS DRAWING

FOR PROJECT:

**EXPERIMENTAL TESTING OF FILLET WELDED T-JOINTS TO EVALUATE
THE NZS3404 SPECIFIED SAFETY FACTORS FOR SEISMIC FILLET WELDS**

- S100 - GENERAL SETUP AND LAYOUT**
- S101 - TEST SPECIMENS AND SET UP DRAWING**
- S102 - TENSILE TEST OF BEASE MATERIAL**
- S201 - WHOLE PIECE PLAN**
- S202 - T-FILLET WELDED TEST SPECIMEN**
- S201-1 - WHOLE PIECE PLAN FOR TEST SPECIMENS WITH GAP**
- S202-1 - T-FILLET WELDED TEST SPECIMEN WITH GAP**
- S203 - MANUFACTURE DRAWING FOR BACK UP PLATE**
- S204 - MANUFACTURE DRAWING FOR CLAMPING ANGLE**
- S205 - MANUFACTURE DRAWING FOR COVER PLATE AND THE ITEM TABLES**
- S206 - SUMMARY FOR PARTS**
- S207 - MANUFACTURE DRAWING FOR GROUND PROTECTION STEEL PLATE**

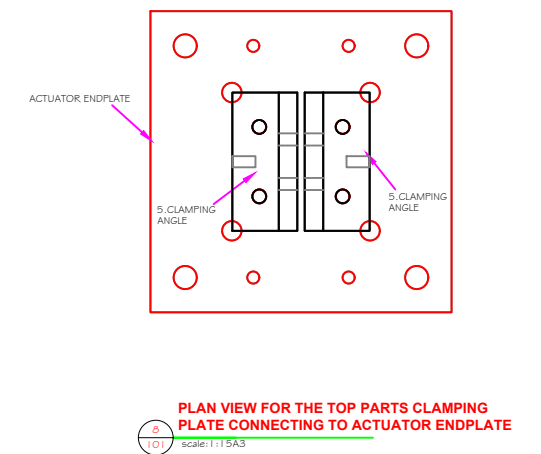
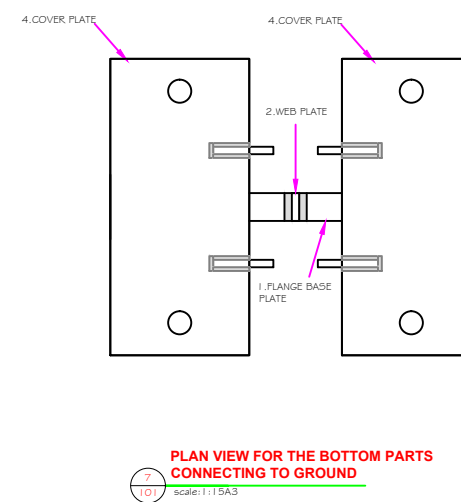
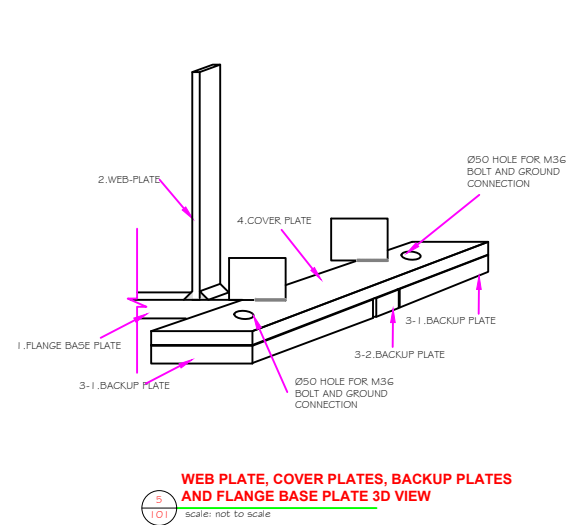
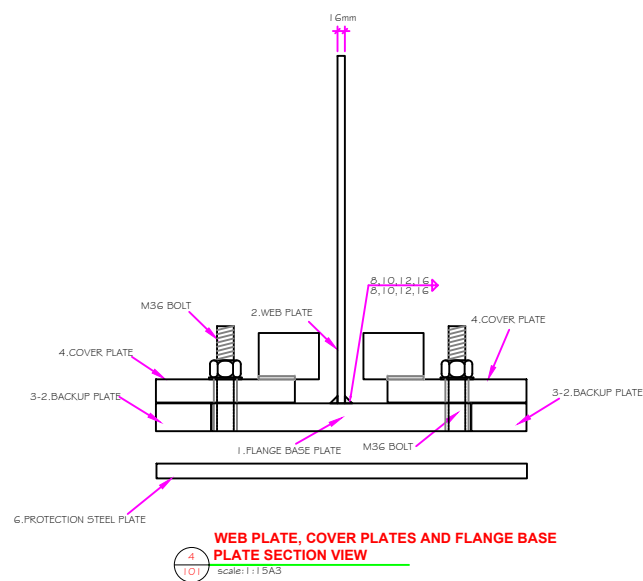
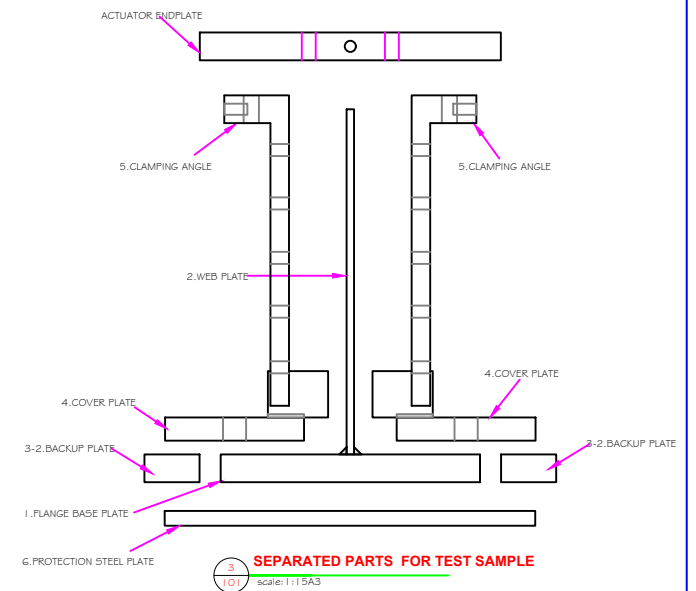
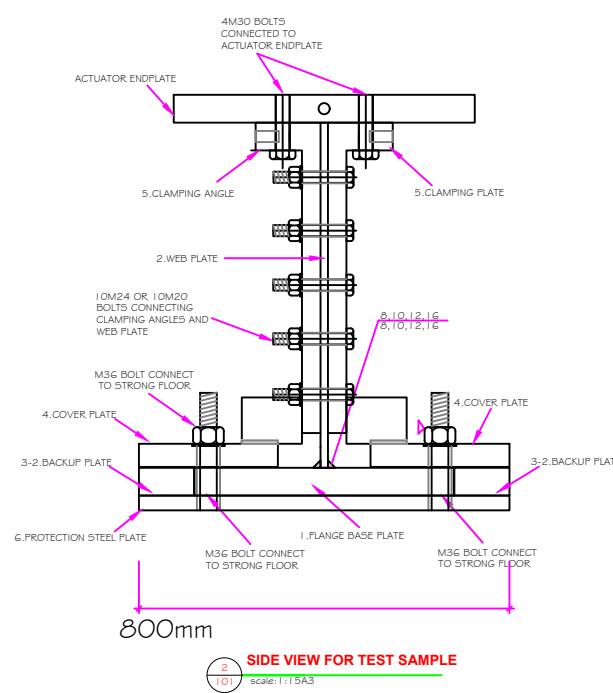
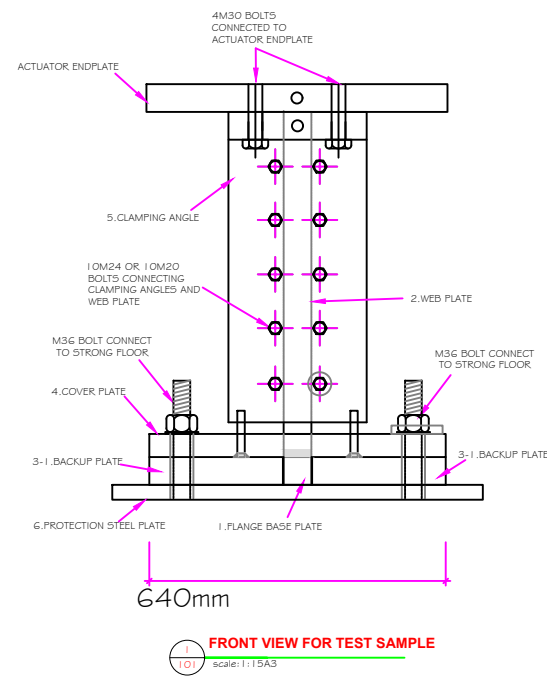


AUT
School of Engineering computer and Mathematical Sciences
Built Environment Engineering

DRAWING TITLE:
General setup and layout

PROJECT TITLE:
Experimental testing of fillet welded T-joints to evaluate the NZS3404 specified safety factors for seismic fillet welds

DRAWN	CHECKED	DRAWING NUMBER	DATE	
Mark Zhang	Dr. Shahab Ramhormozian	100	SCALE	REV.
			1:15	



Note:

- Verify all dimensions prior to commencing any works.
- Either plasma or laser cuts for the holes is acceptable.



AUT

School of Engineering computer and Mathematical Sciences
Built Environment Engineering

DRAWING TITLE:

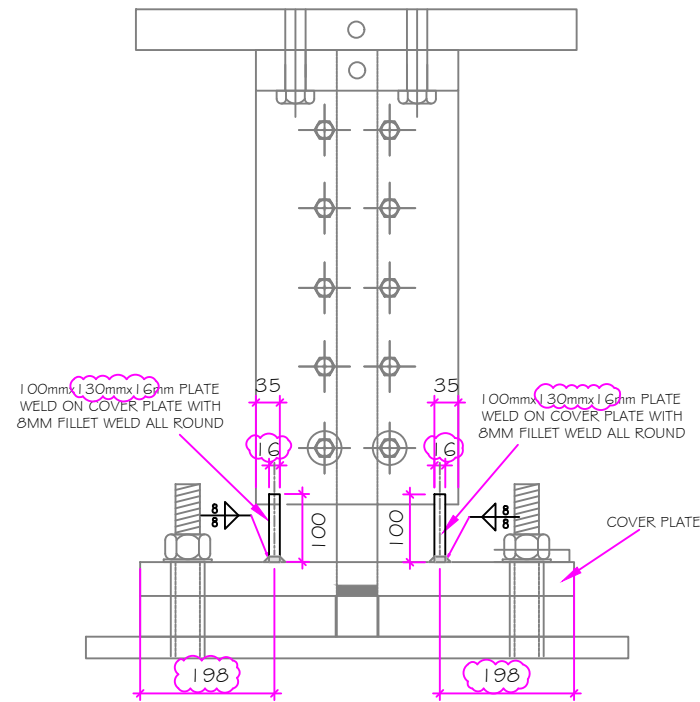
Test specimens and set up drawing

PROJECT TITLE:

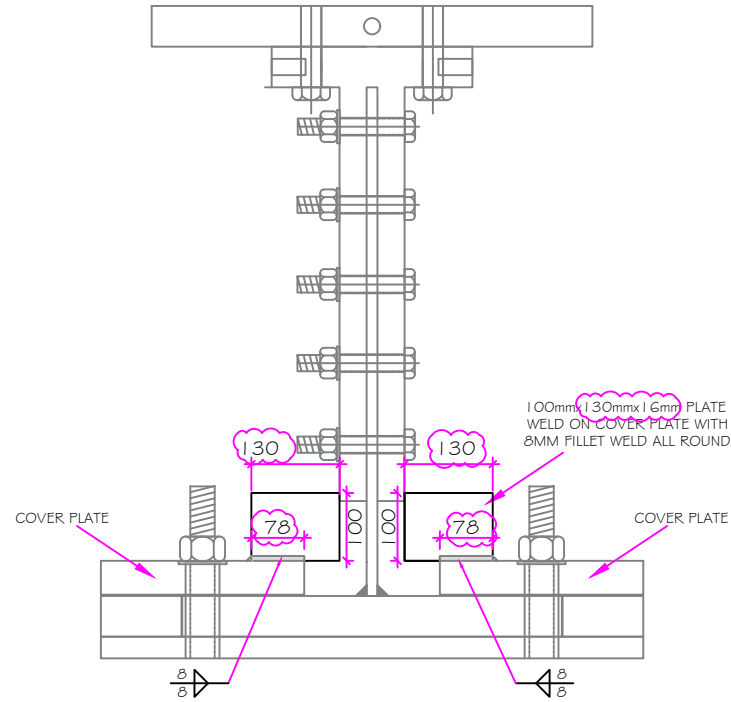
Experimental testing of fillet welded T-joints to evaluate the NZS3404 specified safety factors for seismic fillet welds

DRAWN	CHECKED	DRAWING NUMBER	DATE	
Mark Zhang	Dr. Shahab Ramhormozian	101	SCALE	REV.
			1:15	

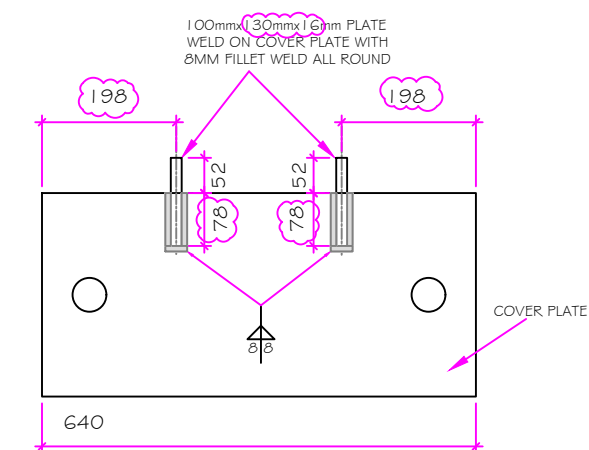
NOTES:
 MANUAL METAL ARC ELECTRODE (AS/NZS 1553.1): E48XX
 NOMINAL TENSILE STRENGTH OF WELD METAL (F_{uw}): 480 MPA



1 FRONT VIEW FOR HOLDING PLATE
 scale: N/A



2 SIDE VIEW FOR HOLDING PLATE
 scale: N/A



3 TOP VIEW FOR HOLDING PLATE AND COVER PLATE
 scale: N/A



AUT
 School of Engineering computer and Mathematical Sciences
 Built Environment Engineering

DRAWING TITLE:
 Holding plate design 1

PROJECT TITLE:
 Experimental testing of fillet welded T-joints to evaluate the NZS3404 specified safety factors for seismic fillet welds

DRAWN	CHECKED	DRAWING NUMBER	DATE
Mark Zhang	Dr. Shahab Ramhormozian	102	
		SCALE	REV.
		1:25	4

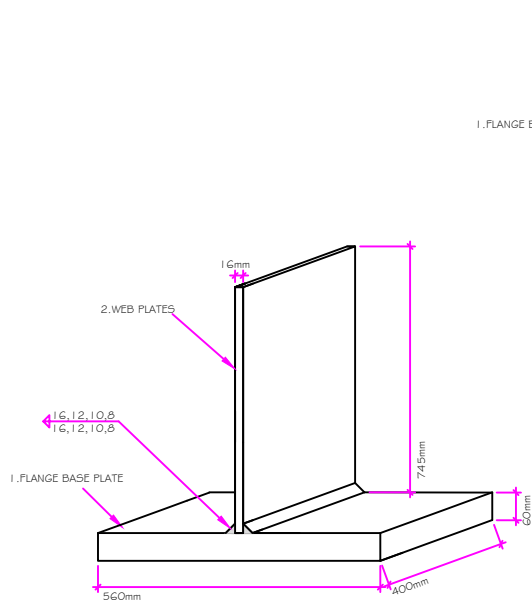
NOTES:

T-FILLET WELDED SPECIMENS ARE MADE AS WHOLE PIECE THEN CUT INTO FIVE SPECIMENS;
 202 IS PLAN FOR SINGLE T-FILLET WELDED SPECIMENS.

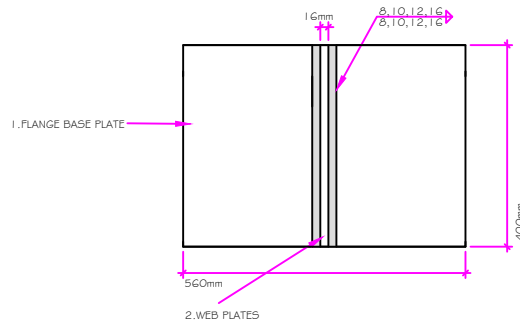
BOTH SURFACES OF THE WEB PLATE ARE TO UNDERGO THOROUGH BLAST CLEANING. THIS IS DESCRIBED AS SA2 IN ISO 8510. THIS SURFACE CONDITION MAY BE OBTAINED USING BOTH:

- AN AUTOMATED SHOT BLASTING MACHINE (SUCH AS A WHEELABRATOR), AND NOT BY HAND.
- SHOT WITH A ROUND PROFILE, (AND NOT GRIT, SAND OR GARNET).

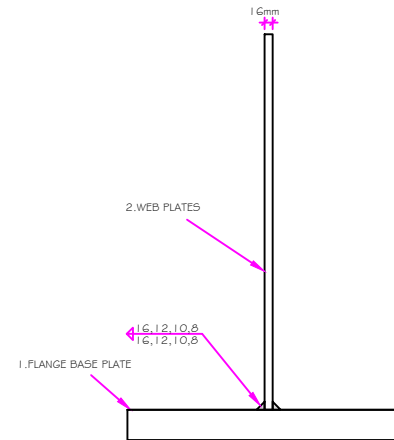
THE SURFACES ARE TO BE KEPT INDOORS IN A DRY LOCATION TO MINIMIZE CORROSION BEFORE PICKUP/DELIVERY.



1
201
 WHOLE PIECE
 GENERAL 3D VIEW
 scale: not to scale



2
201
 WHOLE PIECE
 PLAN VIEW
 scale: not to scale



3
202
 WHOLE PIECE
 SIDE VIEW
 scale: not to scale

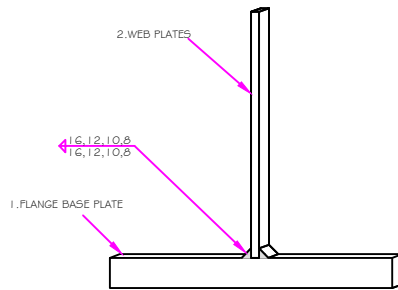
AUT

DRAWING TITLE:
 Whole piece plan

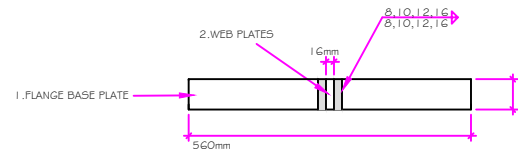
PROJECT TITLE:
 Experimental testing of fillet welded T-joints to evaluate the NZS3404 specified safety factors for seismic fillet welds

Steel Grade 300
 $f_{uw}=490\text{Mpa}$
 Category SP
 128

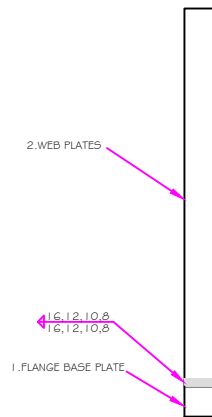
DRAWN	CHECKED	DRAWING NUMBER	DATE	
Mark Zhang	Dr. Shahab Ramhormozian	201	SCALE	REV.
			1:15	



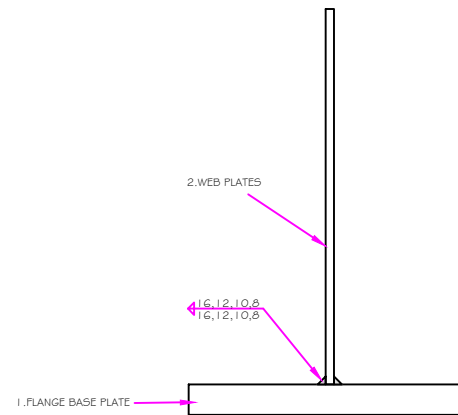
T-FILLET WELDED TEST SPECIMEN
GENERAL 3D VIEW
 1/202 scale: not to scale



T-FILLET WELDED TEST SPECIMEN
PLAN VIEW
 2/202 scale: not to scale



T-FILLET WELDED TEST SPECIMEN
FRONT VIEW
 3/202 scale: not to scale



T-FILLET WELDED TEST SPECIMEN
SIDE VIEW
 4/202 scale: not to scale

AUT

DRAWING TITLE:
 T-Fillet welded test specimens plan

PROJECT TITLE:
 Experimental testing of fillet welded T-joints to evaluate the NZS3404 specified safety factors for seismic fillet welds

Steel Grade 300
 $f_{uW}=490\text{Mpa}$
 Category SP
 129

DRAWN	CHECKED	DRAWING NUMBER	DATE	
Mark Zhang	Dr. Shahab Ramhormozian	202	SCALE	REV.
			1:15	

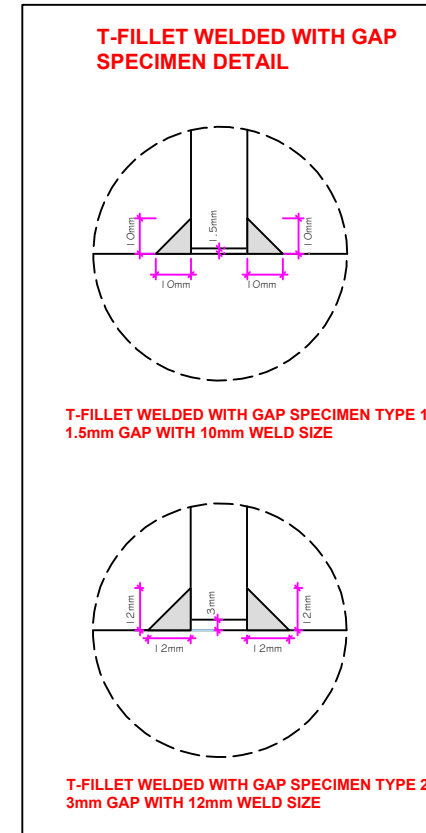
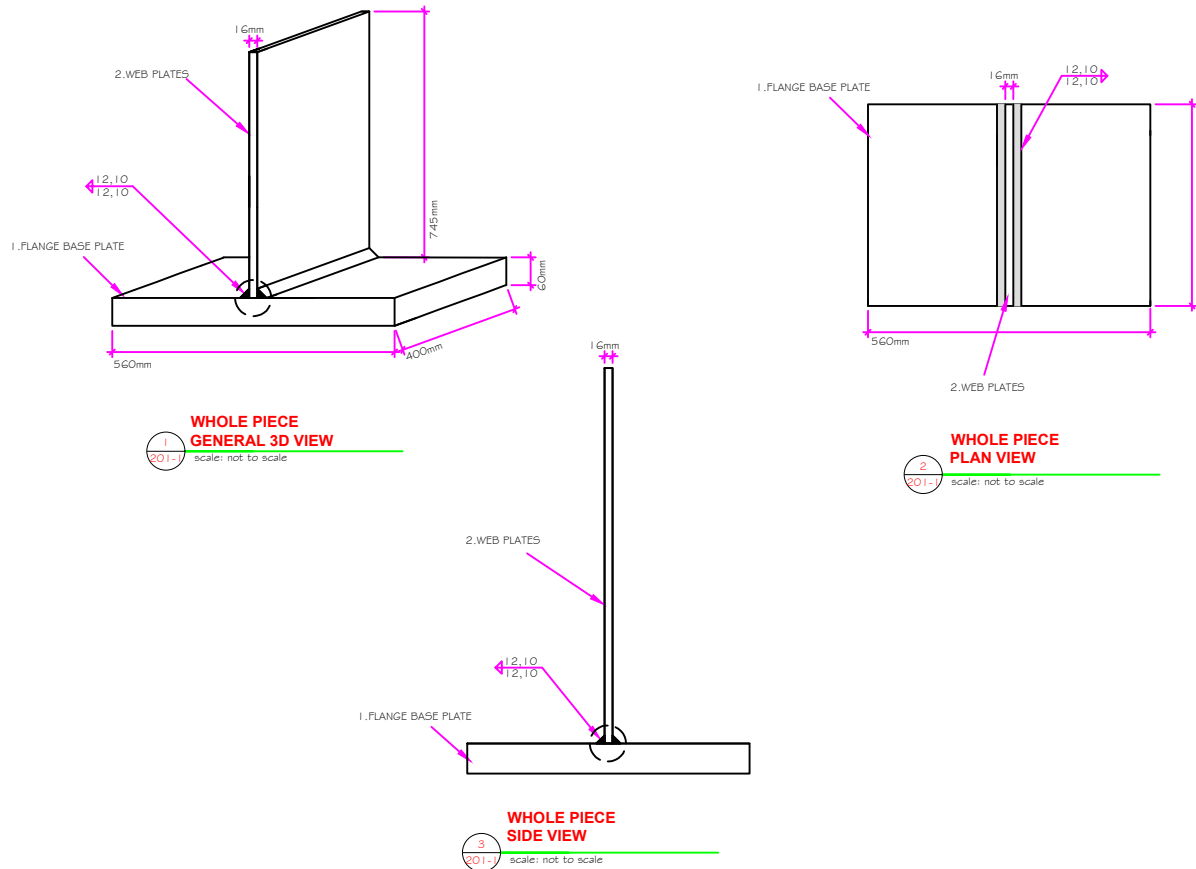
NOTES:

T-FILLET WELDED SPECIMENS ARE MADE AS WHOLE PIECE THEN CUT INTO FIVE SPECIMENS;
202-1 IS PLAN FOR SINGLE T-FILLET WELDED SPECIMENS.

BOTH SURFACES OF THE WEB PLATE ARE TO UNDERGO THOROUGH BLAST CLEANING. THIS IS DESCRIBED AS SA2 IN ISO 8510. THIS SURFACE CONDITION MAY BE OBTAINED USING BOTH:

- AN AUTOMATED SHOT BLASTING MACHINE (SUCH AS A WHEELABRATOR), AND NOT BY HAND.
- SHOT WITH A ROUND PROFILE, (AND NOT GRIT, SAND OR GARNET).

THE SURFACES ARE TO BE KEPT INDOORS IN A DRY LOCATION TO MINIMIZE CORROSION BEFORE PICKUP/DELIVERY.



AUT

DRAWING TITLE:

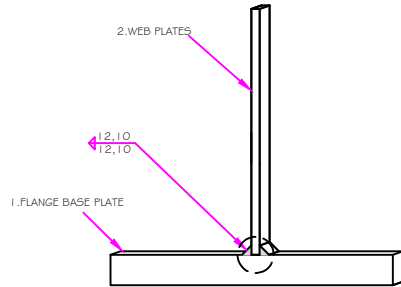
Whole piece plan for test specimens with gap

PROJECT TITLE:

Experimental testing of fillet welded T-joints to evaluate the NZS3404 specified safety factors for seismic fillet welds

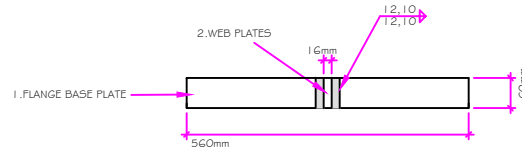
Steel Grade 300
 $f_{uw}=490\text{Mpa}$
Category SP
130

DRAWN	CHECKED	DRAWING NUMBER	DATE	
Mark Zhang	Dr. Shahab Ramhormozian	201-1	SCALE	REV.
			1:15	



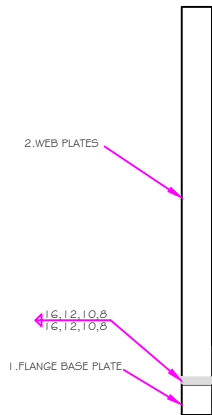
**T-FILLET WELDED TEST SPECIMEN
GENERAL 3D VIEW**

1
202-1 scale: not to scale



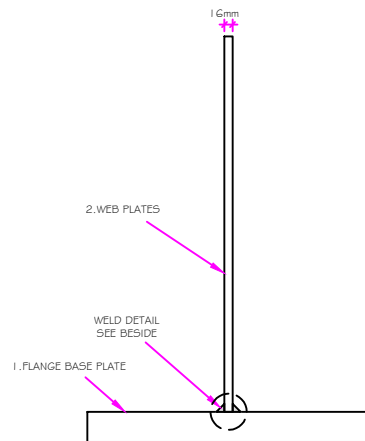
**T-FILLET WELDED TEST SPECIMEN
PLAN VIEW**

2
202-1 scale: not to scale



**T-FILLET WELDED TEST SPECIMEN
FRONT VIEW**

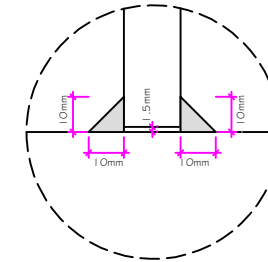
3
202-1 scale: not to scale



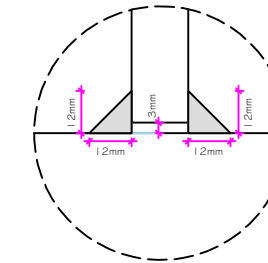
**T-FILLET WELDED TEST SPECIMEN
SIDE VIEW**

4
202-1 scale: not to scale

**T-FILLET WELDED WITH GAP
SPECIMEN DETAIL**



**T-FILLET WELDED WITH GAP SPECIMEN TYPE 1:
1.5mm GAP WITH 10mm WELD SIZE**



**T-FILLET WELDED WITH GAP SPECIMEN TYPE 2:
3mm GAP WITH 12mm WELD SIZE**

AUT

DRAWING TITLE:

T-Fillet welded test specimens plan with gap

PROJECT TITLE:

Experimental testing of fillet welded T-joints to evaluate the NZS3404 specified safety factors for seismic fillet welds

Steel Grade 300

$f_{uW}=490\text{Mpa}$
Category SP
131

DRAWN

Mark Zhang

CHECKED

Dr. Shahab Ramhormozian

DRAWING NUMBER

202-1

DATE

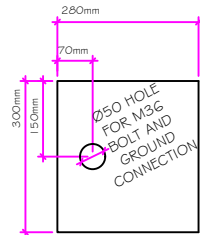
SCALE REV.

1:15

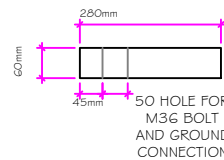
3.BACK UP PLATE:

3-1:
 1-1: LENGTH(mm): 300
 WIDTH(mm): 280
 THICKNESS(mm): 60
 ORDER PIECES: 4
 (STEEL GRADE 350)

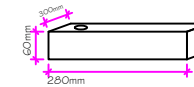
3-2:
 1-2: LENGTH(mm): 120
 WIDTH(mm): 60
 THICKNESS(mm): 60
 ORDER PIECES: 2
 (STEEL GRADE 300)



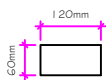
1-1
 203
DETAIL PLAN VIEW
 scale: not to scale



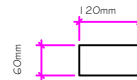
2-1
 203
DETAIL SIDE VIEW
 scale: not to scale



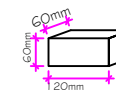
3-1
 203
DETAIL 3D VIEW
 scale: not to scale



1-2
 203
DETAIL PLAN VIEW
 scale: not to scale



2-2
 203
DETAIL SIDE VIEW
 scale: not to scale



3-2
 203
DETAIL 3D VIEW
 scale: not to scale

AUT

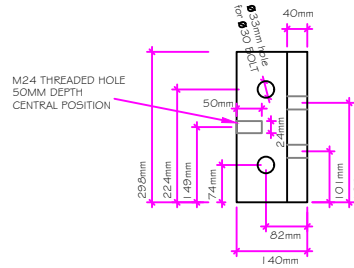
DRAWING TITLE:
 Manufacture drawing
 for back up plate

PROJECT TITLE:
 Experimental testing of fillet
 welded T-joints to evaluate the
 NZS3404 specified safety factors
 for seismic fillet welds

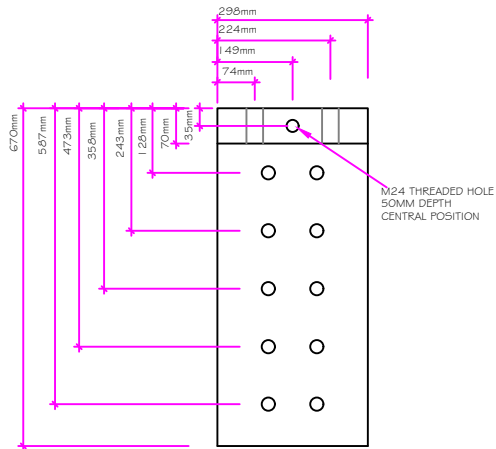
Steel Grade 350
 132

DRAWN	CHECKED	DRAWING NUMBER	DATE	
Mark Zhang	Dr. Shahab Ramhormozian	203	SCALE	REV.
			1:15	

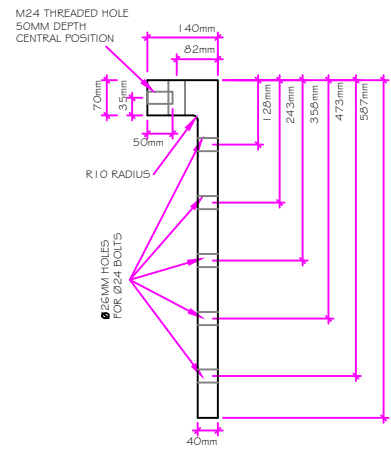
5. CLAMPING ANGLE:
 TO BE MACHINED
 LENGTH(mm): 670
 WIDTH(mm): 298
 THICKNESS(mm):
 70 FOR TOP
 40 FOR BOTTOM
 R10 RADIUS FOR CORNER
 CHAMFER SIZE: 2mm/2mm FOR EACH EDGE



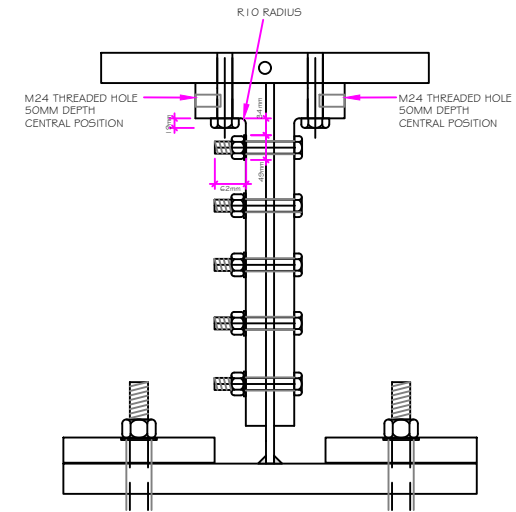
2
 204
DETAIL PLAN VIEW
 scale: not to scale



1
 204
DETAIL FRONT VIEW
 scale: not to scale



3
 204
DETAIL SIDE VIEW
 scale: not to scale



4
 204
DIMENSION AT CORNER
 scale: not to scale

AUT

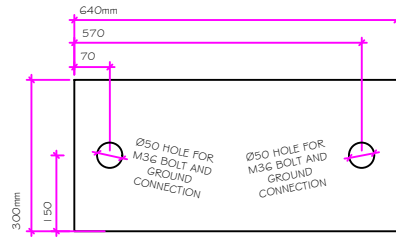
DRAWING TITLE:
 Manufacture drawing
 for clamping angle

PROJECT TITLE:
 Experimental testing of fillet
 welded T-joints to evaluate the
 NZS3404 specified safety factors
 for seismic fillet welds

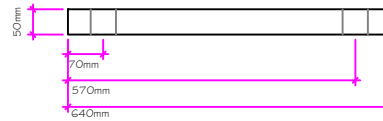
Steel Grade 250
 133

DRAWN	CHECKED	DRAWING NUMBER	DATE	
Mark Zhang	Dr. Shahab Ramhormozian	204	SCALE	REV.
			1:15	

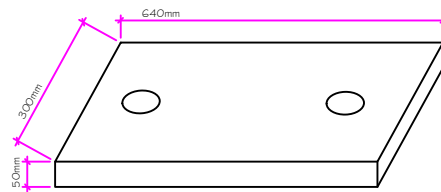
4. COVER PLATE:
 LENGTH(mm): 640
 WIDTH(mm): 300
 THICKNESS(mm): 50
 ORDER PIECES: 2
 (STEEL GRADE 350)



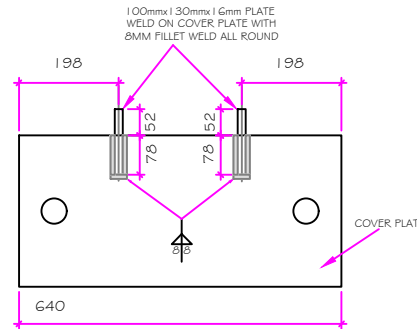
1
205
DETAIL PLAN VIEW
scale: not to scale



2
205
DETAIL SIDE VIEW
scale: not to scale



3
205
DETAIL 3D VIEW
scale: not to scale



4
205
TOP VIEW FOR HOLDING PLATE AND COVER PLATE
scale: N/A

SUMMARY OF THE ITEMS		
DRAWING NO	NAME	PIECES
201	COMPONENTS FROM WHOLE PIECE (8mm weld)	5
201	COMPONENTS FROM WHOLE PIECE (10mm weld)	5
201	COMPONENTS FROM WHOLE PIECE (12mm weld)	5
201	COMPONENTS FROM WHOLE PIECE (16mm weld)	5
201-1	COMPONENTS FROM WHOLE PIECE 1.5mm GAP (10mm weld)	5
201-1	COMPONENTS FROM WHOLE PIECE 3.0mm GAP (12mm weld)	5
203	BACK UP PLATE	4 of 3-1 & 2 of 3-2
204	COVER PLATE	2

OTHER ITEMS TO BE SUPPLIED		
NO	NAME	PIECES
1	M30X120 STRUCTURAL 8.8 BOLT/NUT/WASHER ASSEMBLY	20
2	M24X140 STRUCTURAL 8.8 BOLT/NUT/WASHER ASSEMBLY	60
3	M36X300 STRUCTURAL 8.8 THREAD ROD	20
4	WASHERS FOR M30	10
5	WASHERS FOR M36	30
6	FLAT PLATE WASHERS FOR M36 (70X70X12MM)	30
7	WASHERS FOR M24	20
8	NUTS FOR THREAD ROD	25

NOTES:
 ONE ASSEMBLY INCLUDES ONE BOLT, ONE NUT, AND ONE WASHER.

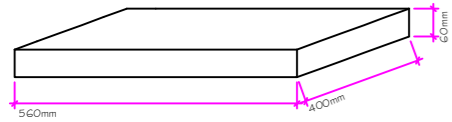
AUT

DRAWING TITLE:
 Manufacture drawing for cover plate and the item tables

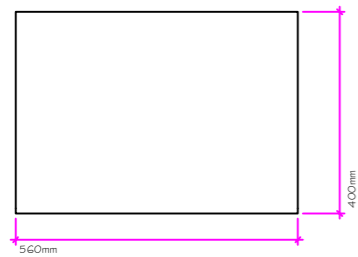
PROJECT TITLE:
 Experimental testing of fillet welded T-joints to evaluate the NZS3404 specified safety factors for seismic fillet welds

Steel Grade 350
 134

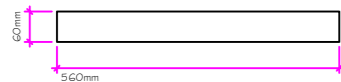
DRAWN	CHECKED	DRAWING NUMBER	DATE	
Mark Zhang	Dr. Shahab Ramhormozian	205	SCALE	REV.
			1:15	



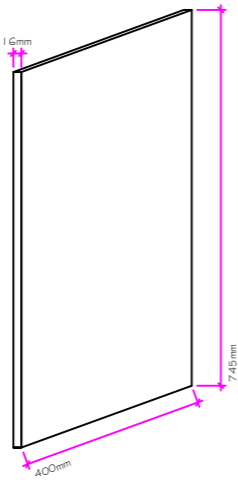
1 PART NO 1: FLANGE BASE PLATE 3D VIEW
scale: not to scale



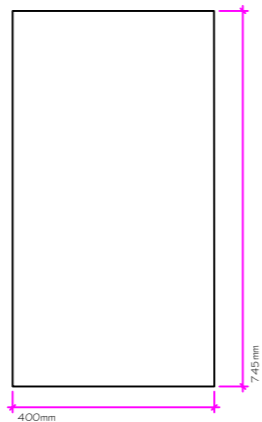
1 PART NO 1: FLANGE BASE PLATE PLAN VIEW
scale: not to scale



1 PART NO 1: FLANGE BASE PLATE SECTION VIEW
scale: not to scale



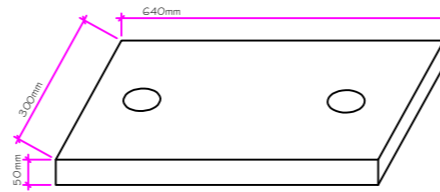
2 PART NO 2: WEB PLATE 3D VIEW
scale: not to scale



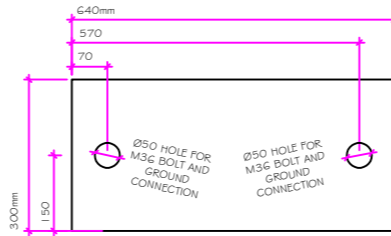
2 PART NO 2: WEB PLATE PLAN VIEW
scale: not to scale



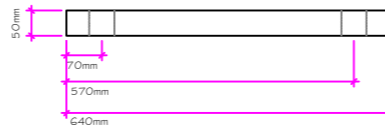
2 PART NO 2: WEB PLATE SIDE VIEW
scale: not to scale



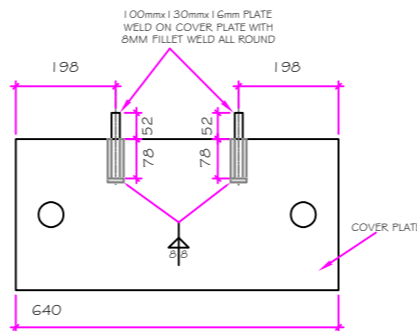
4 PART NO 4: COVER PLATE 3D VIEW
scale: not to scale



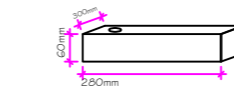
4 PART NO 4: COVER PLATE PLAN VIEW
scale: not to scale



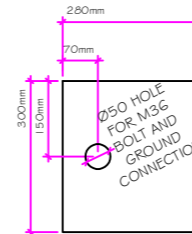
4 PART NO 4: COVER PLATE SECTION VIEW
scale: not to scale



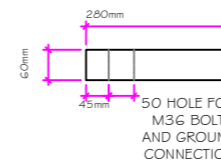
4 TOP VIEW FOR HOLDING PLATE AND COVER PLATE
scale: N/A



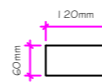
3-1 PART NO 3: BACKUP PLATE 3D VIEW
scale: not to scale



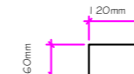
3-1 PART NO 3: BACKUP PLATE PLAN VIEW
scale: not to scale



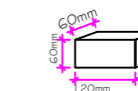
3-1 PART NO 3: BACKUP PLATE SECTION VIEW
scale: not to scale



3-2 DETAIL PLAN VIEW
scale: not to scale



3-2 DETAIL SIDE VIEW
scale: not to scale



3-2 DETAIL 3D VIEW
scale: not to scale

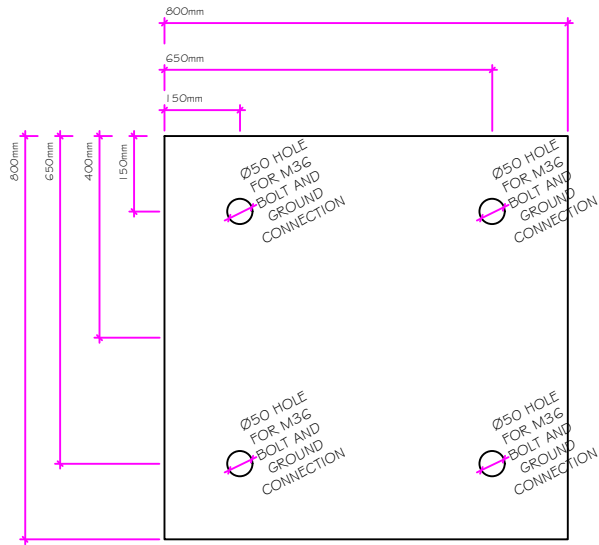
PART LIST

PARTS NO	3D VIEW	MATERIAL / DESCRIPTION	DIMENSIONS	QUANTITY
1		STEEL GRADE 300	PL: 560X400X60	6
2		STEEL GRADE 300	PL: 745X400X16	6
3-1		STEEL GRADE 350	PL: 280X300X60	4
3-2		STEEL GRADE 300	PL: 120X60X60	2
4		STEEL GRADE 350	PL: 640X300X50	2
5		STEEL GRADE 250 (NOT SHOWN IN THIS PAGE)	PL: 670X298X40	2
6		STEEL GRADE 350 (NOT SHOWN IN THIS PAGE)	PL: 800X800X12	1

Note:

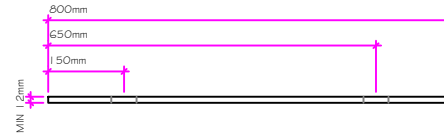
- Verify all dimensions prior to commencing any works.
- Either plasma or laser cuts for the holes is acceptable.

6.GROUND PROTECTION STEEL PLATE:
 TO BE MACHINED
 LENGTH(mm): 800
 WIDTH(mm): 800
 THICKNESS(mm):MIN 1.2mm
 R 10 RADIUS FOR CORNER
 CHAMFER SIZE: 2mm/2mm FOR EACH EDGE

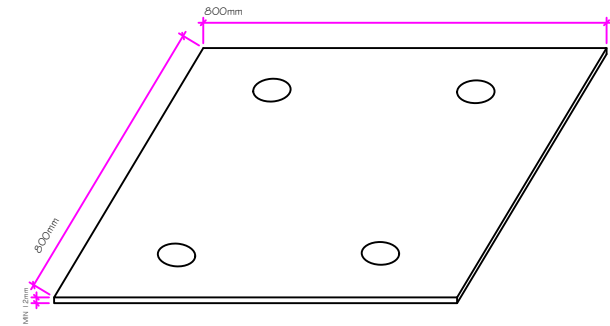


GROUND PROTECTION PLATE

1
20%
DETAIL PLAN VIEW
scale: not to scale



2
20%
DETAIL SIDE VIEW
scale: not to scale



3
20%
DETAIL 3D VIEW
scale: not to scale

AUT

DRAWING TITLE:
 Manufacture drawing
 for ground protection
 steel plate

PROJECT TITLE:
 Experimental testing of fillet
 welded T-joints to evaluate the
 NZS3404 specified safety factors
 for seismic fillet welds

Steel Grade 350
 136

DRAWN	CHECKED	DRAWING NUMBER	DATE	
Mark Zhang	Dr. Shahab Ramhormozian	207	18/10/22	
			SCALE	REV.
			1:15	

Appendix B - Dimensions of Tested samples

Measured size for specimens

		1	2	3	4	5	6	Average value(mm)
No1-20230321- FW10G0R1N3S2	Leg	10.1	10.2	10.3	9.6	9.9	10.5	10.1
	Root	12.5	13.1	12.8	12.5	12.2	12.2	12.55
	Throat	9.2	9.2	9.2	10.4	10.1	11.5	9.93
No2-20230413- FW12G3R1N2S5	Leg	12.9	12.1	11.4	10.7	10.8	12.2	11.68
	Root	12.5	11.8	11.2	10	10.1	12	11.27
	Throat	11	9.3	8.9	7.9	8	9.4	9.08
No3-20230420- FW12G3R0N2S6	Leg	10.3	11	10.9	11	11.2	11.1	10.92
	Root	11.1	10.6	10.1	9.9	10	9.8	10.25
	Throat	9	9	9	7.4	7.8	7.2	8.23
No4-20230420- FW10G0R0N3S3	Leg	9.7	9.4	9.9	9.8	9.5	9.9	9.70
	Root	10.4	9.5	9.8	9.3	9.2	9.2	9.57
	Throat	7.1	7.8	7.9	7.3	7	7	7.35
No5-20230421- FW12G3R0N2S4	Leg	11.3	11.8	12.3	10.8	10.3	10.8	11.22
	Root	9.9	10.4	10.4	10	9.9	10.2	10.13
	Throat	8.4	8.8	8.8	7.8	7.9	7.9	8.27
No6-20230421- FW12G0R0N1S1	Leg	13.8	13.8	14.3	11.7	11.4	11.9	12.82
	Root	13	12.9	12.9	13.2	13.4	13.5	13.15
	Throat	9.2	9.7	9.8	9.9	9.8	9.8	9.70
No7-20230424- FW8G0R0N4S3	Leg	9.4	9.5	9.5	9.2	9.2	9.3	9.35
	Root	11.7	11.4	10.8	10.8	10.3	10.2	10.87
	Throat	7.9	7.2	7.8	8	7.9	7.9	7.78
No8-20230426- FW10G1.5R0N5S2	Leg	11.5	10.4	10	11	11	11	10.82
	Root	13.9	13.2	13.3	13.3	13	13.4	13.35
	Throat	8.9	8.9	8.7	8.8	9.8	9.8	9.15
No9-20230426- FW12G3R0N2S3	Leg	11.7	11.7	11.2	10.9	11	11	11.25
	Root	10.1	9.9	10.3	10.4	10.1	9.9	10.12
	Throat	9	9	9	7.6	7.5	7.8	8.32
No10-20230427- FW12G3R0N2S1	Leg	12.5	11.8	11.4	10.4	9.6	10.8	11.08
	Root	10	10.2	10	10.4	9.6	10.4	10.10
	Throat	8.8	8.8	8.8	7.8	7.3	7.6	8.18

		1	2	3	4	5	6	Average value(mm)
No11-20230501-FW10G0R0N3S4	Leg	9.8	9.7	9.8	9.1	9.8	9.2	9.57
	Root	9.4	9.1	9.6	9.8	9.6	10	9.58
	Throat	6.8	7	7.4	8	8	8	7.53
No12-20230502-FW10G0R1N3S1	Leg	9.9	10.4	11.8	12.2	10.2	9.8	10.72
	Root	10.7	10.9	10.8	10.8	9.2	8.9	10.22
	Throat	7.9	8	8.7	8.2	7	7	7.80
No13-20230503-FW10G0R1N3S5	Leg	10.2	10.8	12.2	10.7	10.1	9.9	10.65
	Root	9.3	9.1	9.1	10.5	10	10	9.67
	Throat	7.2	7.6	8.4	8.8	8.3	8.9	8.20
No14-20230504-FW12G0R1N1S5	Leg	15.9	14.2	13.9	12	12	12.5	13.42
	Root	14.4	12.4	11.9	14	13.1	13.8	13.27
	Throat	9.8	9.7	9.3	9.4	9.9	10.3	9.73
No15-20230504-FW12G3R1N2S2	Leg	12.5	11.5	11.1	11.8	11.8	13.2	11.98
	Root	12.6	10.8	10.3	10.2	9.9	10.8	10.77
	Throat	8.2	7.8	7.8	8.8	8.9	9.5	8.50
No16-20230504-FW16G0R1N6S4	Leg	16	17.8	17.8	17.8	15.7	15.7	16.80
	Root	16.2	16.4	16.9	18.2	18.9	18.9	17.58
	Throat	11.8	12.1	12.1	13.7	12.2	12.5	12.40
No17-20230505-FW16G0R1N6S5	Leg	16.7	16	15.5	16.2	17.4	18	16.63
	Root	18.9	18.7	18.8	18.7	18.8	18.8	18.78
	Throat	12.9	12	12	12.8	13.4	13	12.68
No18-20230505-FW10G1.5R1N5S1	Leg	10.4	11.5	10.9	10.9	10.9	11.3	10.98
	Root	15	13.9	13.7	12.5	12.8	13.2	13.52
	Throat	10.8	10.8	9.8	8.9	8.9	9	9.70
No19-20230505-FW16G0R0N6S1	Leg	15.5	17	16.6	16.4	15.8	14.9	16.03
	Root	19.3	18.3	17.7	18.6	18.7	18.3	18.48
	Throat	11	12.9	13	12	12	11.7	12.10
No20-20230508-FW12G0R1N1S4	Leg	16.9	15.5	14.8	14.9	12.2	12.1	14.40
	Root	12.4	12.6	13.8	15.9	13.5	13.7	13.65
	Throat	9.7	9.7	10	10.9	9.4	9	9.78
No21-20230508-FW16G0R0N6S3	Leg	16.7	16.2	16.2	16.8	17.7	16.4	16.67
	Root	17.9	18.3	18.3	18.2	18.2	17.9	18.13
	Throat	11.8	11.8	11.9	13	13	13	12.42

		1	2	3	4	5	6	Average value(mm)
No22-20230509-FW8G0R0N4S1	Leg	9.4	8.6	8.9	9.8	9.4	9.3	9.23
	Root	10.6	10	9.9	11.8	10.8	10.9	10.67
	Throat	7.8	7.3	7.8	7.9	7.8	7.8	7.73
No23-20230509-FW16G0R0N6S2	Leg	15.5	15	16.5	16.6	15.8	16.8	16.03
	Root	17.3	17.2	17.6	17.6	18.1	18.4	17.70
	Throat	11.9	12	12	12.5	12.5	12.8	12.28
No24-20230509-FW8G0R1N4S2	Leg	9.5	9.4	9.3	9	9	9.9	9.35
	Root	10	9.8	10.8	10.4	10.6	10.8	10.40
	Throat	8.3	8.2	8	7.8	7.7	8.8	8.13
No25-20230510-FW8G0R0N4S5	Leg	8.7	8.4	8.6	9.2	9.8	9.4	9.02
	Root	9.7	9.8	9.9	10.4	11.6	11.4	10.47
	Throat	8	7.8	7.5	8	7.8	8	7.85
No26-20230511-FW10G1.5R0N5S4	Leg	9.7	10	10	11.2	11.1	12.1	10.68
	Root	13.8	13.9	13.5	13.3	12.7	13.2	13.40
	Throat	8.6	8.8	8.7	9.9	10	9.4	9.23
No27-20230511-FW12G0R0N1S3	Leg	12.7	12.7	12.1	13.7	14.3	13.7	13.20
	Root	14.1	13.7	13.8	13.1	13.3	13.6	13.60
	Throat	9.8	9.7	10	9.9	9.7	9.7	9.80
No28-20230512-FW8G0R1N4S4	Leg	10.2	9.9	11.6	9.4	9	8.6	9.78
	Root	11	11	11	11.2	11	10.8	11.00
	Throat	7.6	8	8.8	9	8.1	8	8.25
No29-20230512-FW10G1.5R0N5S3	Leg	9.9	10.3	10.2	11.5	12.2	12.2	11.05
	Root	13.8	14.1	14	13.9	13.4	12.8	13.67
	Throat	9	8.8	8.9	8.9	9.9	10	9.25
No30-20230515-FW10G1.5R0N5S5	Leg	11.4	11.2	10.7	9.4	9.9	10.2	10.47
	Root	11.7	13.6	13.7	14.7	13.1	13	13.30
	Throat	9	9	9.3	9	8.8	9	9.02
No31-20230515-FW12G0R0N1S2	Leg	12.2	12.4	13	13.8	13.8	13.9	13.18
	Root	13.8	14.1	14.1	13.1	13.1	13.3	13.58
	Throat	9.8	10	10.3	9.8	9	9.5	9.73
No32-20230516-FW10G0R0N3S6	Leg	10.6	9.7	9.4	9.4	9.3	9.2	9.60
	Root	9.8	9.9	9.1	9.7	9	9.8	9.55
	Throat	7.4	7	7	7.6	8	7.9	7.48

FW stand for weld size

G stand for gap size

R stand for round about weld. 0 is no round about weld and 1 is having round about weld.

N stand for grouped number and is not related to the sample size.

Appendix C - Tested Data

Summary for tested samples

Failure mode	Sample	Stem's Bottom width (mm)	Throat Length-both side(mm)			Max actual weld total demand (kN)	Average angle of fracture on weld	Theoretical weld design force-both side-capacity (kN/mm)	Actual weld force-both side-capacity or demand (kN/mm)		Ratio of actual/theoretical capacity or actual/theoretica demand		
			Cam Scale(45°)	Etching Test	Failure plane (Actual degree)				Cam Scale	Fracture plane	Cam Scale	Etching Test	Fracture plane
Slip	FW8G0N4S1(M20)	73.8	14.00	15.47		380.78		2.66	4.17		1.57	1.42	
Weld fracture	FW8G0N4S2(M24)	68.2	13.92	15.71	15.60	493.88	14.99	2.66	5.89	5.25	2.21	1.96	1.97
Weld fracture	FW8G0N4S3(M24)	69.4	14.21	15.03	15.43	506.37	17.44	2.66	5.81	5.35	2.18	2.06	2.01
Weld fracture	FW8G0N4S4(M20)	74.3	14.62	14.86	16.65	533.02	13.06	2.66	5.55	4.87	2.09	2.05	1.83
Slip	FW8G0N4S5(M20)	77.2	13.70	15.14		462.96		2.66	4.95		1.86	1.68	
Weld fracture	FW10G0N3S1(M24)	61	14.30	15.59	15.47	453.15	29.34	3.33	7.35	6.79	2.21	2.03	2.04
Pre-test Buckling	FW10G0N3S2(M24)	58.8	15.83	16.65		433.85		3.33	6.59		1.98	1.88	
Weld fracture	FW10G0N3S3(M24)	60.3	13.62	15.99	14.14	444.86	29.84	3.33	7.66	7.38	2.30	1.96	2.22
Slip	FW10G0N3S4(M24)	62.1	13.53	16.37		467.46		3.33	7.87		2.36	1.96	
Weld fracture	FW10G0N3S5(M24)	60.4	14.30	16.53	14.82	416.44	32.78	3.33	6.82	6.58	2.05	1.77	1.98
Weld fracture	FW10G0N3S6(M24)	63.3	13.54	16.20	14.16	447.89	28.16	3.33	7.39	7.07	2.22	1.86	2.12
Slip	FW10G1.5N5S1(M24)	70.7	17.13	18.15		521.99		2.83	5.18		1.83	1.73	
Weld fracture	FW10G1.5N5S2(M24)	68.7	16.90	17.30	17.25	503.14	26.03	2.83	5.21	5.10	1.84	1.80	1.81
Slip	FW10G1.5N5S3(M20)	77.4	17.23	17.51		512.71		2.83	4.62		1.63	1.61	
Slip	FW10G1.5N5S4(M20)	76.6	16.77	17.40		469.64		2.83	4.39		1.55	1.50	
Weld fracture	FW10G1.5N5S5(M24)	71.8	16.54	17.69	17.43	528.66	18.91	2.83	5.35	5.08	1.89	1.77	1.80
Stem fracture	FW12G0N1S1(M24)	73.5	18.31	18.12		536.78	99.42	3.99	6.77		1.70	1.71	
Slip	FW12G0N1S2(M20)	76.5	18.89	18.28		496.75		3.99	5.83		1.46	1.51	
Slip	FW12G0N1S3(M20)	77.5	18.92	18.26		432.18		3.99	5.00		1.25	1.30	
Slip	FW12G0N1S4(M24)	68.1	19.72	17.56		511.76		3.99	6.47		1.62	1.82	
Slip	FW12G0N1S5(M24)	70.6	18.80	18.52		513.89		3.99	6.57		1.65	1.67	

Failure mode	Sample	Stem's Bottom width (mm)	Throat Length-both side(mm)			Max actual weld total demand (kN)	Average angle of fracture on weld	Theoretical weld design force-both side-capacity (kN/mm)	Actual weld force-both side-capacity or demand (kN/mm)		Ratio of actual/theoretical capacity or actual/theoretical demand		
			Cam Scale(45°)	Etching Test	Failure plane (Actual degree)				Cam Scale	Fracture plane	Cam Scale	Etching Test	Fracture plane
Stem fracture	FW12G3N2S1(M24)	62.8	14.92	19.75		442.37	97.31	2.99	6.01		2.01	1.52	
Slip	FW12G3N2S2(M24)	62.6	16.02	20.43		427.62		2.99	5.43		1.81	1.42	
Stem fracture	FW12G3N2S3(M24)	61	15.06	20.46		440.56	96.48	2.99	6.10		2.04	1.50	
Stem fracture	FW12G3N2S4(M24)	62.4	15.05	20.28		452.13	95.04	2.99	6.13		2.05	1.52	
Stem fracture	FW12G3N2S5(M24)	56.8	16.22	20.23		444.93	96.42	2.99	6.15		2.05	1.65	
Stem fracture	FW12G3N2S6(M24)	60.7	14.94	20.39		460.24	95.36	2.99	6.46		2.16	1.58	
Stem fracture	FW16G0N6S1(M24)	72.6	24.28	22.94		543.25	107.96	5.32	6.97		1.31	1.39	
Slip	FW16G0N6S2(M20)	77	23.79	23.33		334.59		5.32	4.13		0.78	0.79	
Slip	FW16G0N6S3(M20)	74.6	24.56	23.73		447.85		5.32	5.53		1.04	1.08	
Slip	FW16G0N6S4(M24)	68.4	24.26	22.97		499.19		5.32	6.81		1.28	1.35	
Slip	FW16G0N6S5(M24)	73.1	24.94	23.77		523.76		5.32	6.50		1.22	1.28	

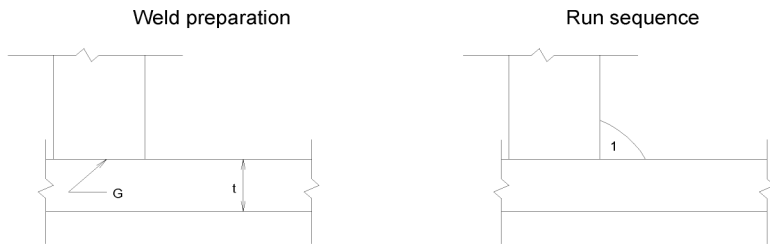
Red: fracture in weld, orange: fracture in stem (i.e. web), Green: test terminated due to sliding, and black: the sample used in first trail test.

Appendix D - Welding Procedures

Welding Procedure Specification

Standard:	AS/NZS 1554.1: 2014	WPS no:	JJS-08-01	Rev:	1
Weld category:	GP & SP	Date qualified:	27/03/2012	Page:	1 of 1
Material spec/grade/type:	Steel types 1 & 4 (note 1)	To:	Steel types 1 & 4 (note 1)		
Joint type:	Fillet - equal leg length with no root gap	PQR reference:	JJS-08		
Process:	FCAW (C)	Type:	Semi-automatic		
Position(s) qualified:	Flat, Horizontal & Overhead	"t" range qualified:	All		
Diameter range qualified:	All	Leg length qualified:	Up to 6.0mm		

Preheat temperature:	10 minimum, Additional preheat may be required see 'Preheat matrix 01' document	
Inter-run temperature:	N/A	Method and check:
Surface finish:	As welded	PWHT:
		Nil



Joint details:

Prequalified no:	F1
To table:	E3
Root gap (G) mm:	Nil
Root face (F) mm:	N/A
Included angle (°):	85-100
Backing (t) mm:	N/A

Welding consumables:

Specification - root:	AS/NZ ISO 17632-B	Remainder:	N/A	Flux:	N/A
Classification - root:	T492T1-1 CAU H10	Remainder:	N/A	AWS A5.20:	E71T-12M H4
Shielding gas 1:	Welding grade C02	Flow rate (l/m):	18 to 25	Shipping class:	ABS 3YSA H10
Shielding gas 2:	N/A	Flow rate (l/m):	N/A	Other:	N/A

Weld run details and parameters:

Run #	Side	Position / Progression	Wire Ø mm	Current / Polarity	Tradename	Amperage	Voltage	Wire speed mm/min	Travel mm/min	Heat input kJ/mm
1	1	F, H, OH	1.2	DC (+)	Any (note 2)	223 - 257	27 - 31	10800	204 - 276	1.3 - 2.3

Technique details:

Technique:	Leading gun angle 10-15°	Run formation:	Single pass - stringer bead
Initial cleaning:	N/A	Electrical stickout:	16-20mm
Inter-run cleaning:	N/A	Backgouge method:	N/A
Metal transfer:	N/A	Backgouge check:	N/A
Post weld cleaning:	Remove slag & spatter		

Notes / revisions: Rev 1: Issued due to revision under AS/NZS 1554.1: 2014

- 1) WPS is qualified for use with other C or C-Mn steels without further qualification testing provided all the items listed in section 4.8(a-d) of the standard are met.
- 2) Approval covers the use of any welding consumable as classified above(excluding AWS) provided all the parameters comply with the consumable manufacturer's recommendations.
- 3) Wire speed recorded is from the PQR and is supplied for informational purposes only.

Fabricator:	John Jones Steel Ltd	Approved by:	C Ayers SWI
Approved by:		Date:	27/03/2020
Date:			

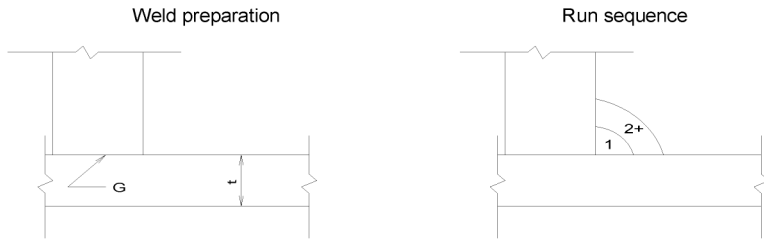


Any changes to the data contained in this record outside of the range of essential variables detailed in the specification requires requalification.

Welding Procedure Specification

Standard:	AS/NZS 1554.1: 2014	WPS no:	JJS-09-01	Rev:	1
Weld category:	GP & SP	Date qualified:	27/03/2012	Page:	1 of 1
Material spec/grade/type:	Steel types 1 & 4 (note 1)	To:	Steel types 1 & 4 (note 1)		
Joint type:	Fillet - equal leg length with no root gap	PQR reference:	JJS-09		
Process:	FCAW (C)	Type:	Semi-automatic		
Position(s) qualified:	Flat, Horizontal & Overhead	"t" range qualified:	All		
Diameter range qualified:	All	Leg length qualified:	8.0mm and above		

Preheat temperature:	10 minimum, Additional preheat may be required see 'Preheat matrix 01' document				
Inter-run temperature:	300 maximum for seismic joints, otherwise N/A	Method and check:	Any		
Surface finish:	As welded	PWHT:	Nil		



Joint details:

Prequalified no:	F1
To table:	E3
Root gap (G) mm:	Nil
Root face (F) mm:	N/A
Included angle (°):	85-100
Backing (t) mm:	N/A

Welding consumables:

Specification - root:	AS/NZS ISO 17632-B	Remainder:	AS/NZS ISO 17632-B	Flux:	N/A
Classification - root:	T492T1-1 CAU H10	Remainder:	T492T1-1 CAU H10	AWS A5.20:	E71T-12M H4
Shielding gas 1:	Welding grade C02	Flow rate (l/m):	18 to 25	Shipping class:	ABS 3YSA H10
Shielding gas 2:	N/A	Flow rate (l/m):	N/A	Other:	N/A

Weld run details and parameters:

Run #	Side	Position / Progression	Wire Ø mm	Current / Polarity	Tradename	Amperage	Voltage	Wire speed mm/min	Travel mm/min	Heat input kJ/mm
1	1	F, H, OH	1.2	DC (+)	Any (note 2)	223 - 257	27 - 31	10800	204 - 276	1.3 - 2.3
2+	1	F, H, OH	1.2	DC(+)	Any (note 2)	223 - 257	27 - 31	10800	298 - 402	0.9 - 1.6

Technique details:

Technique:	Leading gun angle 10-15°	Run formation:	Multi pass - stringer bead
Initial cleaning:	Grind	Electrical stickout:	16-20mm
Inter-run cleaning:	Chip, grind & wire brush	Backgouge method:	N/A
Metal transfer:	N/A	Backgouge check:	N/A
Post weld cleaning:	Remove slag & spatter		

Notes / revisions: Rev 1: Issued due to revision under AS/NZS 1554.1: 2014

- 1) WPS is qualified for use with other C or C-Mn steels without further qualification testing provided all the items listed in section 4.8(a-d) of the standard are met.
- 2) Approval covers the use of any welding consumable as classified above(excluding AWS) provided all the parameters comply with the consumable manufacturer's recommendations.
- 3) Wire speed recorded is from the PQR and is supplied for informational purposes only.

Fabricator:	John Jones Steel Ltd	Approved by:	C Ayers SWI
Approved by:		Date:	27/03/2020
Date:			

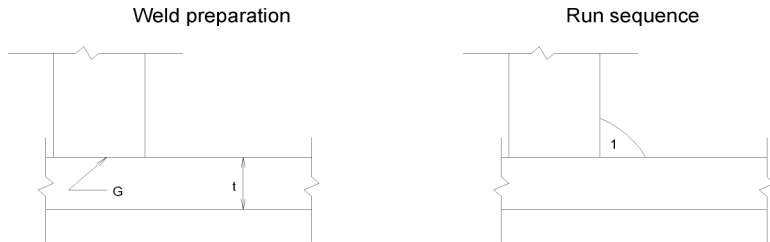


Any changes to the data contained in this record outside of the range of essential variables detailed in the specification requires requalification.

Welding Procedure Specification

Standard:	AS/NZS 1554.1: 2014	WPS no:	JJS-10-01	Rev:	1
Weld category:	GP & SP	Date qualified:	27/03/2012	Page:	1 of 1
Material spec/grade/type:	Steel types 1 & 4 (note 1)	To:	Steel types 1 & 4 (note 1)		
Joint type:	Fillet - equal leg length with no root gap	PQR reference:	JJS-10		
Process:	FCAW (C)	Type:	Semi-automatic		
Position(s) qualified:	Vertical	"t" range qualified:	All		
Diameter range qualified:	All	Leg length qualified:	Up to 7.0mm		

Preheat temperature:	10 minimum, Additional preheat may be required see 'Preheat matrix 01' document	
Inter-run temperature:	N/A	Method and check:
Surface finish:	As welded	PWHT:



Joint details:

Prequalified no:	F1
To table:	E3
Root gap (G) mm:	Nil
Root face (F) mm:	NA
Included angle (°):	85-100
Backing (t) mm:	N/A

Welding consumables:

Specification - root:	AS/NZS ISO 17632-B	Remainder:	N/A	Flux:	N/A
Classification - root:	T492T1-1 CAU H10	Remainder:	N/A	AWS A5.20:	E71T-12M H4
Shielding gas 1:	Welding grade C02	Flow rate (l/m):	18 to 25	Shipping class:	ABS 3YSA H10
Shielding gas 2:	N/A	Flow rate (l/m):	N/A	Other:	N/A

Weld run details and parameters:

Run #	Side	Position / Progression	Wire Ø mm	Current / Polarity	Tradename	Amperage	Voltage	Wire speed mm/min	Travel mm/min	Heat input kJ/mm
1	1	Vertical up	1.2	DC (+)	Any (note 2)	233 - 268	26 - 30	7200	119 - 161	2.3 - 4.1

Technique details:

Technique:	Trailing gun angle 10-15°	Run formation:	Single pass - stringer bead
Initial cleaning:	Grind	Electrical stickout:	16-20mm
Inter-run cleaning:	N/A	Backgouge method:	N/A
Metal transfer:	N/A	Backgouge check:	N/A
Post weld cleaning:	Remove slag & spatter		

Notes / revisions: Rev 1: Issued due to revision under AS/NZS 1554.1: 2014

- 1) WPS is qualified for use with other C or C-Mn steels without further qualification testing provided all the items listed in section 4.8(a-d) of the standard are met.
- 2) Approval covers the use of any welding consumable as classified above(excluding AWS) provided all the parameters comply with the consumable manufacturer's recommendations.
- 3) Wire speed recorded is from the PQR and is supplied for informational purposes only.

Fabricator:	John Jones Steel Ltd	Approved by:	C Ayers SWI
Approved by:		Date:	27/03/2020

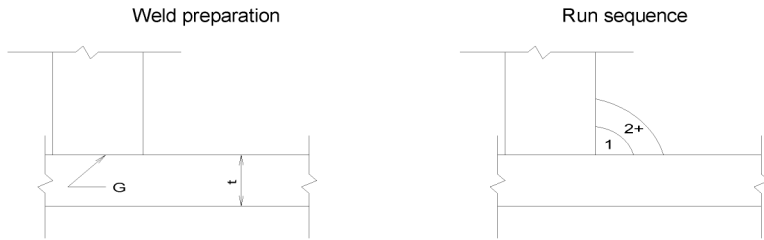


Any changes to the data contained in this record outside of the range of essential variables detailed in the specification requires requalification.

Welding Procedure Specification

Standard:	AS/NZS 1554.1: 2014	WPS no:	JJS-11-01	Rev:	1
Weld category:	GP & SP	Date qualified:	27/03/2012	Page:	1 of 1
Material spec/grade/type:	Steel types 1 & 4 (note 1)	To:	Steel types 1 & 4 (note 1)		
Joint type:	Fillet - equal leg length with no root gap	PQR reference:	JJS-11		
Process:	FCAW (C)	Type:	Semi-automatic		
Position(s) qualified:	Vertical	"t" range qualified:	All		
Diameter range qualified:	All	Leg length qualified:	8.0mm and above		

Preheat temperature:	10 minimum, Additional preheat may be required see 'Preheat matrix 01' document				
Inter-run temperature:	300 maximum for seismic joints, otherwise N/A	Method and check:	Any		
Surface finish:	As welded	PWHT:	Nil		



Joint details:

Prequalified no:	F1
To table:	E3
Root gap (G) mm:	Nil
Root face (F) mm:	N/A
Included angle (°):	85-100
Backing (t) mm:	N/A

Welding consumables:

Specification - root:	AS/NZS ISO 17632-B	Remainder:	AS/NZS ISO 17632-B	Flux:	N/A
Classification - root:	T492T1-1 CAU H10	Remainder:	T492T1-1 CAU H10	AWS A5.20:	E71T-12M H4
Shielding gas 1:	Welding grade C02	Flow rate (l/m):	18 to 25	Shipping class:	ABS 3YSA H10
Shielding gas 2:	Nil	Flow rate (l/m):	N/A	Other:	N/A

Weld run details and parameters:

Run #	Side	Position / Progression	Wire Ø mm	Current / Polarity	Tradename	Amperage	Voltage	Wire speed mm/min	Travel mm/min	Heat input kJ/mm
1	1	Vertical up	1.2	DC (+)	Any (note 2)	233 - 268	26 - 29	7200	119 - 161	2.2 - 4.0
2+	1	Vertical up	1.2	DC (+)	Any (note 2)	233 - 268	26 - 29	7200	119 - 161	2.2 - 4.0

Technique details:

Technique:	Trailing gun angle 10-15°	Run formation:	Multiple run - string & weave bead
Initial cleaning:	Grind	Electrical stickout:	19-20mm
Inter-run cleaning:	Chip and grind	Backgouge method:	N/A
Metal transfer:	N/A	Backgouge check:	N/A
Post weld cleaning:	Remove slag & spatter		

Notes / revisions: Rev 1: Issued due to revision under AS/NZS 1554.1: 2014

- 1) WPS is qualified for use with other C or C-Mn steels without further qualification testing provided all the items listed in section 4.8(a-d) of the standard are met.
- 2) Approval covers the use of any welding consumable as classified above(excluding AWS) provided all the parameters comply with the consumable manufacturer's recommendations.
- 3) Wire speed recorded is from the PQR and is supplied for informational purposes only.

Fabricator:	John Jones Steel Ltd	Approved by:	C Ayers SWI
Approved by:		Date:	27/03/2020
Date:			

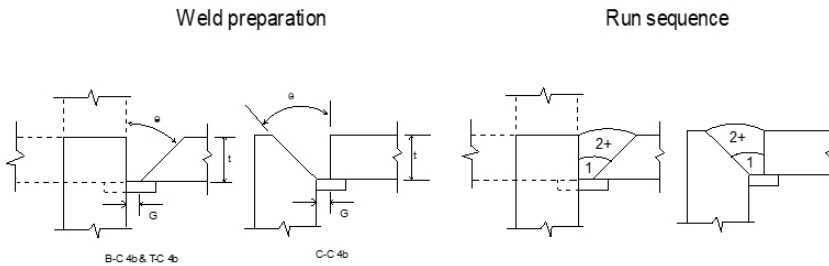


Any changes to the data contained in this record outside of the range of essential variables detailed in the specification requires requalification.

Welding Procedure Specification

Standard:	AS/NZS 1554.1: 2014	WPS no:	JJS-21-01	Rev:	2
Weld category:	SP & GP	Date qualified:	22/05/2019	Page:	1 of 1
Material spec/grade/type:	Steel type 1 & 4 (note 1)	To:	Steel type 1 & 4 (note 1)		
Joint type:	Single bevel butt, welded one side with backing	PQR reference:	JJS-21		
Process:	FCAW (C)	Type:	Semi-automatic		
Position(s) qualified:	Horizontal & Overhead	"t" range qualified:	6mm - 24mm		
Diameter range qualified:	N/A	Leg length qualified:	N/A		

Preheat temperature:	10 minimum, Additional preheat may be required see 'Preheat matrix 01' document	
Inter-run temperature:	300 maximum for seismic joints, otherwise N/A	Method and check:
Surface finish:	As welded	PWHT:



Joint details:

Prequalified no:	B-C4b, T-C4b, C-C4b
To table:	E1
Root gap (G) mm:	4.5 - 12.0
Root face (F) mm:	0.0 - 1.5
Included angle (°):	40 - 50
Backing (t) mm:	5.0 minimum

Welding consumables:

Specification - root:	AS/NZS ISO 17632-B	Remainder:	AS/NZS ISO 17632-B	Flux:	N/A
Classification - root:	T492T1-1 CAU H10	Remainder:	T492T1-1 CAU H10	AWS A5.20:	E71T-12M H4
Shielding gas 1:	CO2	Flow rate (l/m):	20 to 28	Shipping class:	ABS 2YSA H10
Shielding gas 2:	N/A	Flow rate (l/m):	N/A	Other:	N/A

Weld run details and parameters:

Run #	Side	Position / Progression	Wire Ø mm	Current / Polarity	Tradename	Amperage	Voltage	Wire speed mm/min	Travel mm/min	Heat input kJ/mm
1	1	H or OH	1.2	DC(+)	Any (note 2)	234 - 286	28 - 32	9600	255 - 345	1.1 - 2.2
2+	1	H or OH	1.2	DC(+)	Any (note 2)	234 - 289	28 - 32	9600	255 - 345	1.1 - 2.2

Technique details:

Technique:	Dragging gun angle 10-15°	Run formation:	Multiple run - stringer bead
Initial cleaning:	Grind	Electrical stickout:	20-25mm
Inter-run cleaning:	Chip, grind & wire brush	Backgouge method:	N/A
Metal transfer:	N/A	Backgouge check:	N/A
Post weld cleaning:	Remove Spatter & slag		

Notes / revisions: Rev 1: Issued due to revision under AS/NZS 1554.1: 2014. Wire speed recorded is from PQR for informational purposes only.

- 1) WPS is qualified for use with other C or C-Mn steels without further qualification testing provided all the items listed in section 4.8(a-d) of the standard are met.
- 2) Approval covers the use of any welding consumable as classified above(excluding AWS) provided all the parameters comply with the consumable manufacturer's recommendations.

Fabricator:	John Jones Steel Ltd	Approved by:	C Ayers SWI
Approved by:		Date:	27/03/2020



Any changes to the data contained in this record outside of the range of essential variables detailed in the specification requires requalification.

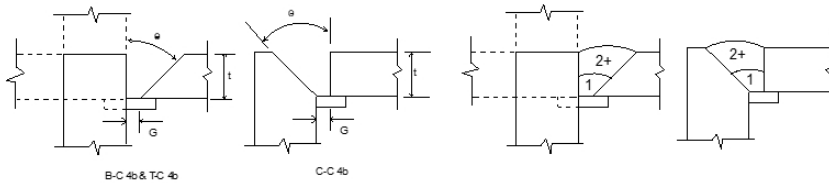
Welding Procedure Specification

Standard:	AS/NZS 1554.1: 2014	WPS no:	JJS-21-02	Rev:	0
Weld category:	SP & GP	Date qualified:	22/05/2019	Page:	1 of 1
Material spec/grade/type:	Steel type 1 & 4 (note 1)	To:	Steel type 1 & 4 (note 1)		
Joint type:	Single bevel butt, welded one side with backing	PQR reference:	JJS-21		
Process:	FCAW (C)	Type:	Semi-automatic		
Position(s) qualified:	Flat	"t" range qualified:	6mm - 24mm		
Diameter range qualified:	N/A	Leg length qualified:	N/A		

Preheat temperature:	10 minimum, Additional preheat may be required see 'Preheat matrix 01' document		
Inter-run temperature:	300 maximum for seismic joints, otherwise N/A	Method and check:	Any
Surface finish:	As welded	PWHT:	Nil

Weld preparation

Run sequence



Joint details:

Prequalified no:	B-C4b, T-C4b, C-C4b
To table:	E1
Root gap (G) mm:	8.5 - 12.0
Root face (F) mm:	0.0 - 1.5
Included angle (°):	40
Backing (t) mm:	5.0 minimum

Welding consumables:

Specification - root:	AS/NZS ISO 17632-B	Remainder:	AS/NZS ISO 17632-B	Flux:	N/A
Classification - root:	T492T1-1 CAU H10	Remainder:	T492T1-1 CAU H10	AWS A5.20:	E71T-12M H4
Shielding gas 1:	CO2	Flow rate (l/m):	20 to 28	Shipping class:	ABS 2YSA H10
Shielding gas 2:	N/A	Flow rate (l/m):	N/A	Other:	N/A

Weld run details and parameters:

Run #	Side	Position / Progression	Wire Ø mm	Current / Polarity	Tradename	Amperage	Voltage	Wire speed mm/min	Travel mm/min	Heat input kJ/mm
1	1	Flat	1.2	DC(+)	Any (note 2)	234 - 286	28 - 32	9600	255 - 345	1.1 - 2.2
2+	1	Flat	1.2	DC(+)	Any (note 2)	234 - 289	28 - 32	9600	255 - 345	1.1 - 2.2

Technique details:

Technique:	Dragging gun angle 10-15°	Run formation:	Multiple run - stringer bead
Initial cleaning:	Grind	Electrical stickout:	20-25mm
Inter-run cleaning:	Chip, grind & wire brush	Backgouge method:	N/A
Metal transfer:	N/A	Backgouge check:	N/A
Post weld cleaning:	Remove Spatter & slag		

Notes / revisions: Wire speed recorded is from PQR for informational purposes only.

- 1) WPS is qualified for use with other C or C-Mn steels without further qualification testing provided all the items listed in section 4.8(a-d) of the standard are met.
- 2) Approval covers the use of any welding consumable as classified above(excluding AWS) provided all the parameters comply with the consumable manufacturer's recommendations.

Fabricator:	John Jones Steel Ltd	Approved by:	C Ayers SWI
Approved by:			
Date:		Date:	27/03/2020



Any changes to the data contained in this record outside of the range of essential variables detailed in the specification requires requalification.

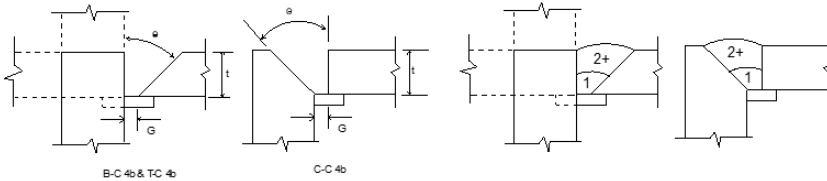
Welding Procedure Specification

Standard:	AS/NZS 1554.1: 2014	WPS no:	JJS-22-01	Rev:	2
Weld category:	SP & GP	Date qualified:	27/03/2012	Page:	1 of 1
Material spec/grade/type:	Steel types 1 & 4 (note 1)	To:	Steel types 1 & 4 (note 1)		
Joint type:	Single bevel T butt with backing	PQR reference:	JJS-22		
Process:	FCAW (C)	Type:	Semi-automatic		
Position(s) qualified:	Vertical	"t" range qualified:	6mm - 24mm		
Diameter range qualified:	N/A	Leg length qualified:	N/A		

Preheat temperature:	10 minimum, Additional preheat may be required see 'Preheat matrix 01' document	
Inter-run temperature:	300 maximum for seismic joints, otherwise N/A	Method and check:
Surface finish:	As welded	PWHT:

Weld preparation

Run sequence



Joint details:

Prequalified no:	B-C4b, T-C4b, C-C4b
To table:	E1
Root gap (G) mm:	4.5 - 12.0
Root face (F) mm:	0.0 - 1.5
Included angle (°):	40 - 55
Backing (t) mm:	6.0

Welding consumables:

Specification - root:	AS/NZS ISO 17632-B	Remainder:	AS/NZS ISO 17632-B	Flux:	N/A
Classification - root:	T492T1-1 CAU H10	Remainder:	T492T1-1 CAU H10	AWS A5.20:	E71T-12M H4
Shielding gas 1:	CO2	Flow rate (l/m):	20 to 28	Shipping class:	ABS 3YSA H10
Shielding gas 2:	Nil	Flow rate (l/m):	N/A	Other:	N/A

Weld run details and parameters:

Run #	Side	Position / Progression	Wire Ø mm	Current / Polarity	Tradename	Amperage	Voltage	Wire speed mm/min	Travel mm/min	Heat input kJ/mm
1	1	Vertical up	1.2	DC(+)	Any (note 2)	162 - 198	23 - 27	4800	196 - 265	0.9 - 1.6
2+	1	Vertical up	1.2	DC (+)	Any (note 2)	162 - 198	23 - 27	4800	196 - 265	0.9 - 1.6

Technique details:

Technique:	Trailing gun angle 10-15°	Run formation:	Multiple run - weave bead
Initial cleaning:	Grinding	Electrical stickout:	20-25mm
Inter-run cleaning:	Chip, grind & wire brush	Backgouge method:	N/A
Metal transfer:	N/A	Backgouge check:	N/A
Post weld cleaning:	Remove slag & spatter		

Notes / revisions: Rev 2: Issued due to revision under AS/NZS 1554.1: 2014. Wire speed recorded is from PQR for informational purposes only.

- WPS is qualified for use with other C or C-Mn steels without further qualification testing provided all the items listed in section 4.8(a-d) of the standard are met.
- Approval covers the use of any welding consumable as classified above(excluding AWS) provided all the parameters comply with the consumable manufacturer's recommendations.

Fabricator:	John Jones Steel Ltd	Approved by:	C Ayers SWI
Approved by:		Date:	27/03/2020



Any changes to the data contained in this record outside of the range of essential variables detailed in the specification requires requalification.